

# **Molecular correlates of visual system development**

Corey Joseph Flynn  
BS, Animal Behavior, Bucknell University 2005

Submitted to the the faculty in the  
Department of Biological Sciences at  
Carnegie Mellon University

In partial fulfillment of the requirements for the degree of  
Doctor of Philosophy

March 2011

# **Abstract**

## **Molecular correlates of visual system development** **Corey Joseph Flynn, March 2011**

The development of neural systems has been shown to be under the influence of both neural activity and molecular paradigms. In the visual system, many classic studies focused on the impact of activity paradigms on the wiring diagram of the system. In these studies it became clear that altered activity patterns resulted in altered anatomy at the first stages of the visual system. At the level of the retina, the lateral geniculate nucleus (LGN), and primary visual cortex (V1) the basic wiring diagram of the system can be manipulated by alteration of activity levels during development. Specifically, much attention has been focused on the processing of visual information from one eye versus the other in this system known as ocular dominance. Both the physiological and anatomical representations of ocular dominance have been shown to be susceptible to altered activity during development.

Over the last few decades, the study of visual development has begun to draw on the tools of molecular biology as well. It is now clear that molecular paradigms are also at work in neural development. The influences of molecular paradigms on neural development work in tandem with those of activity based paradigms. In the visual system, molecular studies have largely focused on the mechanisms governing patterning of topological projections, areal specification, and plasticity mechanisms. There have been relatively few studies targeted at the molecular characterization of ocular dominance development. The main goal of this dissertation is to implement a strategy for charac-

terizing molecular correlates of visual system development with a focus on the development of ocular dominance.

In order to characterize molecular correlates of ocular dominance in the developing visual system, I first implemented a pair-wise proteomic screen of samples from known anatomical correlates of ocular dominance at the level of the retina, LGN, and V1. From these screens, many potential candidates were identified and some of them were further characterized through immunohistochemical methods. One of these candidates, collapsin response mediator protein 4 (CRMP4) was shown to be a novel and developmentally regulated marker for LGN development. CRMP4 expression is present at the interlaminar zones between eye specific laminae in the developing LGN. Further, expression of CRMP4 is constrained to a short window of development in which the final structure of the LGN is determined. I show that CRMP4 expression tracks the morphology of the interlaminar zones of the LGN both in normal animals and in animals with altered retinogeniculate inputs. This finding leads me to hypothesize that the expression of CRMP4 is linked to the interlaminar zones in during the window of development in which it is expressed. Finally, I suggest that the mechanism of CRMP4 action in the developing LGN may be downstream of myelin associated inhibitor signaling. In this scheme, CRMP4 mediates myelin dependent outgrowth inhibition of retinal ganglion cell afferents at the interlaminar zones and fine tunes the boundaries of eye specific lamina in the developing LGN.

# Acknowledgments

The past six years have been a period of profound personal and intellectual growth in my life. I have never before experienced life so fully. My time at Carnegie Mellon has challenged me in ways that I did not think possible and I have become a much better scientist and person because of it. I try to strive for improvement in all that I do and I truly believe that my peers and mentors have facilitated my improvement at every step along the way. I am appreciative of those that have influenced me throughout my tenure in this program.

First and foremost, I would like to thank my advisor. Justin Crowley took a chance on me. I will be forever indebted to him for seeing a budding systems neuroscientist in a young man more accustomed to boot-wearing biology and observational behavior work. Beyond his patience in teaching new methodology, I would like to thank Justin for teaching me his brand of scientific investigation. Justin introduced a level of rigor and determination into my work that I am not sure I would find in many other laboratories. He also encouraged me to tackle large and complex problems that I, and many others, may otherwise have shied away from. I only hope that I can repay these kindnesses with my future endeavors.

Beyond the influence of Justin, I have been positively impacted by all of those that I have been privileged to share lab space with. In particular, I have benefitted from the feedback of Krishnan Padmanabhan throughout my graduate training. For this I will be forever grateful. I would also like to thank David Whitney and Santosh Chandrasekaran for their contributions and conversations over the years. I have benefitted from the

opportunity to mentor many undergraduate students over the years and I would like to thank them for their dedication, effort, and patience.

I would also like to thank the members of my dissertation committee. Nathan Urban has always been an excellent sounding board for a new perspective on scientific data and many other things in my life. Jon Minden's kindness and patience was one of the major ingredients in whatever successes are to be found in this dissertation. Jon allowed me a great deal of access to his laboratory's staff and resources in order to get my work started at Carnegie Mellon and he has continued to be of great support ever since. Peter Strick has been an incredibly valuable source of input at all of my committee's meeting. He has been able to shape the direction of my work for the better in every conversation that I have had with him.

In addition to those at Carnegie Mellon, I would like to thank the people that brought me to the start of my training here. I have benefitted from outstanding mentors from a very young age and my successes are certainly a result of their efforts as much as my own. I would like to acknowledge the efforts of Thatcher Shug, Mark Evans, Robert Cook, Owen Floody, and Elizabeth Capaldi.

For support outside of my professional life, I would like to thank Gail Siewiorek. Gail has been there to share in all of my successes and failures during graduate school and she has been a source of strength through it all. Gail's family has been especially welcoming during my time in Pittsburgh and I would like to thank them for that.

Last, I would like to acknowledge my family. My parents, Don and Susan Flynn, as well as my brother, Micah Flynn,

have been a constant source of feedback and encouragement throughout my education in the past decade. None of what I have done would be possible without their support. For everything that you have done and continue to do each day, thank you.

# List of Abbreviations

- 2D-DIGE** Two dimensional difference gel electrophoresis  
**A** Lamina A of the lateral geniculate nucleus  
**A1** Lamina A1 of the lateral geniculate nucleus  
**C** Laminae C0-C2 of the lateral geniculate nucleus  
**C4RIP** CRMP4-RhoA inhibitor protein  
**CamK2** Calcium/calmodulin protein kinase 2  
**CaV2.2** N-type presynaptic calcium channel  
**CRMP2** Collapsin response mediator protein 2  
**CRMP4** Collapsin response mediator protein 4  
**E\_** Embryonic day \_  
**GAPDH** Glyceraldehyde 3-phosphate dehydrogenase  
**GSK3 $\beta$**  Glycogen synthase kinase 3 $\beta$   
**IEF** Isoelectric focusing  
**IPL** Inner plexiform layer  
**Isl2** Islet-2  
**LGN** Lateral geniculate nucleus  
**MALDI-TOF MS** Matrix assisted laser desorption/ionization time of flight mass spectrometry  
**MAI** Myelin associated inhibitor  
**NgR** Nogo receptor  
**NSD** No significant difference  
**ODC** Ocular dominance column  
**ONH** Optic nerve head  
**OPL** Outer plexiform layer  
**P\_** Postnatal day \_  
**PGN** Perigeniculate nucleus  
**RGC** Retinal ganglion cell  
**ROCK** Rho kinase

**S1** Primary somatosensory cortex

**TTX** Tetrodotoxin

**V1** Primary visual cortex

**V2** Secondary visual cortex

# Contents

<b>1</b>	<b>Introduction</b>	<b>1</b>
1.1	Visual System . . . . .	3
1.1.1	Anatomy . . . . .	3
1.1.2	Physiology . . . . .	6
1.1.3	Visual Cortical Columns . . . . .	7
1.2	Visual Critical Period . . . . .	9
1.3	Spontaneous Activity in the Visual System . . .	11
1.3.1	Retinal Waves . . . . .	11
1.3.2	Spontaneous Activity in the LGN . . . .	13
1.3.3	Spontaneous Activity in V1 . . . . .	14
1.4	The Retinogeniculate Circuit . . . . .	15
1.4.1	Structure of the Retinogeniculate Circuit	15
1.4.2	Development of the Retinogeniculate Circuit . . . . .	15
1.4.3	The Role of Activity in Retinogeniculate Development . . . . .	17
1.4.4	The Role of Molecular Cues in Retinogeniculate Development . . . . .	19
1.5	The Geniculocortical Circuit . . . . .	20
1.5.1	Structure of the Geniculocortical Circuit	20
1.5.2	Development of the Geniculocortical Circuit . . . . .	22

1.5.3	The Role of Activity in Geniculocortical Development . . . . .	24
1.5.4	The Role of Molecular Cues in Geniculocortical Development . . . . .	25
1.6	Methods for Molecular Characterization of the Visual System . . . . .	26
1.7	Mylenation in the Lateral Geniculate Nucleus .	27
<b>2</b>	<b>A novel tissue sampling strategy for the elucidation of molecular correlates of visual development</b>	<b>29</b>
2.1	Introduction . . . . .	31
2.2	Materials and methods . . . . .	34
2.2.1	General animal procedures . . . . .	34
2.2.2	Optical imaging of intrinsic signal . . . . .	34
2.2.3	Retina tissue sampling . . . . .	35
2.2.4	LGN tissue sampling . . . . .	36
2.2.5	Cortical tissue sampling . . . . .	36
2.2.6	Two dimensional difference gel electrophoresis . . . . .	40
2.2.7	Fluorescence gel imaging and image analysis . . . . .	42
2.2.8	Protein spot isolation and identification .	44
2.2.9	Immunohistochemistry . . . . .	45
2.3	Results . . . . .	46
2.3.1	Retinal molecular correlates of visual development . . . . .	46
2.3.2	LGN molecular correlates of visual development . . . . .	53

2.3.3	Cortical molecular correlates of visual development . . . . .	60
2.4	Conclusions . . . . .	73
2.4.1	Summary of findings . . . . .	73
2.4.2	Pitfalls and limitations . . . . .	74
2.4.3	Discussion . . . . .	76
<b>3</b>	<b>Developmentally regulated expression of collapsin response mediator protein 4 in the interlaminar zones of the lateral geniculate nucleus</b>	<b>79</b>
3.1	Introduction . . . . .	80
3.2	Materials and methods . . . . .	82
3.2.1	Ferret and mouse tissue preparation . . .	82
3.2.2	Macaque tissue preparation . . . . .	83
3.2.3	Immunohistochemistry . . . . .	83
3.2.4	Western Blotting . . . . .	84
3.2.5	Myelin staining . . . . .	84
3.2.6	Image analysis . . . . .	84
3.3	Results . . . . .	86
3.4	Conclusions . . . . .	94
3.4.1	Summary of findings . . . . .	94
3.4.2	Pitfalls and limitations . . . . .	95
3.4.3	Discussion . . . . .	96
<b>4</b>	<b>Expression of collapsin response mediator protein 4 in the presence of altered retinogeniculate input</b>	<b>100</b>
4.1	Introduction . . . . .	101
4.2	Materials and methods . . . . .	103

4.2.1	Tissue preparation . . . . .	103
4.2.2	Monocular and binocular enucleation . .	103
4.2.3	Intravitreal application of epibatidine . .	104
4.2.4	Immunohistochemistry . . . . .	104
4.2.5	Myelin staining . . . . .	104
4.2.6	Image analysis for epibatidine disruption of retinothalamic projections . . . . .	104
4.2.7	Image analysis for laminar expression of CRMP4 and Myelin . . . . .	105
4.3	Results . . . . .	105
4.3.1	Transient epibatidine block of retinal ac- tivity disrupts normal retinal projections, normal cytoarchitecture, and normal CRMP4 expression in the LGN . . . . .	105
4.3.2	Monocular or binocular enucleation at birth abolishes normal development of cytoar- chitecture in the LGN and normal inter- laminar CRMP4 expression . . . . .	115
4.4	Conclusions . . . . .	118
4.4.1	Summary of Findings . . . . .	118
4.4.2	Pitfalls and limitations . . . . .	118
4.4.3	Discussion . . . . .	119
<b>5</b>	<b>General Discussion</b>	<b>122</b>
5.1	Toward a molecular characterization of ocular dominance . . . . .	122
5.2	Molecular development of the LGN . . . . .	127
5.3	Hypothesized roles of CRMP4 during LGN de- velopment . . . . .	129

5.3.1	Hypothesis i: CRMP4 serves as a response factor downstream of myelin signaling and mediates myelin dependent outgrowth inhibition in the cell sparse interlaminar zones.	130
5.3.2	Hypothesis ii: CRMP4 serves as a response factor downstream of semaphorin signaling and mediates growth cone collapse in the cell sparse interlaminar zones.	137
5.3.3	Hypothesis iii: CRMP4 serves to modulate calcium signaling in RGC axon terminals in the cell sparse interlaminar zones	140
5.4	Conclusions . . . . .	142
5.4.1	Specific conclusions . . . . .	142
5.4.2	General conclusions . . . . .	143

## **References** 145

# List of Figures

1.1	Organization of the ferret visual system . . . . .	4
1.2	Laminar boundaries and sub-laminar divisions in the ferret LGN . . . . .	5
1.3	The ocular dominance column map in ferret V1	8
1.4	Illustration of anatomical development in the fer- ret visual system and concordant patterns of spon- taneous activity . . . . .	12
1.5	Development of retinogeniculate projections . .	17
1.6	Schematic diagram of ferret V1 . . . . .	21
2.1	Fluorescent micro-dissection of the LGN for 2D- DIGE. . . . .	37
2.2	Isolation 2D-DIGE samples from functionally de- fined maps of ocular dominance. . . . .	39
2.3	Location of protein candidates found to be dif- ferentially expressed across temporal and nasal retina. . . . .	48
2.4	Functions of protein candidates found to be dif- ferentially expressed across temporal and nasal retina. . . . .	49
2.5	Quantification of munc13-3 expression in the flat mounted retina. . . . .	50
2.6	Munc13-3 expression in retinal cross-sections. .	51

2.7	List of protein candidates found to be differentially expressed across the A and A1 LGN laminae.	56
2.8	Functions of protein candidates found to be differentially expressed across the A and A1 LGN laminae. . . . .	57
2.9	Location of protein candidates found to be differentially expressed across contralateral and ipsilateral ocular dominance columns. . . . .	63
2.10	Functions of protein candidates found to be differentially expressed across contralateral and ipsilateral ocular dominance columns. . . . .	64
2.11	Western blot of ipsilateral and contralateral ocular dominance column CRMP2 expression . . .	65
2.12	Time-course of CRMP2 expression in the visual cortex . . . . .	66
2.13	CRMP2 is expressed near the V1/V2 border in the mature visual cortex . . . . .	67
3.1	Developmentally regulated CRMP4 expression in LGN interlaminar zones of the ferret. . . . .	88
3.2	Expression of CRMP4 protein in the ferret LGN. .	89
3.3	Quantification of developmentally regulated CRMP4 expression in the interlaminar zones of the ferret LGN. . . . .	90
3.4	Developmentally regulated expression of CRMP4 in both the LGN interlaminar zones and within layer ON/OFF boundaries. . . . .	91
3.5	CRMP4 expression in the P14 ferret retina. . .	92
3.6	Myelin expression in the normal ferret LGN. . .	93

4.1	Epibatidine treatment alters the pattern of retinothalamic projections into the LGN. . . . .	109
4.2	Epibatidine treatment does not alter the size or segregation of ipsilateral and contralateral retinothalamic projections to the LGN. . . . .	110
4.3	Epibatidine treatment causes a medial shift in the ipsilateral retinothalamic projection to the LGN. . . . .	111
4.4	Epibatidine treatment abolishes normal LGN cytoarchitecture. . . . .	112
4.5	Epibatidine treatment abolishes CRMP4 expression in the ferret LGN. . . . .	113
4.6	Myelination of normal and epibatidine treated LGNs. . . . .	114
4.7	LGN CRMP4 expression in enucleate ferrets. . .	117
5.1	MAI signaling through CRMP4 and RhoA results in myelin dependent outgrowth inhibition. . .	135
5.2	Development of eye specific segregation, interlaminar zones, myelination, and CRMP4 expression in the normal ferret LGN. . . . .	136

# List of Tables

2.1	List of protein candidates found to be differentially expressed across temporal and nasal retina.	52
2.2	List of retinal protein candidates sub-cellular locations and functions. . . . .	53
2.3	List of protein candidates found to be differentially expressed across the A and A1 LGN laminae.	58
2.4	List of LGN protein candidates sub-cellular locations and functions. . . . .	60
2.5	List of protein candidates found to be differentially expressed across ipsilateral and contralateral ocular dominance columns . . . . .	68
2.6	List of cortical protein candidates sub-cellular locations and functions . . . . .	72

# Chapter 1

## Introduction

The mammalian brain is one of the most complex biological structures known to man and it has been the center of intense study for centuries. A rather striking feature of the brain is just how reliably its gross anatomy is preserved across individuals and generations. The fact that complex neuroanatomy is faithfully preserved in such a manner requires that the mechanisms through which brain structures are created in development and maintained throughout life are rather stereotyped as well. Much work has been done, principally in the last half of the last century, in an attempt delineate the precise mechanisms of neural development. Two general classes of neural development models have emerged from this work. The first class of models for neural development are based on activity dependent mechanisms. Under these models, developing neural systems exhibit a profound period of early and exuberant connectivity. Neurons make many early connections, some of which are ultimately appropriate and are maintained. Other inappropriate connections are pruned away in a period of neuronal refinement that follows initial connection events. Neural connections under these models are either strengthened in the case of appropriate connections or weakened in the case of inap-

ropriate connections through synaptic re-weighting based on activity patterns in the system. Under these models the driving force for proper neural development is patterned activity (LeVay et al., 1978). External and internal environmental influences on the system hold sway and have a dramatic effect on the structure and function of the brain. The systematic replication of gross neuronal structure across individuals is thus explained by stereotyped environmental influences on the developing nervous system. The second class of models for neural development are based on molecular cues. Under these models, there is a molecular blueprint that defines the pattern of neural connections. In stark contrast to activity dependent sorting of neural connections, connections are precise at their onset under these models. Here, the structure of the brain is set forth at the most fundamental level. Genetically encoded molecular cues guide axons and dendrites in the developing nervous system to their appropriate targets and there is little need for large-scale rewiring of the system (Sperry, 1963). Environmental influences on the brain are marginalized to a role in which they only fine tune the structure set forth by genetically encoded molecular cues. The striking reliability of gross neuronal structures is thus explained by a preservation of the genetic material which drives the formation of the brain. One of the first neural systems studied in great detail was the visual system (Hubel, 1982). The visual system of binocular mammals has proven to be of great use in characterizing the contribution of activity and molecular cue dependent aspects of neural development. From these studies, it has become clear that both activity and genetically encoded cues shape the development of the brain. The anatomy of the visual system as well as its developmental progression is very

well characterized. Both the activity paradigms and the basics of molecular patterning at work in the developing visual system are well understood, making it an appropriate setting for the work presented in this dissertation. The bulk of the work presented here was undertaken in the ferret. The visual system of the ferret is particularly useful in that a large portion of visual development occurs postnatally. This fact allows for tractable manipulations of visual development that are not possible in other systems.

## 1.1 Visual System

### 1.1.1 Anatomy

Firing patterns of RGC in the retina encode one of the brain's first internal representations of the external visual world. Temporal RGCs encode responses to visual stimuli in the nasal visual field and nasal RGCs encode responses to stimuli in the temporal visual field (**figure 1.1**). RGC axons exit the eye at the optic nerve head and proceed to the optic chiasm. Axons from nasal RGCs cross the optic chiasm en route to the contralateral LGN and axons from temporal RGCs remain uncrossed en route to the ipsilateral LGN. The ferret LGN is composed of two major retinorecipient laminae, A and A1. There are also three minor retinorecipient layers in the lateral aspect of the nucleus known as C, C1, and C2. They are omitted from the main discussion here as my focus on the LGN is largely about gross structural details. Lamina A receives input from the contralateral eye and lamina A1 receives input from the ipsilateral eye. In the ferret, as well as in many higher mammals,

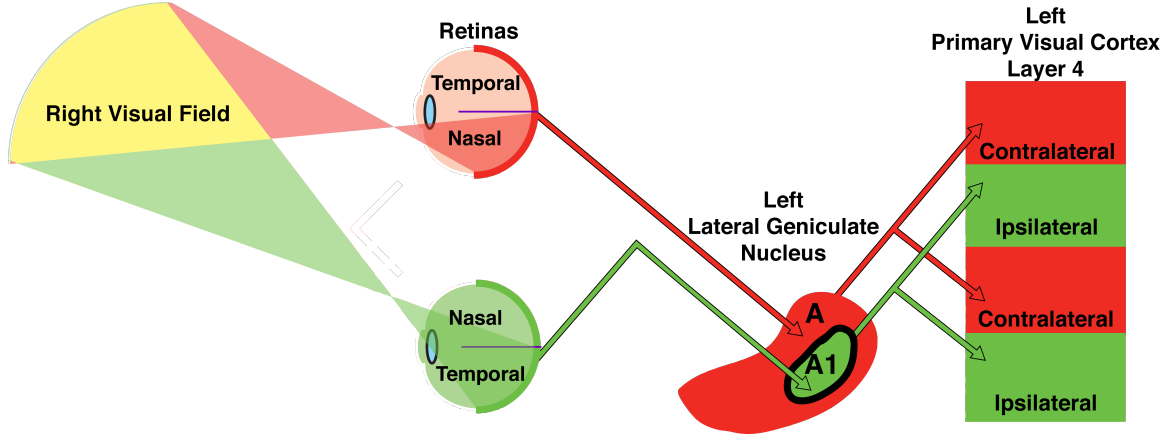


Figure 1.1: Organization of the ferret visual system. The Left side of the visual system is depicted. The right visual field is encoded by the right nasal retina and the left temporal retina. Retinogeniculate afferents from nasal RGCs in the right retina cross the optic chiasm and terminate in the A lamina of the left LGN. Afferents from temporal RGCs in the left retina do not cross the optic chiasm and terminate in the A1 lamina of the LGN. Geniculocortical projections from the A and A1 laminae in the LGN then project to layer 4 of the primary visual cortex (V1). These projections are segregated into non-overlapping patches of cells that respond preferentially to stimuli from either the ipsilateral or contralateral eye depending on the origin of their geniculocortical input. These segregated patches are the anatomical basis for ocular dominance.

the boundaries between these major anatomical divisions in the LGN are cell sparse interlaminar zones (Linden et al., 1981b). Additionally, sublaminar divisions in the ferret LGN between the input of ON and OFF center RGCs to the A and A1 lamina are apparent (see section 1.1.2). The ON/OFF sublaminar boundaries are also characterized by a lower density of cell bodies although not as dramatically as the interlaminar zones between the A and A1 laminae (figure 1.2). Geniculocortical projections from the A and A1 laminae of the retina terminate in layer 4 of primary visual cortex (V1). Geniculocortical projections in to layer 4 of V1 form non-overlapping projections representing contralateral and ipsilateral input from the LGN from lamina A and A1, respectively. As with other binocular

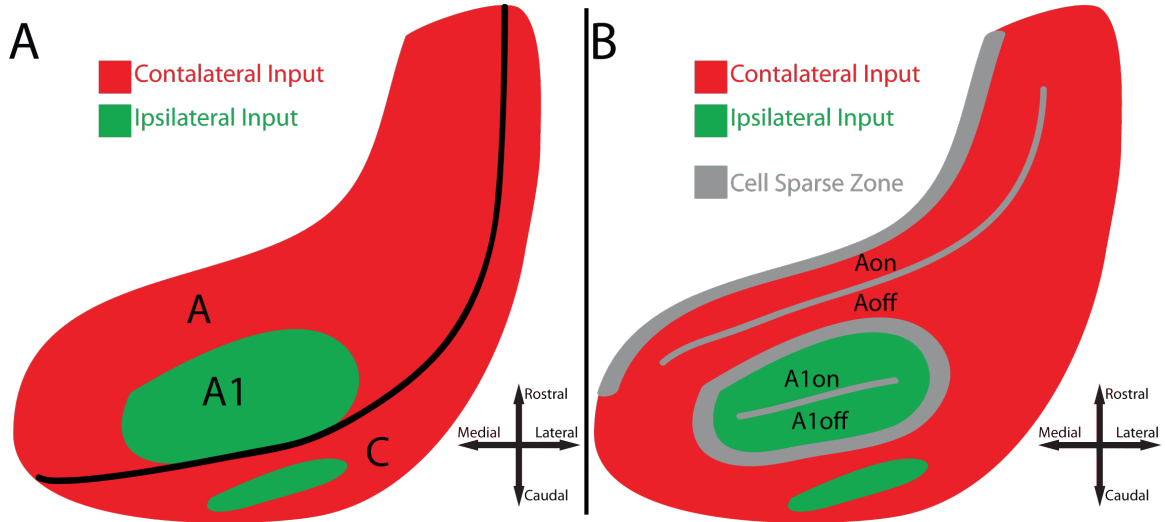


Figure 1.2: Laminar boundaries and sub-laminar divisions in the ferret LGN. Both eyes send input via RGCs into the ferret lateral geniculate nucleus (LGN). Contralateral input to the retina is shown in red and ipsilateral input to lamina A1 is shown in green. A, major divisions of the LGN. The LGN is composed of two major retinorecipient layers, the contralateral A layer and the ipsilateral A1 layer, as well as minor retinorecipient layers collectively depicted here as the C layer. B, laminar boundaries and sublaminar divisions. The medial boundary of the LGN, The A/A1 laminar boundary, and the A1/C laminar boundary are major cell sparse zones. Minor cell sparse zones delineate sub-laminar ON/OFF boundaries within the A and A1 layers.

mammals, this projection pattern forms the anatomical basis for ocular dominance (Hubel and Wiesel, 1962; Hubel and Wiesel, 1969; Hubel and Wiesel, 1972; Hubel and Wiesel, 1998). However, this is not universally the case as rodents lack ocular dominance columns and some new world monkeys show a complete lack of or variable appearance of ocular dominance columns. Additionally, rodents show ocular dominance at a cellular level. The ferret visual system shows classic anatomically and physiologically defined ocular dominance as demonstrated in the cat and macaque and as such the insight gained from these models is applicable here.

### 1.1.2 Physiology

In the retina, visually driven responses of RGCs can be separated into two classes, ON and OFF. For all RGCs, the receptive field is circular and is composed of center and surround. ON RGCs respond well to a light presented in the center of their receptive field and decrease in response magnitude when a light is presented in their surround. OFF RGCs respond in the opposite fashion; light presented to their receptive field's surround increases their response, light presented to their receptive field's center decreases their response. In the ferret LGN, the same receptive field properties are maintained in geniculate relay neurons. Responses driven through ON and OFF RGC input to the LGN are organized into ON and OFF sub-laminar regions in both the A and A1 laminae (Figure 1.2 and Section 1.1.1)(Stryker and Zahs, 1983). LGN cells responding to ipsilateral and contralateral inputs are also segregated in the LGN lamina (see Section 1.1.1). In layer IV of the primary visual cortex, receptive fields of neurons receiving direct input from the LGN become elongated in form are optimally driven by stimuli that are linear and oriented at a specific angle (Hubel and Wiesel, 1962). These receptive fields are the product of convergence by collinear LGN receptive fields onto a target layer IV neuron (Chapman et al., 1991). Additionally, layer IV cells in primary visual cortex begin to integrate synaptic input from both ipsilateral and contralateral inputs. This integration leads to physiologically defined ocular dominance in which some cells respond preferentially to ipsilateral stimuli, some to contralateral stimuli, and some to both. Depending on the species of binocular mammal, the ratio of cells driven

by stimulation of ipsilateral, contralateral, or both eyes varies. In many large binocular mammals, groups of cells sharing similar eye-specificity are arranged in periodic and interdigitated columns oriented orthogonal to the pial surface (Figure 1.3). Physiological grouping of cells in this manner is observed as a result of segregated, eye specific, and spatially periodic input to the cortex from LGN thalamocortical projections (see Section 1.1.1).

### 1.1.3 Visual Cortical Columns

The visual cortex represents many features of visual stimuli using columnar systems. The entire collection of a columnar system for a particular stimulus feature is referred to as a map of that feature (see Figure 1.3 for an example of one such map). Some of these maps such as the map of retinotopy vary continuously across the cortex (Van Essen et al., 1984), while others such as ocular dominance are spatially periodic (Hubel and Wiesel, 1968). Other classes of maps such as that of orientation are both periodic (single orientations are separated by others in the map) and continuous (the progression from one orientation through all other back to the original is smoothly mapped)(Hubel and Wiesel, 1974; Bonhoeffer and Grinvald, 1991). Maps in both V1 and secondary visual cortex (V2) share these basic properties. Ocular dominance columns are a feature of the visual system of many higher mammals. Rodents show ocular dominance at the cellular level, but they lack the columnar organization seen in animals such as the macaque, cat and ferret. Instead, the visual system of rodents is organized into a binocular response zone inside of a larger contralateral response

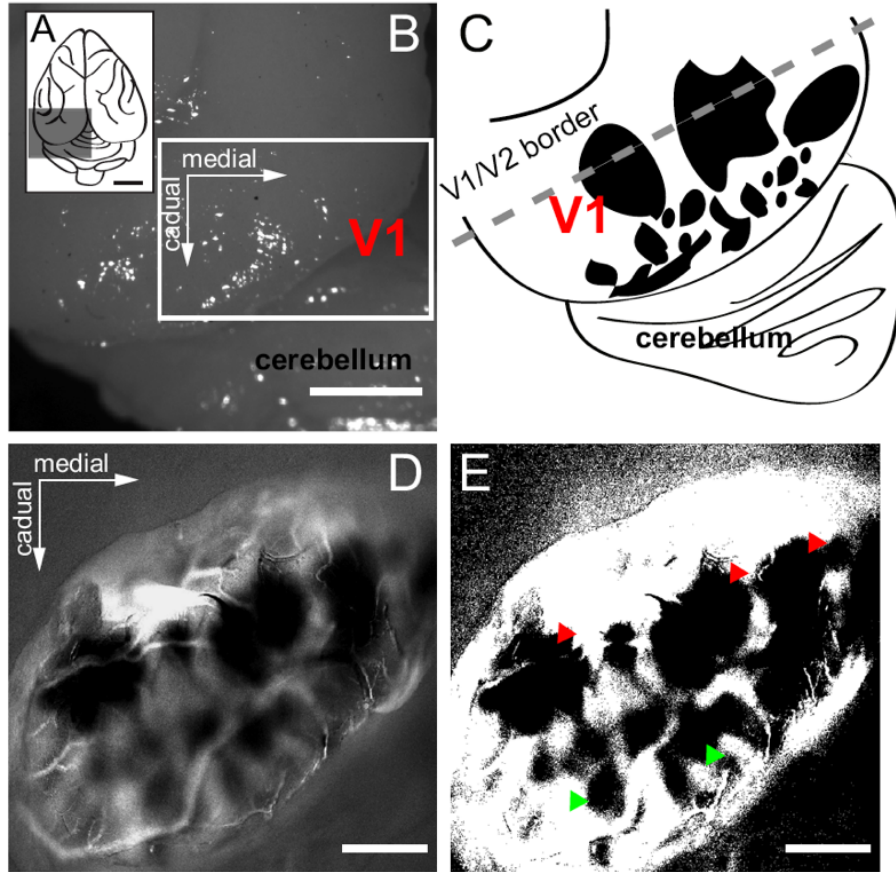


Figure 1.3: The ocular dominance column map in ferret V1. (A-B) Dorsal surface of the ferret cortex (A) Illustration of the ferret cortex with the caudal pole highlighted. (B) V1 is located on the dorsal ridge of the caudal most part of the ferret's cortex. Scale bar=0.2 cm. (C) An illustration of the map of ocular dominance in the ferret with projections from one eye represented in black and the V1/V2 border represented as a gray line. (D) Intrinsic signal optical image of eye specific responses in V1. Black patches correspond to responses from one eye while lighter patches correspond to responses from the other eye. Scale bar = 1mm. (E) Thresholded image of (B1) illustrates the unique organizational pattern of the ocular dominance column map in the ferret. Large blobs are located at the V1/V2 border (red arrows) and smaller columns are located at caudal pole (green arrows). Scale bar = 1 mm. Figure courtesy of K. Padmanabhan.

zone (Hubener, 2003). Single unit recording studies in higher mammals have shown that cells in V1 are arranged into spatially periodic ocular dominance columns in higher mammals (Hubel and Wiesel, 1962; Hubel and Wiesel, 1977). The size

of ODCs varies roughly with the size of the animal in which they are studied. Ferret ODCs are on the order of 200-400m (Issa et al., 1999), whereas macaque ODCs vary between 500-800m (Hubel and Wiesel, 1969). Within a given species, the statistics of ODC size can vary from individual to individual but genetically similar animals (litter-mates for example) tend to share similar ODC sizes and distributions (Kaschube et al., 2002; Kaschube et al., 2003). Column size and shape were traditionally thought to be relatively stable throughout development, but recent evidence suggests that columns may change in their geometric properties throughout development (Kaschube et al., 2009).

## 1.2 Visual Critical Period

In neuronal systems, critical periods are epochs of development in which circuits are maximally sensitive to changes in the pattern of neuronal activity (Hubel and Wiesel, 1962, 1970; Hubel et al., 1977). Changes in the activity pattern of circuits during the critical period lead to sculpting of the circuit. In the visual system, there are two identifiable critical periods. The first is the critical period for proper eye specific segregation and laminar targeting in the retinogeniculate circuit. In the ferret, this period extends from birth to P25 and corresponds roughly to the period of time in which the retina is known to exhibit spontaneous activity in the form of retinal waves (see section 1.3.1) (Penn et al., 1998b; Penn and Shatz, 1999; Stellwagen and Shatz, 2002). The retinogeniculate critical takes place before eye opening and thus is driven by endogenous activity patterns. Activity in the retina during this developmental epoch can be

thought of as instructing the proper segregation and laminar targeting of RGCs in the LGN (Huberman et al., 2008). This idea is important for the work that I present in chapter 4 because I employ an established method for manipulation of retinal activity from P0-P10 in order to alter the normal projection and lamination patterns of RGC afferents in the LGN (Huberman et al., 2002). The second critical period in the visual system is the geniculocortical critical period for ocular dominance plasticity in which the response of neurons in V1 can be shaped by the modification of external stimuli. The geniculocortical critical period for ocular dominance plasticity in the ferret begins at P35 and ends at P70-80 (Issa et al., 1999). Unlike the retinogeniculate critical period, the geniculocortical critical period for ocular dominance plasticity occurs after eye opening. Importantly, this means that the major source of activity in the system during this developmental phases is non-endogenous and that the geniculocortical critical period occurs after the initial formation of ocular dominance columns (Hubel and Wiesel, 1962; Hubel and Wiesel, 1963; Issa et al., 1999; Crowley and Katz, 2000). This critical period can thus be thought of as a period of time in which the visual system is capable of sculpting its existing architecture to fit the constraints placed upon it by the specific anatomy of the animal and the environment in which the animal lives. Deprivation of one eye from external stimulation during this critical period results in a shift of responses in V1 neurons toward the non-deprived eye as well as a reduction in the size of deprived eye ocular dominance columns. This process is mediated by a retraction of geniculocortical axons from the deprived eye and an elaboration of those from the non-deprived eye (Hubel et al., 1977; LeVay et al., 1980).

Geniculocortical critical periods for ocular dominance plasticity have been identified in many mammalian species including the cat (Wiesel and Hubel, 1963; Hubel and Wiesel, 1970), primate (Hubel et al., 1977; Horton and Hocking, 1997), and the ferret (Issa et al., 1999). The opening at of this critical period in the ferret at P35 directly follows eye opening at P30-35. In the work presented here, I perform the imaging experiments described in chapter 2 during the geniculocortical critical period in an attempt to characterize the molecular profile of visual cortex during this developmentally relevant epoch.

## 1.3 Spontaneous Activity in the Visual System

Spontaneous activity during the development of the visual system is observed at the level of the retina, the LGN and V1. All of these sources of spontaneous activity occur at different points during development, but they all occur before the onset of externally driven activity in the system and are correlated with the maturation of normal anatomy throughout the system (figure 1.4). In all discussion below, the timing of spontaneous activity is reported for the ferret.

### 1.3.1 Retinal Waves

At birth, endogenous activity in the retina takes the form of traveling waves of cholinergic activity initiated in starburst amacrine cells (Feller et al., 1996; Penn et al., 1998b; Feller, 1999). This pattern of activity persists in the retina for the first two weeks of postnatal life (figure 1.4). These traveling waves are composed of bursting patterns that last from 1 to 8 seconds

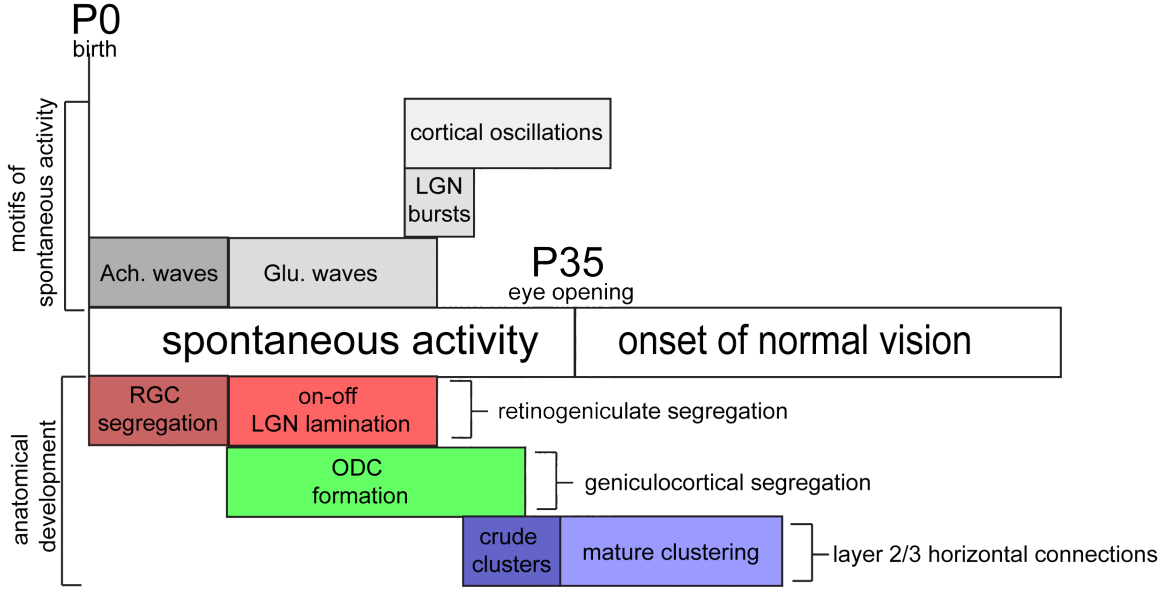


Figure 1.4: Illustration of anatomical development in the ferret visual system and concordant patterns of spontaneous activity. (Adapted from Issa, Trachtenberg, et al 1999). Timeline begins at P0 with birth. Between P0 and P25, retinal waves dominate as the principle type of spontaneous activity (reviewed by, Wong 1999, Huberman, Feller, et al, 2008). In the third postnatal week of life LGN bursts have been identified (Weliky and Katz, 1999). During the same time, cortical oscillations have been recorded (Chiu and Weliky, 2002). During the period of spontaneous activity, the retinogeniculate circuit (red), the geniculocortical circuit (green) and the corticocortical connections (blue) in V1 are undergoing maturation. Figure courtesy of K. Padmanabhan.

and occur from 30 to 60 times per hour (Wong et al., 1993). cholinergic retinal waves appear to be involved in the proper segregation of and laminar targeting of eye specific inputs into the LGN. Disrupting these waves dramatically impacts both the initial and final projection scheme of the RGC afferents in the LGN (Huberman et al., 2002) During the second week of postnatal life, a second kind of retinal wave is observed. The second class of retinal wave are mediated by glutamate transmission, begin at P10, and last at least as long as P25 (Wong and Oakley, 1996; Stacy and Wong, 2003; Kerschensteiner and Wong, 2008). Glutamate mediated retinal waves manifest themselves

differently across the ON and OFF populations of RGCs. The ON RGCs are relatively less active than the OFF centered cells as measured by burst frequency. The ON cells fire 50 burst per hour where the OFF cells may reach activity levels of up to 250 bursts per hour (Wong and Oakley, 1996; Kerschensteiner and Wong, 2008). Glutamate mediated retinal waves are necessary for both the maintenance of eye specific segregation and the formation of ON/OFF sublaminar boundaries in the LGN.

### 1.3.2 Spontaneous Activity in the LGN

Prior to eye opening in the ferret, the LGN exhibits spontaneous activity in the form of bursting activity that propagate across the nucleus (figure 1.4). These waves of activity, known as spindle waves, tend to propagate from the along the dorsal ventral axis of the nucleus (Bal et al., 1995; Kim et al., 1995; McCormick et al., 1995). Spindle waves in the LGN are well correlated within laminae (A, A1, C), but not across laminae (Weliky and Katz, 1999). Retinal and cortical inputs to the LGN appear to play a large role in shaping LGN bursting activity prior to eye opening. When the eyes are removed, the LGN continues to burst but there is a much lower correlation within each lamina in the bursting pattern observed (Weliky and Katz, 1999). If V1 is removed, the bursting activity in the LGN stops entirely, suggesting that the geniculocortical and corticogeniculate circuits are required for the maintenance of LGN bursting (Weliky and Katz, 1999). The loss of LGN bursting in the absence of V1 is most likely due to both severing of geniculocortical afferents and the loss of corticogeniculate feedback to the LGN (Blumenfeld and McCormick, 2000). LGN bursting appears to

have an influence on the development of geniculocortical projections in V1. When the LGN is prevented from bursting using an infusion of TTX for activity block in the kitten, The spatial spread of individual LGN afferents in V1 is greater. This increased projection is either a spread in the normal projection or a failure to prune aberrant connections (Catalano and Shatz, 1998).

### 1.3.3 Spontaneous Activity in V1

In V1, spontaneous activity takes the form of oscillations that are distributed across the cortical sheet from P24 to P29 (figure 1.4). These oscillations appear to be most well correlated across spatial scales of around 800m, suggesting a relationship with the geometry of ocular dominance columns. In fact, there is a high correlation of spontaneous activity between sites in the cortex with the same ocular preference (Chiu and Weliky, 2001). However, the periodic pattern cannot be completely explained by a correlation with the underlying geometry of ocular dominance columns. The correlation of spontaneous activity across V1 is instead better thought of as a function of both ocular dominance and orientation preference (Chiu and Weliky, 2001; Chiu and Weliky, 2002). The degree to which spontaneous activity in V1 may be shaping the anatomy of V1 connections is unclear. It is unlikely that spontaneous activity instructs the formation of ocular dominance columns because geniculocortical afferents are already in place before the onset of spontaneous activity in V1 (Crowley and Katz, 2000). However, the development of orientation preference may be a different story. It is thought that orientation preference is shaped by the development of horizon-

tal projections in layer 2/3 (Ruthazer and Stryker, 1996; Bosking et al., 1997). At the onset of spontaneous activity in V1, layer 2/3 neurons are migrating into place and the structure of horizontal connections between different locations in layer 2/3 are crude at best (Jackson et al., 1989; Ruthazer and Stryker, 1996). It is therefore possible that spontaneous activity in V1 serves to guide the development of orientation tuning and layer 2/3 horizontal projections before the onset of vision.

## 1.4 The Retinogeniculate Circuit

### 1.4.1 Structure of the Retinogeniculate Circuit

The projection pattern of RGCs into the LGN define the different lamina in the LGN. The major projection into the LGN from the contralateral eye defines the A lamina, the major projection of the ipsilateral eye defines the A1 layer, and the minor projections of the eyes define the C0, C1, and C2 layers (Linden et al., 1981a)(figure 1.2). The A and A1 laminae are further divided into ON and OFF sublaminar regions into which ON and OFF center RGCs project, respectively.

### 1.4.2 Development of the Retinogeniculate Circuit

The stereotyped morphology of the retinogeniculate circuit is not present and early stages of visual development. The final structure of the circuit is instead gradually refined during early development (Huberman et al., 2008). In the ferret, initial projections into the LGN arrive from the contralateral retina and diffusely spread throughout the nucleus. Shortly after contralateral projections arrive, projections from the ipsilateral retina

innervate the nucleus and also spread over a large portion of the nucleus. The resulting pattern is one of heavy overlap between the contralateral and ipsilateral projections into the nucleus at birth. Over the course of the next ten days, the projections of the two eyes selectively prune back into their final eye specific laminae (Linden et al., 1981b; Cucchiaro and Guillory, 1984)(figure 1.5a). During the first period of overlap, the afferents from the two eyes form functional synapses which are capable of driving LGN activity of cells located in the both nascent A and A1 laminae (Shatz and Kirkwood, 1984). Inappropriate synapses are eliminated through a competition dependent process. Eliminating competition between the two eyes through either binocular enucleation or treatment with TTX results in a mature nucleus that lacks segregation of retinal inputs. (Sretavan and Shatz, 1986; Shatz and Stryker, 1988). During the same developmental epoch, the cytoarchitecture of the mature LGN is beginning to develop. At birth, the cell sparse interlaminar zones that are the hallmark of LGN laminae in the adult nucleus are not present. Over the course of the first two postnatal weeks, cell sparse interlaminar zones begin to develop at the PGN/A, A/A1, and A1/C boundaries. After the fourth postnatal week, the cell sparse interlaminar zones are in their adult form(Linden et al., 1981a). Additionally, the A and A1 laminae are divided by minor cell sparse regions into ON and OFF leaflets (Stryker and Zahs, 1983; Zahs and Stryker, 1988; Cramer and Sur, 1997)(figure 1.5b).

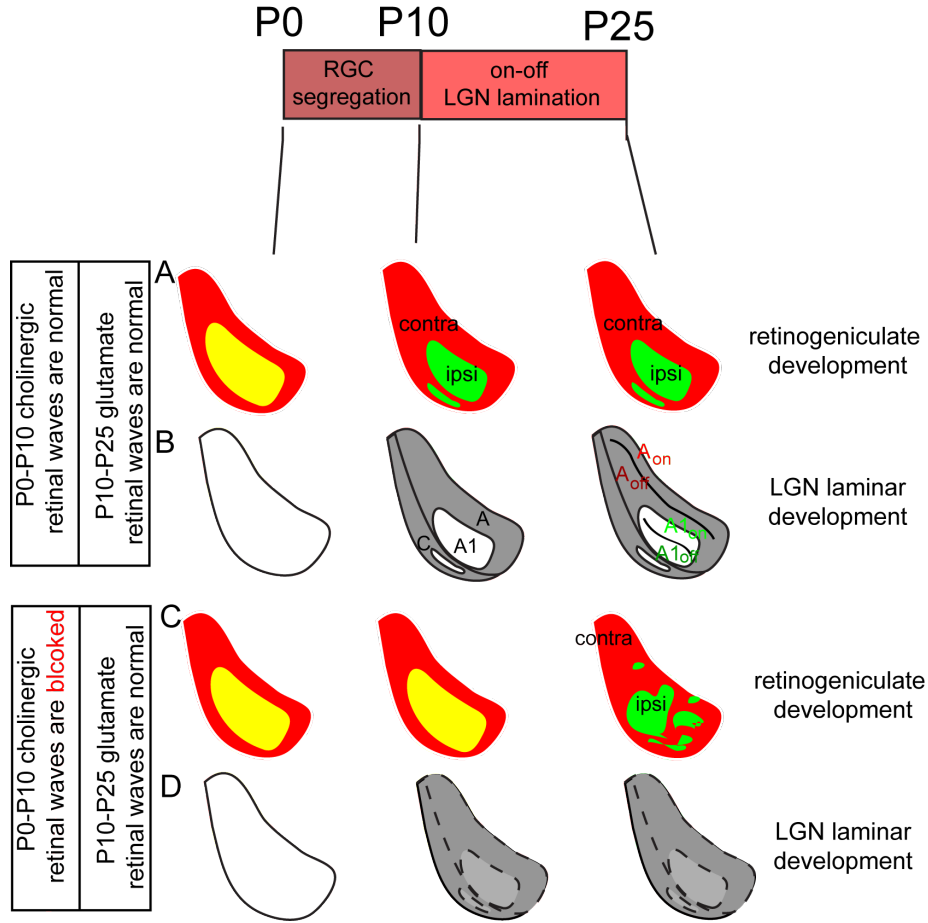


Figure 1.5: Development of retinogeniculate projections. Development of retinogeniculate projections (A) The developmental segregation of retinogeniculate projections between P0 and P25. (B) Laminar maturation of the LGN between P0 and P25. (C) The developmental segregation of retinogeniculate projections between P0 and P25 when cholinergic retinal waves are blocked between P0 and P10 and glutamate waves are normal between P10 and P25. (D) Laminar maturation of the LGN between P0 and P25 when cholinergic retinal waves are blocked between P0 and P10 and glutamate waves are normal between P10 and P25. Figure courtesy of K. Padmanabhan.

### 1.4.3 The Role of Activity in Retinogeniculate Development

The proper development of the retinogeniculate projection is dependent on the influence of endogenous retinal activity in the form of retinal waves (see section 1.3.1). If cholinergic retinal waves are disrupted during the first ten days of life with either the cholinergic antagonist epibatididine (Penn et al., 1998a;

Huberman et al., 2002; Huberman et al., 2003) or the sodium channel blocker TTX (Shatz and Stryker, 1988), the initial overlap of retinal projections observed at birth is preserved (figure 1.5c). If only one of the eyes is subjected to disruption of retinal waves, segregation does occur. Unlike in the normal animal, the projection territory of the manipulated eye in both LGN is much reduced (Penn et al., 1998a). This result frames the segregation of eye specific projections in the LGN as an activity dependent process. Further evidence of implicating eye specific segregation as an activity dependent process is found when the activity of one eye is artificially increased through the application of the cAMP agonist forskolin. When treated with forskolin, the projections of the treated eye expand relative to their normal territory (Stellwagen et al., 1999; Stellwagen and Shatz, 2002). Even though eye specific segregation is not observed at P10 after blockade of cholinergic retinal waves in the ferret, if the animal is allowed to recover until P25 (Huberman et al., 2002) or later (P30, see chapter 4), eye specific segregation does occur. However, the normal pattern of projections is disrupted and normal LGN laminae do not develop (Huberman et al., 2002, chapter 4, figure 1.5c and d). Under this scheme, cholinergic retinal waves are disrupted until P10, but glutamatergic retinal waves remain normal from P10 to P25. Glutamatergic retinal waves are thus sufficient to drive eye specific segregation, but not normal formation of LGN laminae. This observation allows the two processes to be studied independently if cholinergic retinal waves are disrupted until P10. I make use of this manipulation in chapter 4 to characterize the relationship of a novel molecular marker for LGN development,

collapsin response mediator protein 4 (CRMP4), to eye specific segregation and laminar development in the LGN.

#### **1.4.4 The Role of Molecular Cues in Retinogeniculate Development**

At the level of the optic chiasm, molecular cues play a large role in the proper targeting of retinal afferents to either the ipsilateral or contralateral LGN. ventrot temporal RGCs normally project to the ipsilateral LGN and dorsomedial RGCs normally project to the contralateral LGN. When deficient in key molecular cues, this normal projection scheme of retinal afferents is altered. Contralateral projecting RGCs normally express the transcription factor Islet-2 (Isl2), but when Isl2 expression is knocked out in the mouse, there is a significantly larger ipsilateral projection (Pak et al., 2004). Conversely, defects in the expression of the transcription factor Zic2 or cell surface receptors such as EphBs result in a significantly larger contralateral projection (Williams et al., 2003; Pak et al., 2004). Additionally regulation of these markers occurs through the action of other transcription factors. Foxd1 expression is in the ventromedial retina and is linked to ipsilateral afferent targeting (Herrera et al., 2004). Contralateral targeting programs are driven by the expression of Foxg1(Tian et al., 2008). Once in the LGN, the elaboration of retinal afferents into the appropriate topographic and eye specific target regions has also been shown to be under the control of molecular cues. Targeting of RGC afferents is guided by matching the expression of various Eph cell surface receptors to gradients of the ligands, the Ephrins, in the LGN (Flanagan and Vanderhaeghen, 1998; Frisen et al., 1998;

Huberman et al., 2005; Pfeiffenberger et al., 2005). Additional guidance of topographic projection is driven by cues such as Ten-m3(Leamey et al., 2007). Further evidence that retinogeniculate circuit patterning is subject to molecular influences comes from the study of the A2/A3/A5 triple knockout of the Ephrin A family in the mouse. In this line, the mapping of visual space along the azimuth is completely abolished (Cang et al., 2005; Cang et al., 2008b; Cang et al., 2008a) and the pattern of eye specific projections resembles that of the LGN after blockade of cholinergic retinal waves.

## 1.5 The Geniculocortical Circuit

### 1.5.1 Structure of the Geniculocortical Circuit

In most mammalian species, geniculocortical afferents from eye specific laminae in the LGN terminate into layer 4 of the cortical sheet in a periodic fashion. This periodic eriodic termination pattern of geniculocortical afferents into visual cortex is the anatomical basis of ocular dominance columns (Hubel and Wiesel, 1969; Hubel and Wiesel, 1972). In the ferret, the organization of eye specific terminations into visual cortex form ocular dominance columns, but the organization of ocular dominance columns is unique among mammals (Redies et al., 1990; White et al., 1999b). The termination pattern of geniculocortical afferents in the visual cortex of the ferret is composed of three distinct domains (figure 1.6). The first domain receives input from the most caudal binocular portion of the LGN and is the rostral most termination site of LGN afferents (blue area iii, figure 1.6). Lamina A of the LGN innervates contralat-

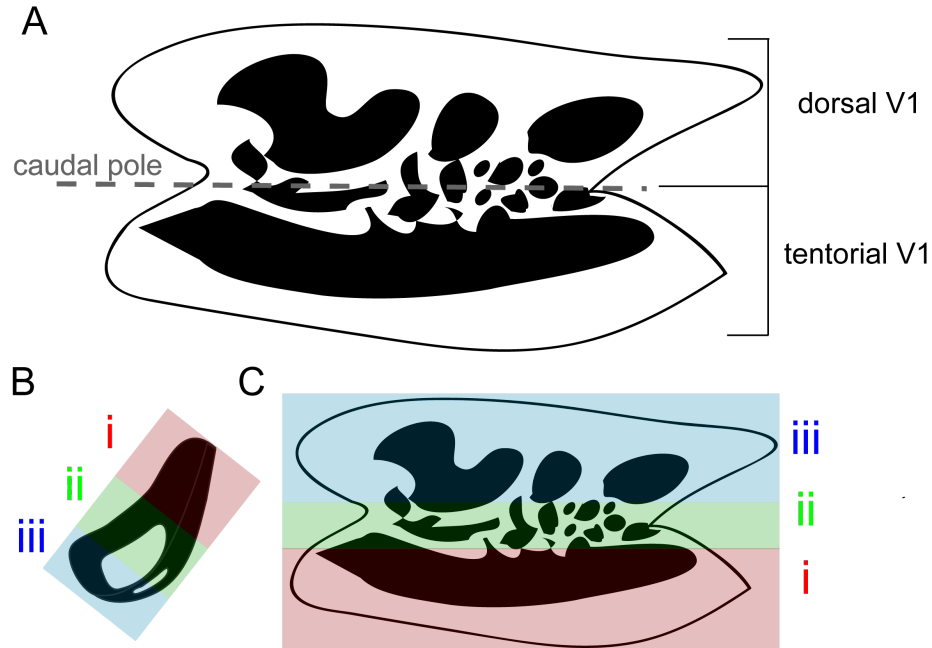


Figure 1.6: Schematic diagram of ferret V1. (A) Schematic of a surface reconstruction of ferret V1 with the ocular dominance column termination pattern illustrated. The caudal pole is identified with a gray dashed line. The dorsal surface of V1 is composed of regular ocular dominance columns and the V1/V2 border columns. The tentorial (ventral part of cortex that begins at the caudal pole) surface is composed of regular ocular dominance columns and a continuous projection from the lamina A. Contralateral ocular dominance columns from lamina A are illustrated in black. The interleaving white domains correspond to ipsilateral ocular dominance columns from lamina A1. (B) Schematic of the LGN and the (C) cortex as in A. Three different regions of the LGN geniculocortical axons project to the three regions of V1. (red) Region i from the rostral lamina A in the LGN forms the geniculocortical projection to the continuous contralateral projection on the tentorial surface. (green) Region ii from the binocular LGN sends projections from both lamina A (black) and lamina A1 (white) to the tentorial surface and the dorsal surface of V1. (blue) Region iii from the binocular LGN sends projections from both lamina A (black) and lamina A1 (white) to the dorsal surface of V1 to form the large ocular dominance that compose the V1/V2 border. Figure courtesy of K. Padmanabhan.

eral columns and lamina A1 of the LGN innervates ipsilateral columns. This domain is composed of both V1 and V2 ocular dominance columns and columns here can be as large as 1mm. The cytoarchitectural makeup of this area is homogenous and lacks defined boundaries between V1 and V2 as is observed in

the cat and primates (Rockland, 1985; Law et al., 1988). As a consequence, the only reliable way to define the V1/V2 border in the ferret is through physiological mapping of visual space (White et al., 1999, but also see section 2.3.3). The second geniculocortical projection domain in the ferret visual cortex receives input from the central binocular portion of the LGN and is located at the caudal pole of the visual cortex (green area ii, figure 1.6). Similar to the first domain, contralateral columns are innervated by projections from lamina A of the LGN and ipsilateral columns are innervated by afferents from lamina A1. Ocular dominance columns in this region are definitively part of V1 and are 400m in size. These columns are similar in size and shape to those found in the cat. The third domain receives input from the rostral most portion of the LGN and is located on the tentorial (ventral) surface of the cortex after it has wrapped around the caudal pole (area i, figure 1.6). This area receives monocular input from the contralateral eye at the extreme peripheral visual field. Consequently, projections from the LGN in this area form a continuous band (Redies et al., 1990). Along with the first two projection domains, this domain completes the full map of direct retina to LGN to Visual cortex projections.

### 1.5.2 Development of the Geniculocortical Circuit

Our most current model of geniculocortical circuit development is composed of discrete steps; migration of geniculocortical axons to the subplate of the developing cortex, synapse formation in the subplate, and finally migration into and synapse formation with layer 4 of V1. Initially, geniculocortical axons in the

ferret migrate to the subplate between embryonic day 30 (E30) and E35, some 10-14 days before birth (Herrmann et al., 1994). Once in the subplate, the growth of geniculocortical axons is temporarily arrested and synapses are formed with the cortical subplate (Shatz and Luskin, 1986; Ghosh and Shatz, 1992a, b). The pattern of these synapses is thought to direct the future formation of geniculocortical afferents into ocular dominance columns. If the subplate is destroyed using an immunotoxin a number of cortical defects result, including the failure of ocular dominance column development (Kanold et al., 2003). While geniculocortical axons are in the subplate, layer 4 neurons in the ferret cortex differentiate migrate into place (Jackson et al., 1989). Once layer 4 is in place, geniculocortical axons leave the subplate and innervate layer 4 in segregated patches that form the anatomical basis for ocular dominance columns (Herrmann et al., 1994; Crowley and Katz, 2000). These patches are visible through direct visualization of geniculocortical afferents in the cortex as early as P16, a few days after the first arrival of geniculocortical afferents in layer 4 (Crowley and Katz, 2000). The early segregation of these afferents in layer 4 of ferret V1 called into question previous reports that the initial projection pattern of geniculocortical afferents was highly overlapping and ocular dominance columns were formed by selective pruning driven by hebbian mechanims under visual experience (LeVay et al., 1978). The work of Crowley and Katz instead argued that the initial establishment geniculocortical synapses in layer 4 laid that foundation for the spatially periodic ocular dominance structures observed in adult animals. They further hypothesized that the patterning and maintenance of these con-

nections was likely to have a molecular or genetic component (Crowley and Katz, 2000, 2002; Katz and Crowley, 2002).

### 1.5.3 The Role of Activity in Geniculocortical Development

The work of Crowley and Katz suggests that the initial formation of ocular dominance columns is relatively independent of activity and proceeds the visual critical period for ocular dominance plasticity in which retinal activity holds sway over the anatomy and physiology of ocular dominance columns (Crowley and Katz, 2002). Many studies have been done that implicate retinal activity in the refinement of ocular dominance in the primate (Hubel et al., 1977; LeVay et al., 1980) and lower mammals such as the cat (Stryker, 1978; Stryker and Harris, 1986; Antonini and Stryker, 1993, 1996; Antonini et al., 1998). However, these studies were carried out after the initial establishment of ocular dominance columns and as such can only speak to the role of activity in the maintenance of ocular dominance columns and not their establishment (Horton and Hocking, 1996, 1997; Crowley and Katz, 2002). The establishment of ocular dominance columns appears to be highly resistant to alterations of retinal activity and form in the absence of visually driven activity in the retina. Adult-like ocular dominance columns in the macaque are well formed at birth (Horton and Hocking, 1996) and the same is seen in the developing ferret before the onset of vision (Crowley and Katz, 2000). Nascent ocular dominance columns are even observed in the ferret when the eyes are removed at birth even though these animals have undergone a dramatic manipulation to their visual system (Crowley and Katz, 1999). Further studies have

shown that the formation of geniculocortical afferents into ocular dominance columns is unchanged in ferrets treated with epibatidine from P0-P10. Blockade of retinal waves using epibatidine (see section 1.4.3) in this developmental period results in a scrambled retinal projection to the LGN. Despite abnormal (and sometimes binocular) retinal input LGN afferents still form the remnants of the A and A1 laminae still project to layer 4 of V1 in a segregated and spatially periodic fashion (Padmanabhan, 2008). These results point to a strong molecular component to the establishment of ocular dominance columns.

#### **1.5.4 The Role of Molecular Cues in Geniculocortical Development**

The initial parcellation of the cerebral cortex into different cortical areas is known to be under the control of a wide variety of molecular players including the transcription factors Emx2, Pax6 (Bishop et al., 2000; Bishop et al., 2002; Bishop et al., 2003). These transcription factors drive the expression of a wide array of other transcription factors, cell adhesion molecule, and axon guidance molecules implicated in areal specification of the cortex (Bulfone et al., 1999; Miyashita-Lin et al., 1999; Rubenstein et al., 1999). More specifically, it is known that the different layers of the ferret visual cortex exhibit a distinct molecular profile (Krishna et al., 2009; Rowell et al., 2010). However, all of appear to be at work during the initial formation of the cortex and may have little to do with the specific patterning of the geniculocortical circuit. There is a relative lack of evidence to date of molecular cues exerting a direct patterning force on the geniculocortical projection, but there are a few examples. One

of the best characterized molecular patterning forces at work during geniculocortical development is the graded expression of ephrins in the cortex. The proper formation of retinotopy in the visual cortex is known to be influenced by gradients of ephrin expression (Frisen et al., 1998; Dufour et al., 2003; Vanderhaeghen and Polleux, 2004; Cang et al., 2005; Ellsworth et al., 2005; Vanderhaeghen, 2007; Cang et al., 2008a). Other molecular players have been implicated in maintenance and plasticity of the geniculocortical circuit during the critical period. These molecules include MHC1 (Huh et al., 2000), trkB (Cabelli et al., 1997), and BDNF (Cabelli et al., 1995; Huang et al., 1999; Lein et al., 2000; Lein and Shatz, 2000). In chapter 2, I present a novel tissue sampling strategy for the identification of more molecular candidates that may be playing a role in either the establishment or maintenance of the geniculocortical circuit.

## 1.6 Methods for Molecular Characterization of the Visual System

An array of techniques have been applied the characterization of molecular mechanisms that may be active in the developing visual system. A pioneering study by corriveau et al in made use of differential mRNA display in order to identify novel players in visual system plasticity (Corriveau et al., 1998). In this study, tissue from tetrodotoxin (TTX) treated and LGN and control LGN were successfully compared for differences in mRNA levels and a novel player in visual system plasticity, MHC1, was identified (Corriveau et al., 1998; Huh et al., 2000; Goddard et al., 2007). In another series of studies, two dimensional difference gel electrophoresis (2D-DIGE)(Unlu et al., 1997) was success-

fully applied to the study of developing visual cortex (Van den Bergh et al., 2003; Van den Bergh et al., 2006a; Jacobs et al., 2008). DNA microarrays and RT-PCR have also been applied to the study of the molecular impact of altered neural activity and normal development in the visual cortex with excellent results (Tropea et al., 2006; Lyckman et al., 2008; Tropea et al., 2009). It has also been demonstrated that similar techniques are very effective in characterizing the molecular profile of the LGN specifically (Horng et al., 2009). All of these methods are targeted at characterizing molecular phenomena that either drive development or plasticity in the visual system at the level of the LGN or cortex, but they do not address the issue of molecular contribution to eye specific circuit development. In order to elucidate the molecular mechanisms that may be at work during eye specific circuit development, Kawasaki et al performed fluorescent guided micro-dissection of the A and A1 laminae of the LGN and compared them using a custom DNA microarray (Kawasaki, 2004). Using this approach, the authors were able to identify molecular markers that distinguished the A and A1 laminae from the C laminae and others that defined the LGN as a whole. In chapter 2, I use a similar method to characterize the proteomic differences between the A and A1 laminae.

## 1.7 Mylenation in the Lateral Geniculate Nucleus

In humans and monkeys, the interlaminar zones of the LGN appear to be more heavily myelinated than the main layers of the LGN (Snider and Lee, 1961; Woolsey et al., 2003). The boundaries between eye specific laminae in the LGN of these

species can easily be visualized with standard myelin stains. In chapter 3 and 4, I show that a similar pattern is observed in the ferret. In Chapter 5, I suggest a mechanism through which this myelination pattern may help to refine the structure of retinogeniculate projections during development.

# Chapter 2

## A novel tissue sampling strategy for the elucidation of molecular correlates of visual development

### Abstract

Throughout visual development, a series of complex connections are established between the retina, lateral geniculate nucleus (LGN), and primary visual cortex (V1). The extent to which retina, LGN, and V1 substructures may be molecularly distinct from one another has only just begun to be explored. Here we outline a novel tissue sampling strategy to further characterize molecular influences on the developing visual system, with a specific focus on the development of ocular dominance. We employ a series of dissection, fluorescent tracing, and optical imaging of intrinsic signal experiments in order to isolate substructures of the retina, LGN, and V1 that provide the anatomical basis of ocular dominance in the ferret. As an example application of this tissue sampling strategy, isolated tissue is used for proteomic analysis with Two Dimen-

sional Difference Gel Electrophoresis (2D-DIGE). Briefly, we isolate pairs of fresh tissue samples from temporal and nasal retina, A and A1 LGN layers (corresponding to the contralateral and ipsilateral eyes, respectively), and ipsilateral and contralateral V1 ocular dominance domains for proteomic analysis. 2D-DIGE is used to compare and quantify the protein compliment of these paired tissue samples. Protein candidates showing differential expression are identified using MALDI-TOF mass spectrometry. Immunohistochemistry and western blot of protein candidates are then used to visualize these differences directly and to characterize their spatiotemporal patterns.

## 2.1 Introduction

In forward looking mammals with overlapping visual fields, segregated eye specific responses to visual stimuli are found in the lateral geniculate nucleus (LGN) and in primary visual cortex (V1). In the LGN, eye specific projections of retinal ganglion cells (RGCs) are segregated into inputs that range from physiologically distinct projections in the rodents to physiologically and anatomically distinct eye specific laminae in higher mammals. In the V1, eye specific responses are organized into a salt and pepper distribution of eye specific cells in rodents and into ocular dominance columns in many higher mammals. The development of these structures in the visual circuit is influenced by both the pattern of neuronal activity in the circuit driven by external stimuli or endogenous activity and patterned gene expression. Hubel and Wiesel's seminal work based on electrode recordings from both normal and visually deprived cats laid the foundation for exploration of the impact of neuronal activity on visual system development. In the decades since their work, a large and robust literature has been built up around experimental approaches centered on variations from normal activity as a window on developmental mechanisms. It has also become clear that there is a strong molecular component to the development of the visual system (Tropea et al., 2009). At the level of the retina, LGN, and V1 there are molecular influences on the structure and function of the visual circuit. In the retina, RGCs express a suite of known markers that dictate their decussation pattern including transcription factors such as Foxd1 (Herrera et al., 2004), Foxg1 (Tian et al., 2008), Zic2 (Herrera et al., 2003), and Isl2 (Pak et al., 2004) as well as cell surface

receptors such as EphB receptors (Williams et al., 2003). In large part due to these cues, the LGN can be considered to receive nasal retinal input from the contralateral eye and temporal retinal input from the ipsilateral eye. At the level of the LGN, RGCs express markers that guide their elaboration into appropriate topographic and eye specific target regions such as the Ephrins and Eph receptors which mediate proper retinogeniculate targeting (Flanagan and Vanderhaeghen, 1998; Frisen et al., 1998; Huberman et al., 2005; Pfeiffenberger et al., 2005) and Ten-m3 which affects ipsilateral afferent targeting (Leamey et al., 2007). In V1, correct topology formation is dependent on EphrinAs and EphAs (Cang et al., 2005) and molecular GABA expression levels shape the width of ocular dominance columns (Hensch, 2005). While we are beginning to understand the impact of many molecular regimes on the developing visual system, it is clear that there is much to learn. We have a good understanding of the role of only a minority of the full complement of proteins present in the developing visual system. It is critical that we begin to identify a larger set of proteins at work during visual development in order to diversify and expand our understanding of how patterned gene expression influences visual development. In order to identify a larger set of proteins involved in visual development, broad based unbiased screening techniques must be employed. Within the past fifteen years, genetic and proteomic screens have begun to be employed in the study of the developing visual system. One of the first studies of this kind was demonstrated by Corriveau et al in 1998 when they used differential mRNA display to identify class 1 MHC as a novel player in visual system plasticity (Corriveau et al.,

1998). More recently, a notable study was done by Tropea et al in 2006 using DNA microarrays and RT-PCR in conjunction with visual deprivation to identify parvalbumin as a novel player in visual system plasticity as well as identifying many other candidates involved in modulating the transduction of inputs to cells in visual cortex (Tropea et al., 2006). In addition to genetic screens, proteomic based screens have recently been leveraged to study visual development. Two dimensional difference gel electrophoresis (2D-DIGE) has been used to identify protein candidates that are regulated throughout visual development and are responsive to visual deprivation including synaptotagmin 1 (Cnops et al., 2007a; Cnops et al., 2007c), CRMP2 and CRMP4 (Cnops et al., 2006; Van Den Bergh et al., 2006b; Cnops et al., 2007a; Cnops et al., 2007b). In addition to comparative studies of age or deprivation condition, 2D-DIGE has been used to characterize the proteome of the visual system relative to other brain areas. 2D-DIGE revealed a list of candidates for areal markers in the cortex including brain type creatine kinase as a novel marker for primary somatosensory cortical (S1) boundaries (Jacobs et al., 2008). Here, we introduce a methodology for the identification of novel molecular correlates of ocular dominance in the visual system. We employ a suite of anatomically and functionally guided isolations of ocular dominance substrates in the retina, LGN, and V1 followed by 2D-DIGE and MALDI-TOF mass spectroscopy in order to identify molecular candidates associated with ocular dominance in the developing ferret visual system.

## 2.2 Materials and methods

### 2.2.1 General animal procedures

All animal procedures were carried out in accordance with approved protocols for the care and use of animals at Carnegie Mellon University. For all experiments, animals were deeply anesthetized with either an overdose of sodium pentobarbital delivered through and IP injection (retina and LGN tissue samples) or with 5% isoflurane in 1:1 O<sub>2</sub>:N<sub>2</sub>O (cortical tissue samples) before tissue sample collection. After collection, all tissue samples were handled in the same manner as described below in Section 2.2.6.

### 2.2.2 Optical imaging of intrinsic signal

Ferrets ranging in age between P30 and P100 were used for optical imaging of intrinsic signal experiments. Animals were anesthetized and maintained with isoflurane (0.5-1.5%) and O<sub>2</sub>:N<sub>2</sub>O (1:1) for surgical preparation of a cranial imaging window over V1 and V2. A large craniotomy (5mm) was opened through the skull and the dura resected. An imaging chamber was constructed over the exposed arachnoid and cortex by interposing a 1% agarose in 0.9% sodium chloride saline solution between the brain and a custom coverslip. This chamber was then secured to the skull using dental cement. Animals were next paralyzed with pancuronium bromide (0.02mg/kg/hr) and artificially respiration through an endotracheal tube. Optical imaging of intrinsic signal was carried out using a tandem microscope lens mounted on a CCD camera (M60; Dalsa, Waterloo, Ontario, Canada) controlled by a commercial data acqui-

sition package (Optical Imaging, Inc., New York, NY 10019) as described previously (Frostig et al., 1990; Bonhoeffer and Grinvald, 1996). Using this technique, it is possible to track localized cortical metabolic activity *in vivo* based on changes the optical properties of the tissue. Briefly, differential reflection of 700nm light off of the exposed V1/V2 cortical surface was recorded in response to visual stimuli generated using a commercial stimulus generator (ViSaGe; Cambridge Research Systems, Rochester, England) presented on a Sony 24 monitor. Ocular dominance mapping stimuli consisted of drifting full field square wave grating patterns at a spatial frequency of .125 cycles/degree. Grating patterns were drifted back and forth along the axis orthogonal to the grating orientation at a velocity of 2 cycles/second. Grating patterns at 0,45,90, and 135 degrees were presented separately to each eye and the differential response between eyes across all patterns presented was taken as the map of ocular dominance.

### **2.2.3 Retina tissue sampling**

Ferrets ranging in age from P15 to P20 were used for retina sample generation. After injection with sodium pentobarbital, both of the eyes were removed and all further procedures were carried out on ice. First, the frontal segment and vitreous humor of eye was removed. The retina was then carefully removed from the retinal pigmented epithelium while leaving it in tact. The retina was then cut along the ventral to dorsal axis isolating the temporal and nasal portions of the retina from one another. Samples were pooled between the two retinas for each animal to form single animal temporal and nasal samples for

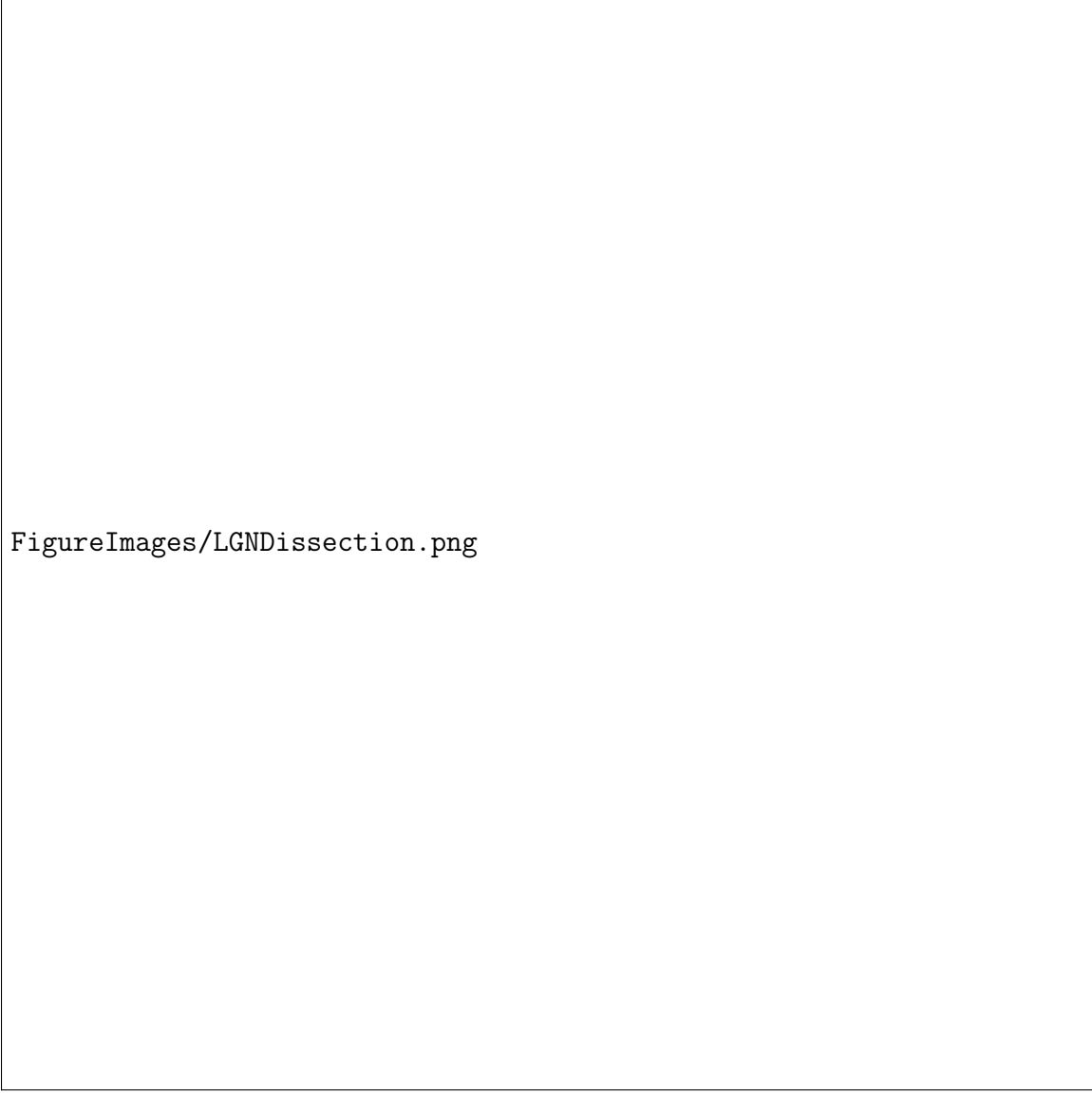
further processing Samples were then homogenized in  $30\mu\text{l}$  of lysis buffer (7M urea, 4% CHAPS, 2M thiourea, 10mM DTT) prior to 2D-DIGE.

#### **2.2.4 LGN tissue sampling**

Ferrets ranging in age from P15 to P20 were used for LGN tissue sample generation. Two days before LGN tissue sample collection, one eye was injected with cholera toxin  $\beta$ -subunit conjugated to alexa-488 and the other with cholera toxin  $\beta$ -subunit conjugated to alexa-555 under isoflurane anesthesia in order to visualize the organization of the retinogeniculate projection. After injection with sodium pentobarbital, the brain was removed from the skull and the thalamus removed from the brain. The lateral aspect of the thalamus was sectioned at 300 $\mu\text{m}$  using a vibratome. The alexa labeled LGN laminae were then isolated using under fluorescently guided micro-dissection as described previously (Kawasaki, 2004)(figure 2.1). The A and A1 laminae samples were pooled across the two LGNS to form single animal A and A1 samples and homogenized in  $30\mu\text{l}$  of lysis buffer (7M urea, 4% CHAPS, 2M thiourea, 10mM DTT) prior to 2D-DIGE.

#### **2.2.5 Cortical tissue sampling**

Ocular dominance maps generated using optical imaging of intrinsic signal were segmented into regions of high ocular preference (defined as pixels falling in the first and fourth quartiles of the difference image pixel value distribution). Segmented ocular dominance maps were used in conjunction of with a green light (546nm) image of cortical surface vasculature to target tis-



FigureImages/LGNDissection.png

Figure 2.1: Fluorescent micro-dissection of the LGN for 2D-DIGE. A, schematic of the LGN in sagittal section. Sagittal sections allow for easy visualization and isolation of labeled laminae. B, intact LGN. C, LGN with C laminae removed. D, isolation of the A1 lamina. E, the A lamina before separation from the perigeniculate nucleus (PGN) at the ventromedial boundary of the LGN. F, the A laminae isolated from the rest of the thalamus. Scale bar = 250m, applies to all.

sue biopsies of functionally defined ocular dominance columns (Figure 2.2a-d). Tissue biopsies were taken using one of two approaches. In the first, fluorescent tracer injections of red and green fluorescent microspheres were used to visualize oc-

ular dominance columns during postmortem dissection of the visual cortex (Figure 2.2e). In the second approach, a blunted 25 gauge needle (inner diameter =  $300\mu\text{m}$ ) attached to a suction line was lowered into the cortex to a depth of  $500\mu\text{m}$ . The needle was then slowly removed from the cortex. The resulting biopsies were spatially confined to the inner diameter of the needle and minimally disturbed the surrounding tissue. Biopsies included only cortical grey matter while leaving the underlying white matter in tact, as confirmed by post-mortem inspection of the biopsy site (Figure 2.2f). Tissue biopsies from 2-3 ocular dominance columns were pooled into two sample tubes according to eye preference. Samples were then homogenized in  $30\mu\text{l}$  of lysis buffer (7M urea, 4% CHAPS, 2M thiourea, 10mM DTT) prior to 2D-DIGE.

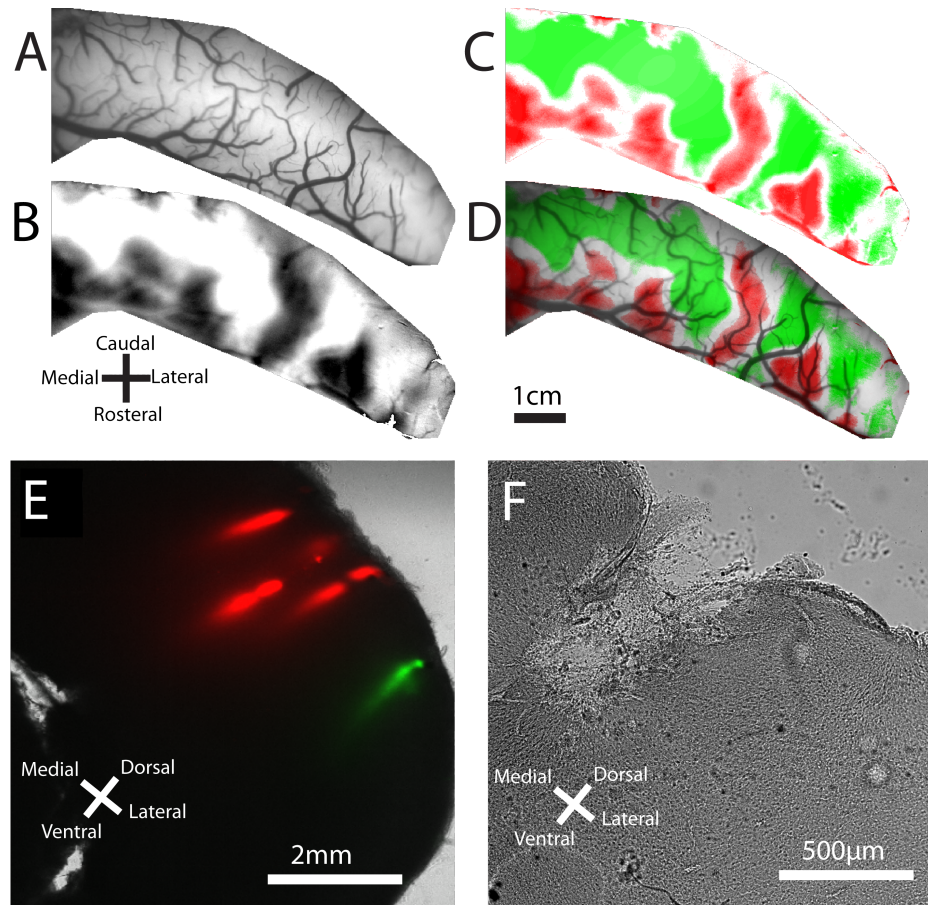


Figure 2.2: Isolation 2D-DIGE samples from functionally defined maps of ocular dominance. A, blood vessel map of the dorsal surface of ferret visual cortex illuminated under green light (546nm). B, functional map of ocular dominance generated using intrinsic signal optical imaging under red light (700nm). The light patches in B are preferentially responsive to stimuli presented to the contralateral eye, patches in black respond to stimuli presented to the ipsilateral eye. C, example map of 2D-DIGE suction biopsy target sites. Contralateral targets are pseudo-colored in green and ipsilateral targets in red. D, overlay of biopsy targets onto the blood vessel map from A. This image is used to visualize the functional map relative to the blood vessel map in order to manually target either fluorescent tracer injections or suction biopsies. E, postmortem coronal section through a set of tracer injections. Tracers are used for fluorescence guided micro-dissection of ipsilateral and contralateral responsive domains. F, postmortem coronal section through a biopsy site. The biopsy extends 750m into the cortex and is 400m in diameter. Biopsies of this size and shape are ideal for specific biopsy of ocular dominance columns *in vivo*. Blood vessel and functional map courtesy of D.E. Whitney.

## **2.2.6 Two dimensional difference gel electrophoresis**

Sample protein concentration was estimated using a Bradford assay. The optical density of protein samples was measured at 595nm and compared to a standard curve ranging from .5 mg/ml to 2.5 mg/ml. Typical sample concentrations were between 1 and 2 mg/ml. Sample concentrations were then used to balance protein load across sample types for each experiment. Typical experiments yielded approximately 100? $\mu$ g of total protein between the two ocular dominance sample types. Each sample was minimally labeled with either propyl-Cy3 or methyl-Cy5 dyes (Amersham Biosciences/GE healthcare Piscataway, NJ 08855). The labeling reaction for these dyes is carried out at sub-stoichiometric conditions, resulting in approximately 5% of the proteins forming a single bond to a dye molecule. These dyes are charge and mass matched and run together through 2D-DIGE. The unlabeled portion of the sample runs slightly faster on the gel with a predictable shift, allowing for easy isolation of this protein pool based on the location of the minimally labeled protein pool. For labeling, protein samples were made up to 80? $\mu$ l in lysis buffer. Proteins solutions were minimally labeled with propyl-Cy3 or methyl-Cy5 dyes by incubation with 1? $\mu$ l of the appropriate dye for 15 minutes in the dark and on ice. Immediately thereafter, non-reacted dye was quenched with an incubation in 1? $\mu$ l of a solution of 5M methylamine-HCl and 10mM HEPES at pH 8.0 for 30 minutes. The two differentially labeled samples were then mixed together in preparation for co-electrophoresis. In order to ensure that enough protein was run in our gels for successful identification using mass spectrometry, an unlabeled sample of V1 homogenate was added

to the labeled sample mixture. We have found that increasing the total protein load in our gels using this background sample results in a large increase the number of successfully identified candidate proteins. As an example, only 12%(3 of 25) spots sampled (see section 2.2.8) from an experiment run without a background were identified and 83%(10 of 12) samples from an experiment with a background were identified. The unlabeled V1 homogenate was derived from a mixture of V1 homogenate from a P33 and a P89 normal ferret. These time points represent the beginning and the end of the critical period in ferret and served as an unbiased background of protein pooled across both development and ocular dominance column type. After sample labeling, isoelectric focusing (IEF) was carried out to separate our samples by pH. IEF was done using a nonlinear immobilized pH gradient strip ( pH 3-10 NL, 13 cm Immobiline DryStips, Amersham Biosciences/GE healthcare) on an IPGphor IEF apparatus (Amersham Biosciences/GE Healthcare), following the manufacturers instructions. IEF was carried out using 500V for 1 hour, 4000V for 1 hour, 8000V for 2 hours, and 8000V until a total of 40kVh was reached. A typical IEF run took approximately 15 hours to complete using these settings. After IEF, the immobiline strips were equilibrated for 15 minutes each in two equilibration solutions. Each equilibration solution contained 50mM Tris, 6M Urea, 30% glycerol, 2% SDS, 1% IPG buffer, and a few grains of bromophenol blue. Additionally, The first equilibration solution contained 1% DTT and the second contained 2.5% iodoacetimide. After equilibration, the IPG strips were run on a 1mm thick 10-15% SDS-polyacrylamide gradient gel in the vertical Protean II xi cell (BioRad, Hercules, CA 94547) at 20mA/gel at 4C. Typical second dimension gel runs

lasted between 10 and 12 hours. After electrophoresis was complete, the final 2D-DIGE gel was fixed in a solution of 40% HPLC grade methanol and 1% glacial acetic acid for at least two hours prior to fluorescence imaging for protein spot localization.

### 2.2.7 Fluorescence gel imaging and image analysis

2D-DIGE gels were imaged using a custom built fluorescent imager in the laboratory of Jonathan Minden of the department of biological sciences at Carnegie Mellon University (Unlu et al., 1997; Viswanathan et al., 2006). The imager consists of a motorized stage (New England Affiliated Technology, Lawrence, MA 01841) enclosed in a light-tight cabinet fitted with two 250W quartz-tungsten-halogen light sources (Oriel, Irvine, CA 92606) for gel illumination. For Cy3 or Cy5 specific illumination, light from the light sources is passed through an appropriate band-pass wavelength filter (Chroma Technology, Rockingham, VT 05101 USA) and directed onto the gel via fiber optic light guides (Oriel). Emission from excited dye molecules is recorded using a cooled 16-bit CCD camera (Photometrics/Roper Scientific, Tucson, AZ 85706) fitted with a 105-mm macro lens (Nikon, Melville, NY 11747-3064, U.S.A.). By moving the stage relative to the stationary illumination and imaging system under control of custom software, a mosaic image of the entire 20cmx20cm gel is created with a resolution of 135 $\mu$ m/pixel sufficient for both qualitative and quantitative protein spot identification. Mosaic gel images were created by exposing all portions of the gel to 30 seconds of illumination at the excitation wavelength of Cy3 followed by 30 seconds of

exposure to the excitation wavelength of Cy5. This exposure time was chosen in order to bring the brightest pixels in the image close to but not above the saturation point of the CDD camera. Photobleaching was not observed during the imaging sessions.

Qualitative differences between the Cy3 and Cy5 signals within a gel were appraised using false colored images generated from the raw fluorescence data using ImageJ. Raw images were log transformed in order to facilitate the visualization of both low and high abundance proteins in the same image. Next, both images were adjusted for overall brightness to compensate for uneven fluorescence yields between the two dyes. A red and green overlay image was then constructed from the two adjusted grayscale images. Protein spots visibly appearing red or green in this overlay image were said to differentially expressed across the samples in the gel. Quantitative differences between the Cy3 and Cy5 signals were detected using custom software written in MATLAB. The raw data images were log transformed and additionally median filtered with a 3x3 kernel to remove shot noise. The centers of all detectable protein spots in the two pre-processed images were found using a custom blob detection algorithm. Once spot centers were identified, a 9-pixel (1.215mm) diameter region of interest around each center was taken into consideration for further analysis. For each spot center, the ratio and difference between the Cy3 and Cy5 image was calculated. From these measurements, a population of ratios and differences was constructed. Those spot measurements falling two standard deviations above or below the mean difference or ratio were considered to be differentially expressed across the samples in the gel.

## **2.2.8 Protein spot isolation and identification**

Protein spots determined to be differentially expressed between sample types were excised from the 2D-DIGE gel using an automated spot cutter (Applied Precision, Inc, Issaquah, WA 98027) built into the imager used to image the gels. Protein spots were cut out of the gel under the control of custom software and placed in a 96-well automated protein digester plate (Digilab/Genomic Solutions, Ann Arbor, MI 48108) filled with 1% glacial acetic acid. After spot cutting, the wells of the plate were drained of liquid and the excised gel pieces were stored at -80°C until further processing. For peptide extraction, gel pieces were thawed and subjected to in-gel tryptic digestion using 20? $\mu$ g of sequencing grade modified trypsin (Promega, Madison, WI 53711 USA) in a ProGest automated protein digester (DigiLab/Genomic Solutions) according to the manufacturers instructions. Peptide extracts were then desalting and concentrated using ZipTip C18 reverse-phase chromatography (Millipore, Billerica, MA 01821). The tip was rinsed twice in 100% acetonitrile and twice in .2% formic acid. Peptide samples were loaded onto the tip by aspirating the peptide extract through the tip ten times. The tip was then washed twice in .2% formic acid and eluted into a sample tube by aspirating ten times with 2.5 $\mu$ l of a 1:1 100% ACN:.2% formic acid solution.

Following desalting and concentration, peptide samples were immediately prepared for matrix-assisted laser desorption/ionization time of flight (MALDI-TOF) mass spectrometry. Samples were spotted in a 1:1 ratio with Alpha-Cyano-4- hydroxycinnamic acid matrix (Agilent Technologies, Santa Clara, CA, 95051) on a 100 well stainless steel sample plate (PerSeptive Biosystems/Applied

Biosciences, Foster City, Ca, 94404) and allowed to dry. MALDI-TOF mass spectrometry was then carried out on a Voyager-DE STR mass spectrometer (Applied Biosciences, Foster City, Ca, 94404).

A voltage of 20kV was applied to the sample plate and the matrix was excited with 337nm light from a nitrogen laser. A peptide survey spectrum was acquired from 750 to 3800 m/z. A peak list for each spectrum was generated through analysis with Data Explorer (Applied Biosciences, Foster City, Ca, 94404). Protein identifications were determined by matching sample MALDI-TOF peak lists to the MASCOT MS Fingerprint database (Perkins et al., 1999). MASCOT searches were carried out with a fixed modification of carboxymethyl, variable modification of methionine oxidation, one possible missed trypsin cleavage, and within a range of 50ppm.

### **2.2.9 Immunohistochemistry**

All immunohistochemical stains were carried out using primary antibodies at a dilution of 1:500 (CRMP4, cat. #AB5454, Millipore, Billerica, MA; munc13-3, cat. #ab2707 Abcam, Cambridge, MA; CRMP2, gift from Dr. Rajesh Khanna, Indiana University). For munc13-3 and CRMP4 stains, expression was assayed with a primary antibody followed by a fluorescent secondary antibody (Alexa 594 or Alexa 488, 1:500 dilution, Invitrogen, Carlsbad, CA). For CRMP2 stains, a biotinylated secondary antibody (cat. #BA-1000, Vector Laboratories, Burlingame, CA) was detected using the Vectastain Elite ABC kit (cat. #PK-6101, Vector Laboratories, Burlingame, CA).

## 2.3 Results

### 2.3.1 Retinal molecular correlates of visual development

Three 2D-DIGE experiments were conducted on retinal tissue derived from temporal and nasal tissue as described in 2.2.3. From these three experiments, eleven protein candidates were found to be differentially expressed. No protein candidate was found in more than one experiment. Four of the candidates were expressed in the temporal retina and seven were expressed in the nasal retina (table 2.1). The isolated proteins were localized primarily in the cytoplasm (6, 54.55%) , with a minority of the proteins in the set localized to the cytoskeleton (2, 18.18%), nucleus (2, 18.18%), and the plasma membrane (1, 9.09%) (figure 2.3). The functional roles of protein candidates were dominantly structural in nature(4, 36.36%). Minority fractions of the candidates were involved in chaperone (2, 18.18%), enzyme (2, 18.18%), splicing (1, 9.09%), metabolic (1, 9.09%), and neurotransmitter release (1, 9.09%) functions (figure 2.4).

From the list of protein candidates differentially expressed between the temporal and nasal retina, munc13-3 was chosen for further validation by immunohistochemistry. In one 2D-DIGE experiment, munc13-3 was found to be expressed in higher abundance in the temporal portion of the retina. The munc13 family regulates synaptic transmission by catalyzing the partial formation of SNARE complexes required for neurotransmitter release (Pang and Sudhof, 2010). Munc13 proteins are known regulators of ribbon synapses in retinal photoreceptors and are therefore of potential importance in the formation and maintenance of retinothalamic projections (tom Dieck et

al., 2005). Munc13-3 is primarily expressed in non-cortical neural tissues and is hypothesized to work in concert with munc13-1 to regulate synaptic transmission in these tissues (Augustin et al., 1999). Immunohistochemistry against munc13-3 in two flat mounted ferret retinas aged P17 and P25 show a trend of relative over expression of munc13-3 in the temporal aspect of the retina (figure 2.5). To further characterize the expression of munc13-3 in the developing retina, immunohistochemistry against munc13-3 was carried out in horizontal sections of P13 retinas. Munc13-3 appeared to stain puncta in the retinal ganglion cell layer of both the temporal and nasal portions of the retina. Stained puncta were more dense in the temporal retina than in the nasal retina (figure 2.6). This result taken with the observed temporal bias in expression from P17 and P25 flat mounted retinas do not definitively confirm the temporal bias in expression found in the temporal/nasal 2D-DIGE screen, but lend support to it.

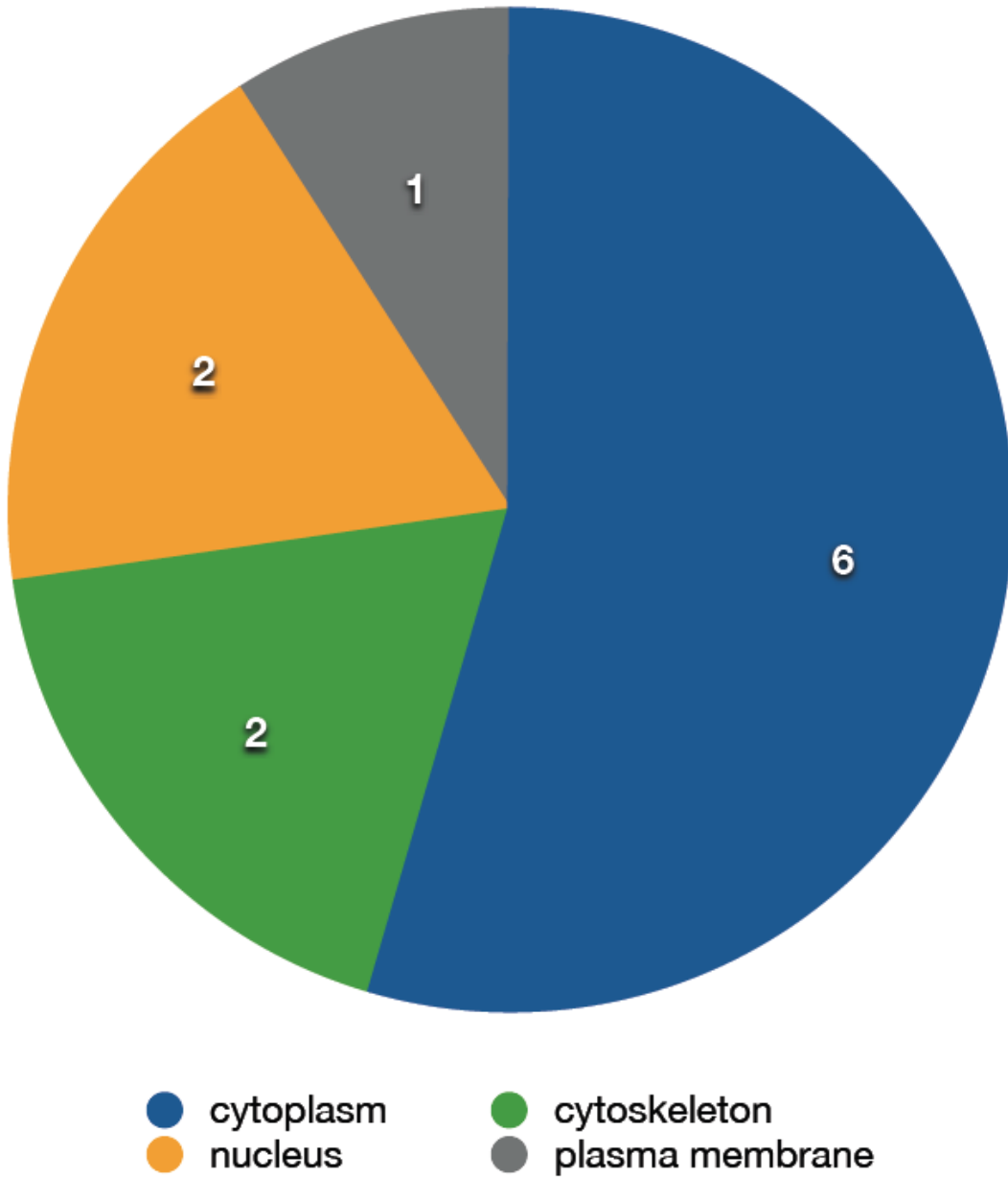


Figure 2.3: Location of protein candidates found to be differentially expressed across temporal and nasal retina. Eleven protein candidates were found to be differentially expressed across the temporal and nasal retina. The number of candidates found in each sub-cellular location is displayed inside of each pie slice. The majority of protein candidates are localized to the cytoplasm (6, 54.55%) with a minority found in the cytoskeleton (2, 18.18%), nucleus (2, 18.18%), and the plasma membrane (1, 9.09%).

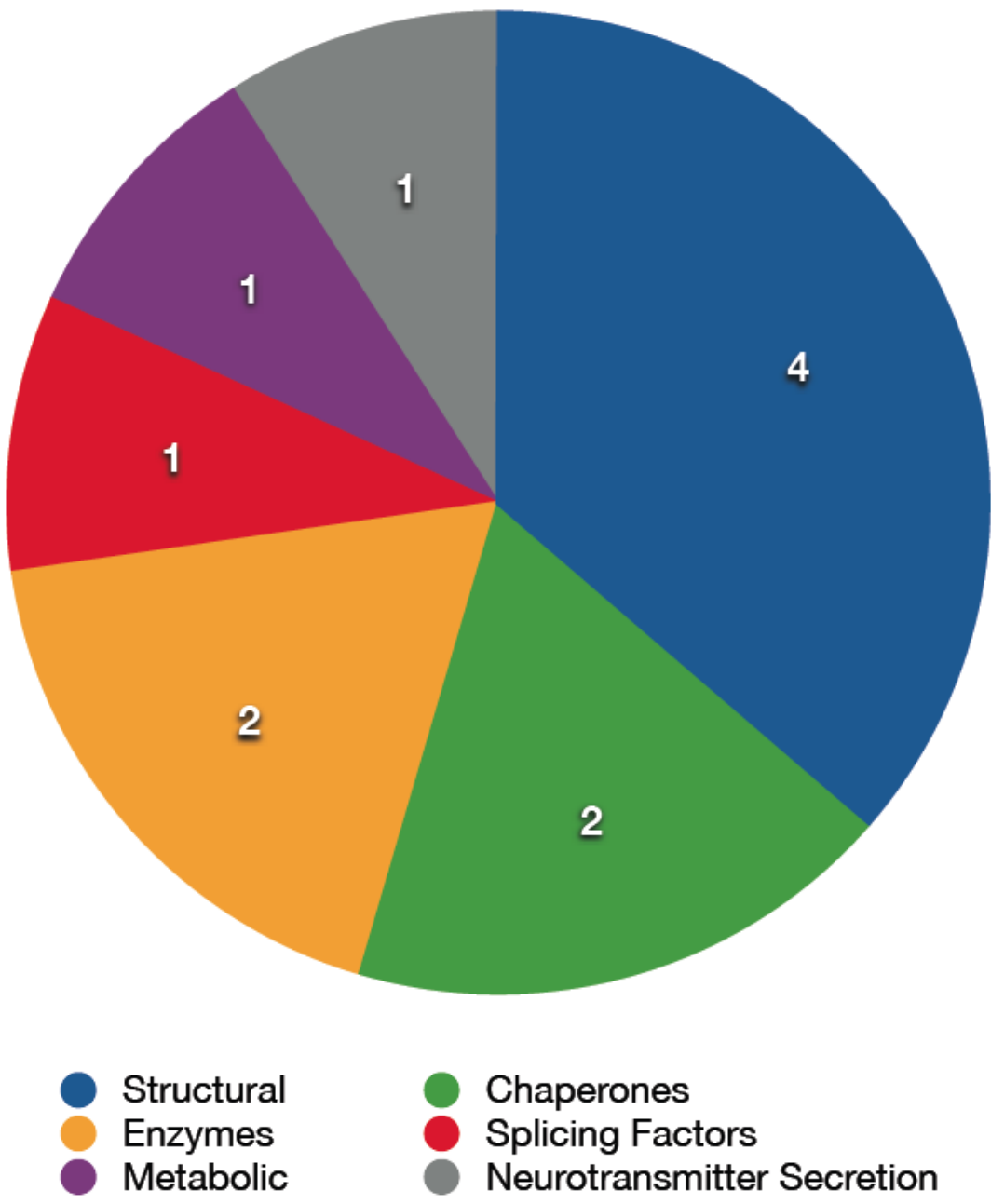


Figure 2.4: Functions of protein candidates found to be differentially expressed across temporal and nasal retina. Eleven protein candidates were found to be differentially expressed across the temporal and nasal retina. The number of candidates found in each functional category is displayed inside of each pie slice. The majority of protein candidates are structural in nature(4, 36.36%). Minority fractions of the candidates are involved in chaperone (2, 18.18%), enzyme (2, 18.18%), splicing (1, 9.09%), metabolic (1, 9.09%), and neurotransmitter release (1, 9.09%) functions.

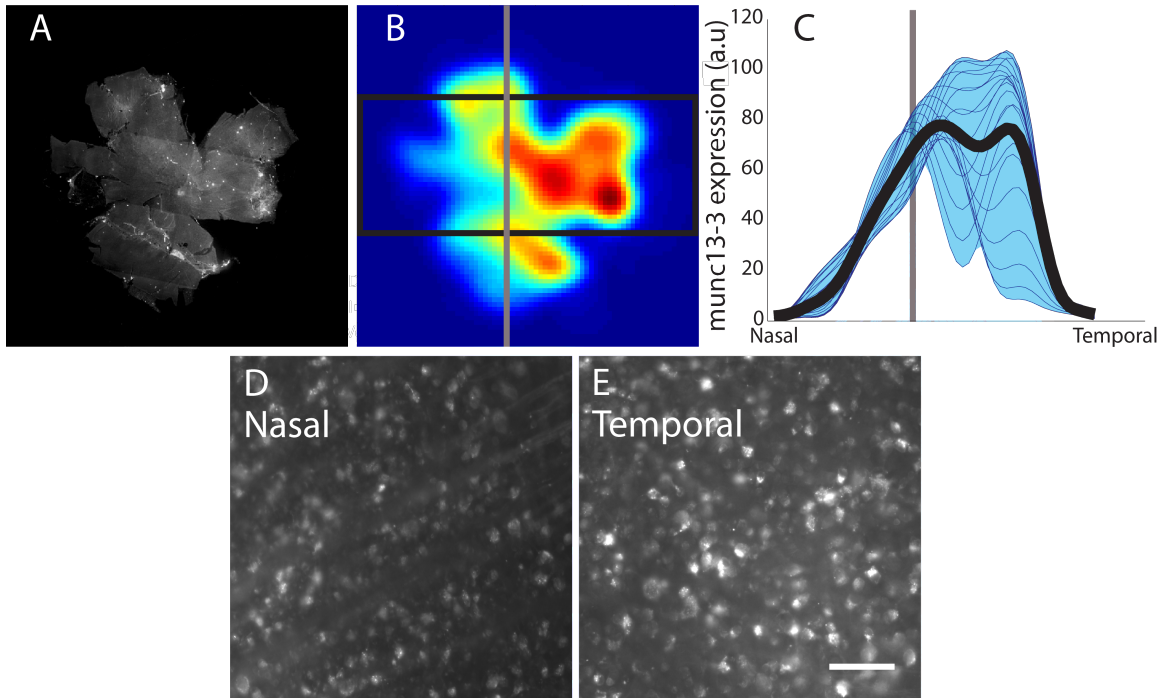


Figure 2.5: Quantification of munc13-3 expression in the flat mounted retina. A, flat mount view of a P17 retina stained for munc13-3. There is a trend of higher expression on in the temporal leaflet when compared to the nasal leaflet. B, The same image smoothed and then binned into 20m domains for quantification. The domains over the center of the retina (black box in B) were used to compute nasal to temporal linescans shown in C. The location of the optic nerve head is shown by the gray line in B and C. C, each nasal to temporal linescan is shown in blue with the average linescan shown in black. There is higher munc13-3 expression on the nasal portion of the retina as defined by the location of the optic nerve head. D, high magnification view of munc13-3 expression in the nasal leaflet of a P17 retina. E, high magnification view of munc13-3 expression in the temporal leaflet of a P17 retina. When normalized to the total number of cells in the field of view, 25% of the nasal cells and 29% of the temporal cells express munc13-3. Scale bar=50m and applies to both D and E.

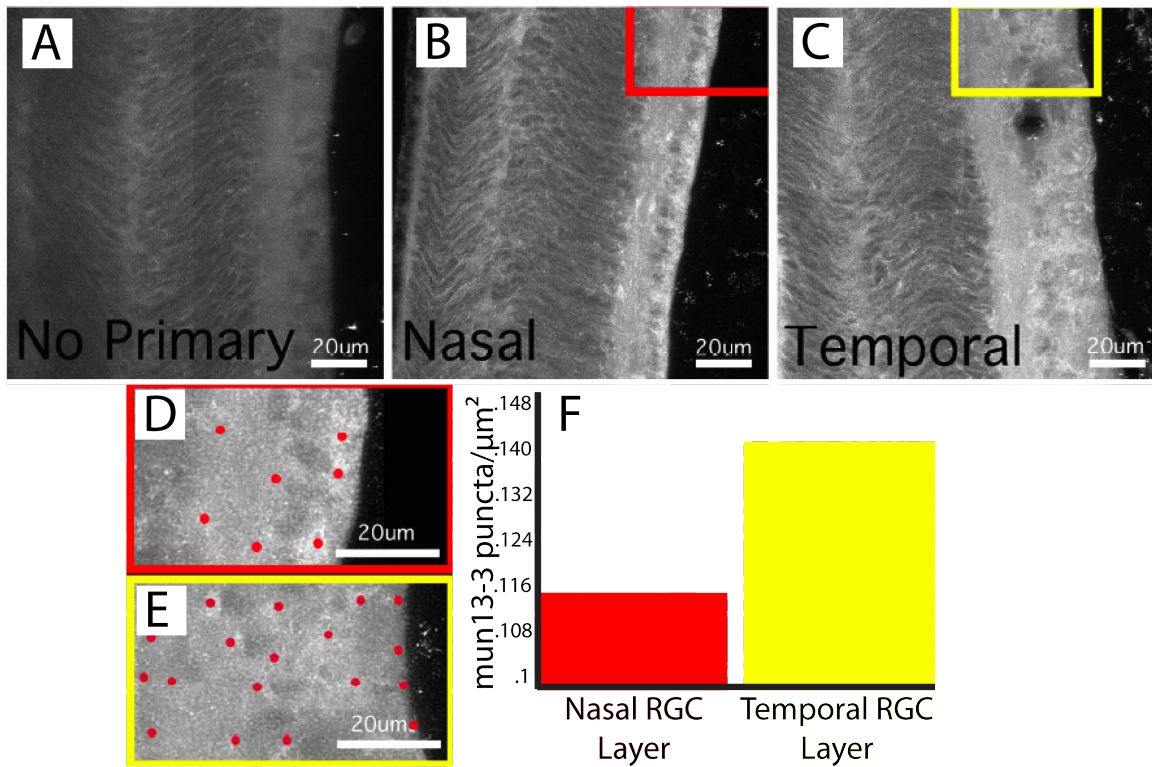


Figure 2.6: Munc13-3 expression in retinal cross-sections. A, no primary control in a section through a P13 retina. There is observable autofluorescence in all layers of the retina. B and C, munc13-3 stain in the temporal and nasal portions of the same retina. There is specific expression above the baseline autofluorescence of munc13-3 in both the nasal and temporal retina. D and E, enlarged view of the boxes in D and C with the locations of munc13-3 positive puncta overlaid by red dots. F, the density of munc13-3 positive puncta is higher in the nasal retina than in the temporal retina.

Table 2.1: List of protein candidates found to be differentially expressed across temporal and nasal retina.

Protein Name	Expression Direction	Total Hits	EI (T-N) / (T+N)	Matched Species	MW (Da)	pH	Score	Coverage
14-3-3 epsilon	Temporal	1	1	<i>Mus musculus</i>	20115	4.51	100	57
alpha tubulin	Temporal	1	1	<i>Macaca mulatta</i>	43315	4.94	165	55
beta A1 crystallin	Nasal	1	-1	<i>Cavia porcellus</i>	23668	6.38	138	61
beta B1 crystallin	Nasal	1	-1	<i>Bos taurus</i>	28354	7.66	172	48
dnaK-type molecular chaperone	Temporal	1	1	<i>Rattus norvegicus</i>	71112	5.43	170	34
hsp72								
guanine nucleotide-binding protein, beta-1 subunit	Nasal	1	-1	<i>Canis familiaris</i>	38151	5.6	76	36
heat shock 70kDa protein 8	Nasal	1	-1	<i>Homo sapiens</i>	53580	5.62	230	44
Heterogeneous nuclear ribonucleoprotein F (hnRNP F)	Nasal	1	-1	<i>Canis familiaris</i>	45942	5.32	72	31
Hexokinase, type I (HK I)	Nasal	1	-1	<i>Canis familiaris</i>	120076	8.88	81	15
munc13-3	Temporal	1	1	<i>Macaca mulatta</i>	254083	5.76	73	10
protein phosphatase 1, catalytic sub-unit	Nasal	1	-1	<i>Homo sapiens</i>	37945	5.84	79	33

Protein candidates are listed alphabetically. EI: expression index defined as (Temporal expression - Nasal Expression)/(Temporal expression + Nasal Expression). Matched Species: identity of the species to which the MS data was matched. MW: predicted molecular weight in daltons. pH: predicted pH. Score: MASCOT score. Coverage: percent of sequence covered by the MASCOT match.

Table 2.2: List of retinal protein candidates sub-cellular locations and functions

Protein Name	Protein Location	Protein Function
14-3-3 epsilon	cytoplasm	Structural
alpha tubulin	cytoskeleton	Structural
beta A1 crystallin	plasma membrane	Structural
beta B1 crystallin	cytoplasm	Structural
dnaK-type molecular chaperone hsp72	cytoplasm	Chaperones
guanine nucleotide-binding protein, beta-1 subunit	cytoskeleton	Enzymes
heat shock 70kDa protein 8	cytoplasm	Chaperones
Heterogeneous nuclear ribonucleoprotein F (hnRNP F)	cytoplasm	Splicing Factors
Hexokinase, type I (HK I)	cytoplasm	Metabolic
munc13-3	nucleus	Neurotransmitter Secretion
Protein phosphatase 1, catalytic subunit	nucleus	Enzymes

Protein candidates are listed alphabetically. All sub-cellular location and function category assignments are based off of protein candidate entries in the Uniprot online database (Jain et al., 2009).

### 2.3.2 LGN molecular correlates of visual development

A Total of fourteen differentially expressed protein candidates were identified in four 2D-DIGE experiments on A and A1 LGN laminae as described in 2.2.4. Three of the candidates were identified in two different experiments, the rest were only identified once. Seven of the candidates were expressed in the A lamina, six were expressed in the A1 lamina, and one candidate was found to be expressed once in the A lamina and once in the A1 lamina (table 2.2). LGN protein candidates displayed a similar sub cellular pattern to that the observed pattern in retinal 2D-

DIGE experiments (2.3.1). The majority of protein candidates are were localized to the cytoplasm (8, 57.14%) with a minority found in the cytoskeleton (3, 21.43%), nucleus (1, 7.14%), mitochondria (1, 7.14%), and the endoplasmic reticulum (1, 7.14%) (figure 2.7). The functional properties of LGN protein candidates were again dominantly structural in nature(5, 35.71%). Minority fractions of the candidates were involved in chaperone (2, 14.29%), enzyme (1, 7.14%), metabolic (2, 14.29%), axon guidance (3, 21.43%), and proteolytic (1, 7.14%) functions (figure 2.8).

From the list of identified LGN candidates, collapsin response mediator protein 4 (CRMP4) was chosen for further analysis. CRMP4 was identified in one 2D-DIGE experiment and was found to be relatively over expressed in the A lamina of the LGN. CRMP family members have been implicated in growth cone dynamics and guidance and are differentially expressed across the central nervous system (Wang and Strittmatter, 1996). CRMP2, CRMP4, and CRMP5 show developmentally regulated expression profiles in cat primary visual cortex, indicating a possible role for the CRMP family in visual system patterning (Cnops et al., 2004; Cnops et al., 2006; Van Den Bergh et al., 2006b). Consistent with a putative role in neural patterning, juvenile CRMP4 expression is high and adult expression is low (Cnops et al., 2004; Cnops et al., 2006; Van Den Bergh et al., 2006b). Immunostaining against CRMP4 in a P30 LGN demonstrated that CRMP4 was more highly expressed in both the cell sparse interlaminar zones and ON/OFF sub-laminar boundaries than the main lamina (A, A1, C) of the nucleus (see chapter 3, fig 3.1). The observed CRMP4 expression pattern

was found to be developmentally regulated and is characterized in chapter 3. Further, the expression of CRMP4 in the LGN was found to be sensitive to the local arrangement of the cytoarchitecture in the nucleus. This result is reported in chapter 4. The organization of CRMP4 expression in the LGN does not confirm CRMP4 as a marker for the A lamina of the LGN. The observed CRMP4 expression pattern indicates that the appearance of CRMP4 as an A lamina candidate likely resulted from a sampling error in the micro-dissection of LGN laminae during sample generation.

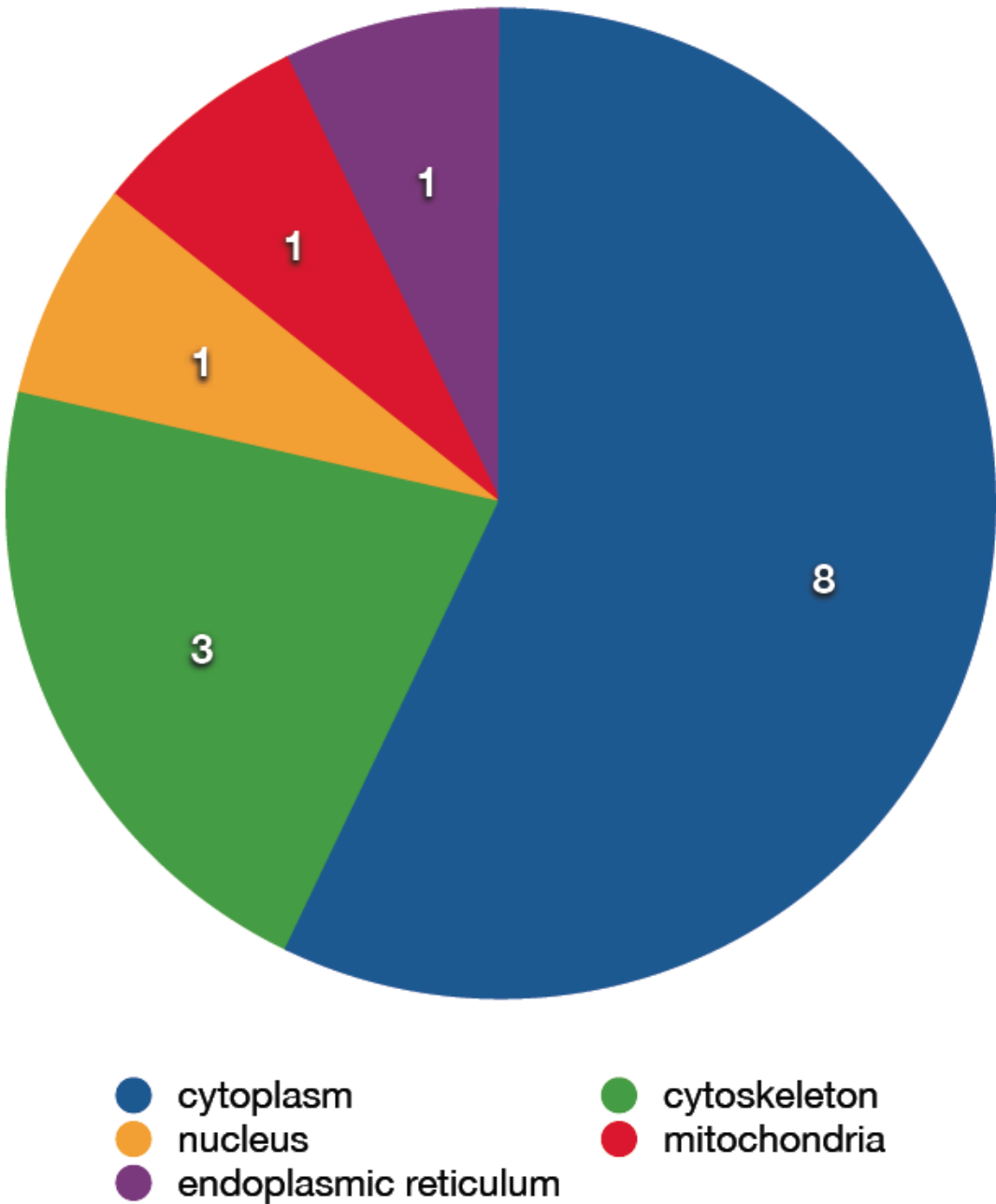


Figure 2.7: List of protein candidates found to be differentially expressed across the A and A1 LGN laminae. Fourteen protein candidates were found to be differentially expressed across the A and A1 LGN laminae. The number of candidates found in each sub-cellular location is displayed inside of each pie slice. The majority of protein candidates are localized to the cytoplasm (8, 57.14%) with a minority found in the cytoskeleton (3, 21.43%), nucleus (1, 7.14%), mitochondria (1, 7.14%), and the endoplasmic reticulum (1, 7.14%).

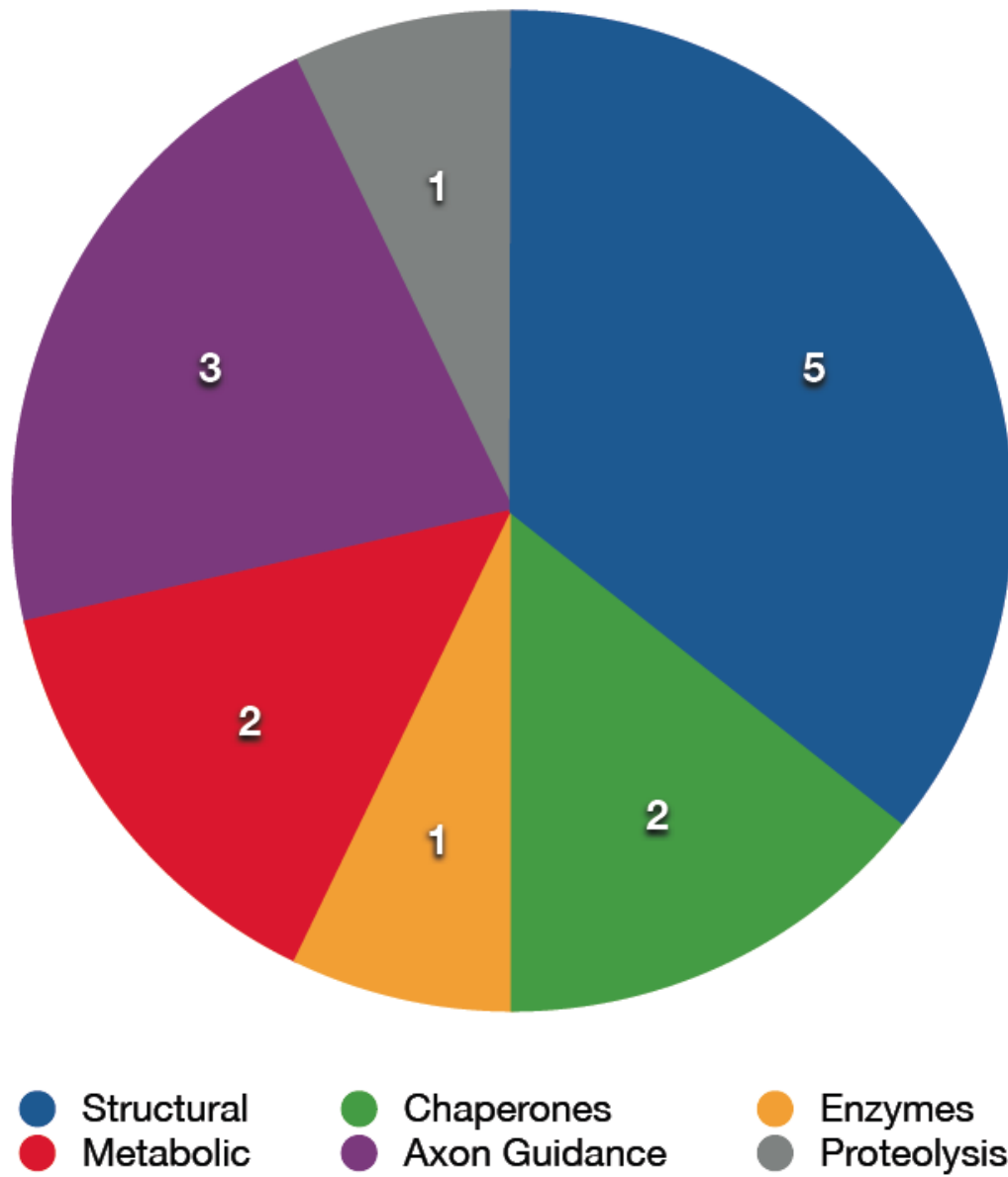


Figure 2.8: Functions of protein candidates found to be differentially expressed across the A and A1 LGN laminae. Fourteen protein candidates were found to be differentially expressed across the A and A1 LGN laminae. The number of candidates found in each functional category is displayed inside of each pie slice. The majority of protein candidates are structural in nature(5, 35.71%). Minority fractions of the candidates are involved in chaperone (2, 14.29%), enzyme (1, 7.14%), metabolic (2, 14.29%), axon guidance (3, 21.43%), and proteolysis (1, 7.14%) functions.

Table 2.3: List of protein candidates found to be differentially expressed across the A and A1 LGN laminae.

Protein Name	Expression Direction	Total Hits	EI (A1-A) /(A1+A)	Matched Species	MW (Da)	pH	Score	Coverage
collapsin response mediator protein								
	None	2	0	Canis familiaris	74229	5.98	172	70
2								
Chain A, Cysteine Structure Of Bovine Hsc70(Aa1-554)e213aD214A MUTANT	A1	2	1	Bos taurus	60977	6.05	159	59
alpha tubulin								
	A1	2	1	Macaca mulatta	46781	4.96	101	56
aconitase 2, mitochondrial isoform 3								
	A	1	-1	Canis familiaris	86409	8.07	201	36
collapsin response mediator protein								
	A	1	-1	Canis familiaris	74485	6.67	126	48
1								
collapsin response mediator protein	A	1	-1	Bos taurus	74398	5.98	72	42
4								
GDP dissociation inhibitor 1 (predicted)	A1	1	1	Rhinolophus ferrumequinum	51060	4.96	77	36
beta actin	A1	1	1	Mus musculus	39446	5.78	94	35
Creatine kinase B-type (Creatine kinase B chain) (B-CK) isoform 1								
Continued on next page								

ubiquitin										
carboxyl-										
terminal	es-	A	1	-1	Sus scrofa	25186	5.22	101	64	
terase L1										
dystonin	iso-				Canis	Famil-				
form 1 isoform	A	1	-1		iaris	632401	5.51	71	17	
17										
Heat-Shock										
Cognate	70kd	A1	1	1	Bos taurus	42557	7.03	91	71	
Protein										
beta tubulin	A1	1	1		Homo sapiens	50274	4.78	299	49	
keratin 1	A	1	-1		Homo sapiens	66149	8.16	70	19	

Protein candidates are ordered by highest number of repeat hits from top to bottom. EI: expression index defined as  $(A1 \text{ expression} - A \text{ Expression}) / (A1 \text{ expression} + A \text{ Expression})$ . Matched Species: identity of the species to which the MS data was matched. MW: predicted molecular weight in daltons. pH: predicted pH. Score: MASCOT score. Coverage: percent of sequence covered by the MASCOT match.

Table 2.4: List of LGN protein candidates sub-cellular locations and functions

Protein Name	Protein Location	Protein Function
aconitase 2, mitochondrial isoform 3	mitochondria	Metabolic
alpha tubulin	cytoskeleton	Structural
beta actin	cytoskeleton	Structural
beta tubulin	cytoskeleton	Structural
Chain A, Crystal Structure Of Bovine Hsc70(Aa1-554)e213aD214A MUTANT	nucleus	Chaperones
collapsin response mediator protein 1	cytoplasm	Axon Guidance
collapsin response mediator protein 2	cytoplasm	Axon Guidance
collapsin response mediator protein 4	cytoplasm	Axon Guidance
Creatine kinase B-type (Creatine kinase B chain) (B-CK) isoform 1	cytoplasm	Metabolic
dystonin isoform 1 isoform 17	cytoplasm	Structural
GDP dissociation inhibitor 1 (predicted)	endoplasmic reticulum	Enzymes
Heat-Shock Cognate 70kd Protein	cytoplasm	Chaperones
keratin 1	cytoplasm	Structural
ubiquitin carboxyl-terminal esterase L1	cytoplasm	Proteolysis

Protein candidates are listed alphabetically. All sub-cellular location and function category assignments are based off of protein candidate entries in the UniProt online database (Jain et al., 2009).

### 2.3.3 Cortical molecular correlates of visual development

Forty-two differentially expressed protein candidates were identified in eleven 2D-DIGE experiments on contralateral and ipsilateral ocular dominance columns as described in 2.2.5. One of the candidates was identified in four different experiments, four were identified in three different experiments, and four were identified in two different experiments. All other candidates were only identified once. Twenty-two of the candidates were expressed in contralateral ocular dominance columns, eighteen

were expressed in ipsilateral ocular dominance columns, and two candidates were found to be expressed evenly across ocular dominance column types (table 2.3). As with the retina and LGN candidates described 2.3.1 and 2.3.2, the majority of cortical protein candidates were localized to the cytoplasm (24, 57.14%) with a minority found in the cytoskeleton (4, 9.52%), nucleus (4, 9.52%), mitochondria (8, 19.04%), endoplasmic reticulum (1, 2.38%), and plasma membrane (1, 2.38%) (figure 2.10). The breakdown of cortical candidate functional properties showed more candidates involved in enzymatic processes (11, 26.19%) than candidates from retina and LGN experiments. Minority fractions of the candidates were involved in structural (10, 23.81%), metabolic (8, 19.05%), chaperone (5, 11.94%), axon guidance (2, 4.76%), and proteolysis (1, 2.38%), or other (5, 11.94%) functions (figure 2.11).

Collapsin response mediator protein 2 (CRMP2) was chosen for further analysis by immunohistochemistry and western blot. CRMP2 was identified in two 2D-DIGE experiments and was found to be more highly expressed in ipsilateral ocular dominance columns than in contralateral dominance columns. As described in 2.3.2, the CRMP family is implicated in axon dynamics and is potentially involved in visual system development. Western blot against CRMP2 in two animals (P36 and P270) showed a higher level of expression in ipsilateral ocular dominance column samples than in contralateral ocular dominance column samples, indicating that there the relative expression of CRMP2 may be biased toward ipsilateral columns throughout visual development (figure 2.12).

Immunohistochemical stains against CRMP2 in P12 and P16 animals identified an early phase of CRMP2 expression (figure

2.13, A and B) in which discrete patches of CRMP2 expression are visible in the the neuropil of the visual cortex. These CRMP2 patches are variable in their size and spacing and are not evenly distributed across the cortex as would be expected of a pattern mirroring the distribution of ocular dominance columns (figure 2.13, C). Animals in the early visual critical period do not appear to CRMP2 expression in immunohistochemical stains. At the end of the visual critical period, the expression of of CRMP2 is only apparent toward near the V1/V2 border. At this age and into adulthood, CRMP2 expression is limited to a discrete band of cells across the cortex near the V1/V2 border. In the ferret, it has been observed that there is a large band of V2 cells responsive to ipsilateral inputs at the V1/V2 border (White et al., 1999b). The location of the CRMP2 positive band of cells appears to localize well with this large ipsilateral response domain (figure 2.14). These experiments along with the finding that CRMP2 is expressed in the A1 lamina of the LGN in a 2D-DIGE experiment lend support to the hypothesis that CRMP2 may be involved in visual development and/or maintenance in the ferret. Specifically, CRMP2 may be involved in the maintenance of the V1/V2 border in early development and adulthood.

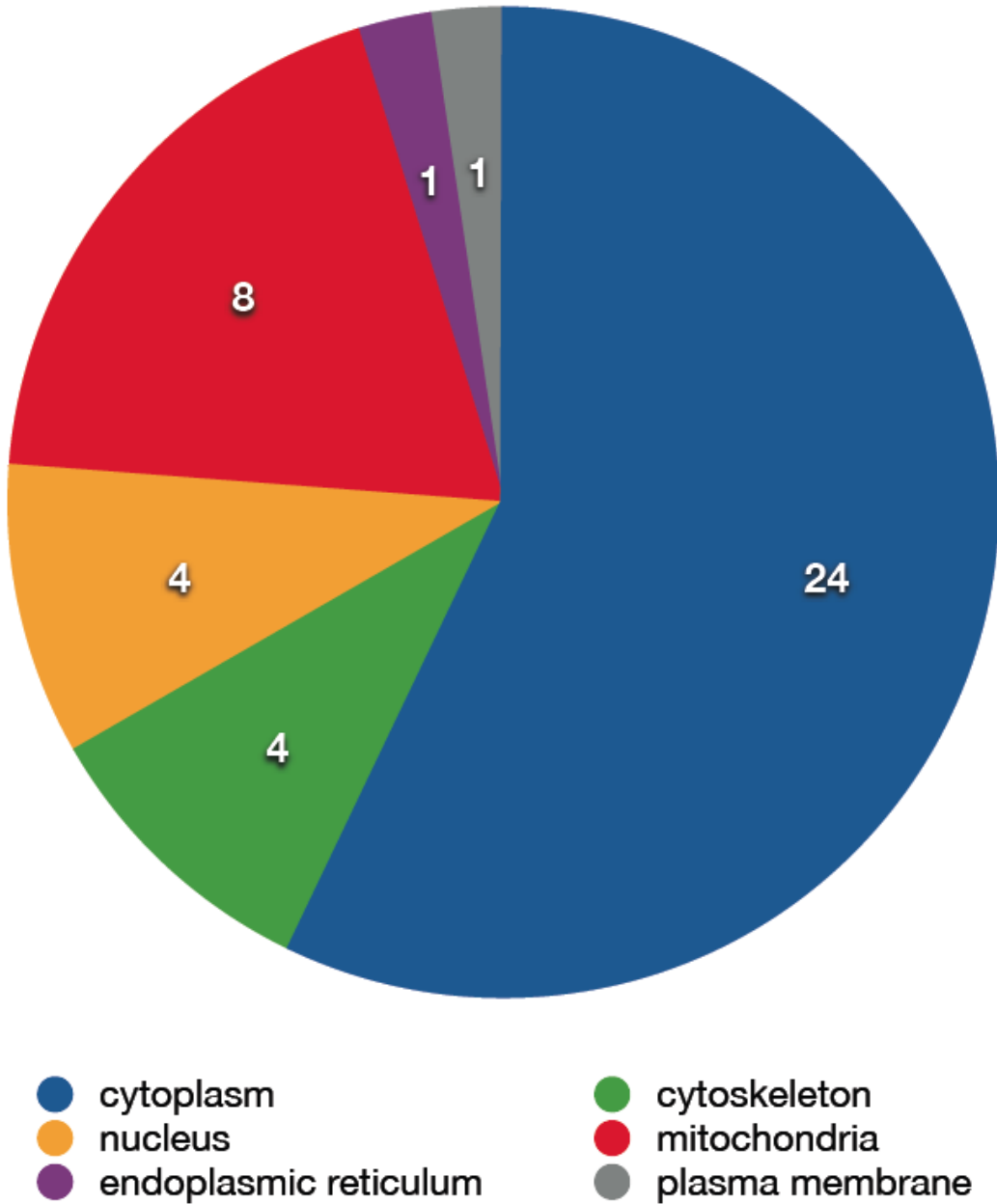


Figure 2.9: Location of protein candidates found to be differentially expressed across contralateral and ipsilateral ocular dominance columns. Forty-two protein candidates were found to be differentially expressed across contralateral and ipsilateral ocular dominance columns. The number of candidates found in each sub-cellular location is displayed inside of each pie slice. The majority of protein candidates are localized to the cytoplasm (24, 57.14%) with a minority found in the cytoskeleton (4, 9.52%), nucleus (4, 9.52%), mitochondria (8, 19.04%), endoplasmic reticulum (1, 2.38%), and the plasma membrane (1, 2.38%).

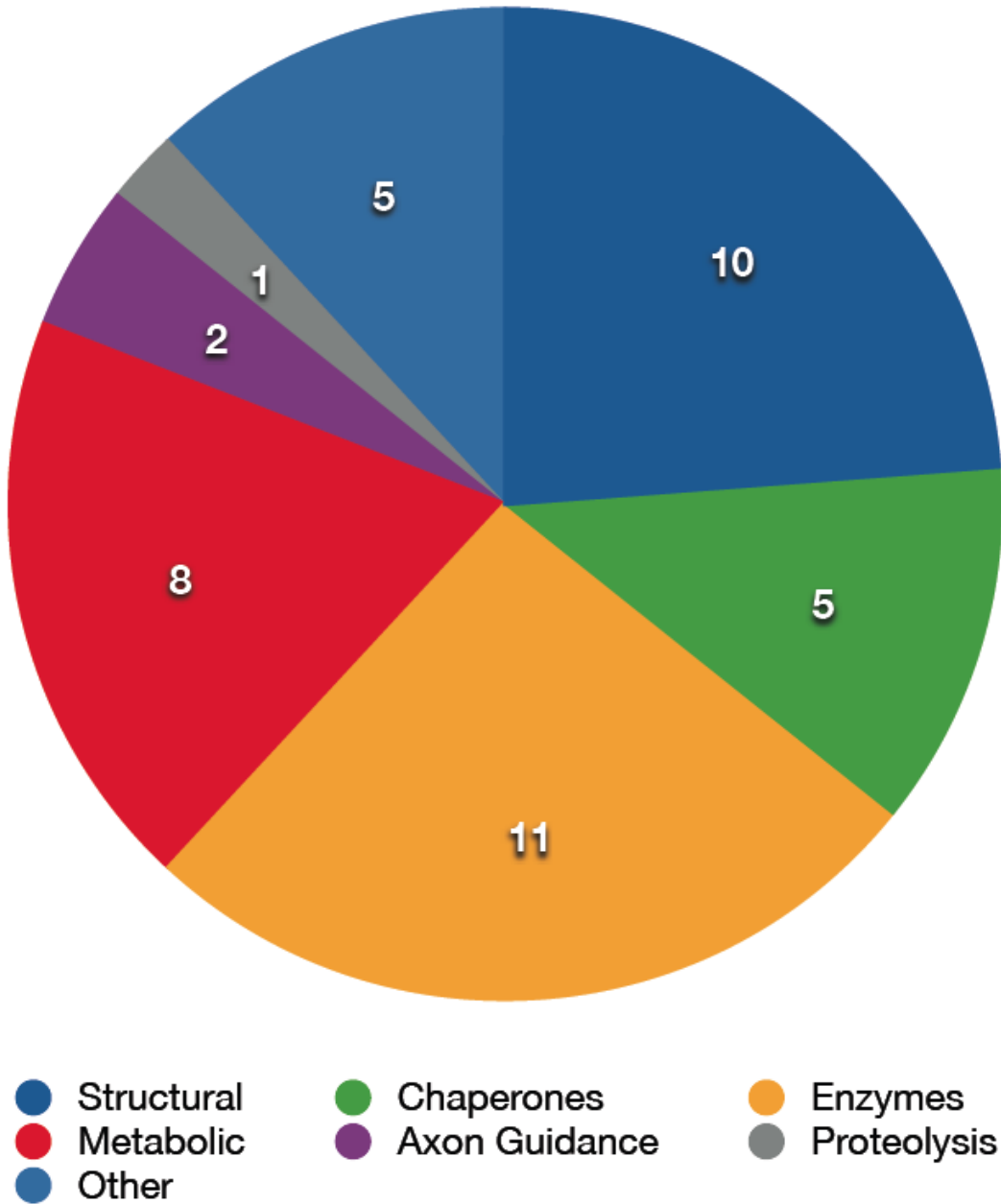


Figure 2.10: Functions of protein candidates found to be differentially expressed across contralateral and ipsilateral ocular dominance columns. Forty-two protein candidates were found to be differentially expressed across contralateral and ipsilateral ocular dominance columns. The number of candidates found in each functional category is displayed inside of each pie slice. The majority of protein candidates were enzymes (11, 26.19%). Minority fractions of the candidates were involved in structural (10, 23.81%), metabolic (8, 19.05%), chaperone (5, 11.94%), axon guidance (2, 4.76%), and proteolysis (1, 2.38%), or other (5, 11.94%) functions.

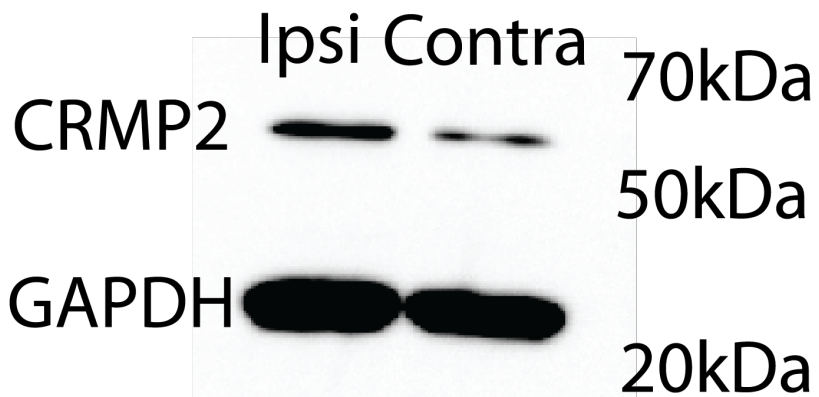


Figure 2.11: Western blot of ipsilateral and contralateral ocular dominance column CRMP2 expression. Western blot reveals a relative abundance of CRMP2 expression in ipsilateral ocular dominance column samples relative to contralateral ocular dominance column samples. Glyceraldehyde 3-phosphate dehydrogenase (GAPDH), a ubiquitous metabolic protein found in the brain is used as a control. CRMP2 bands run at 60 kDa in good agreement with the known mass of human CRMP2 at 62,294 Da.

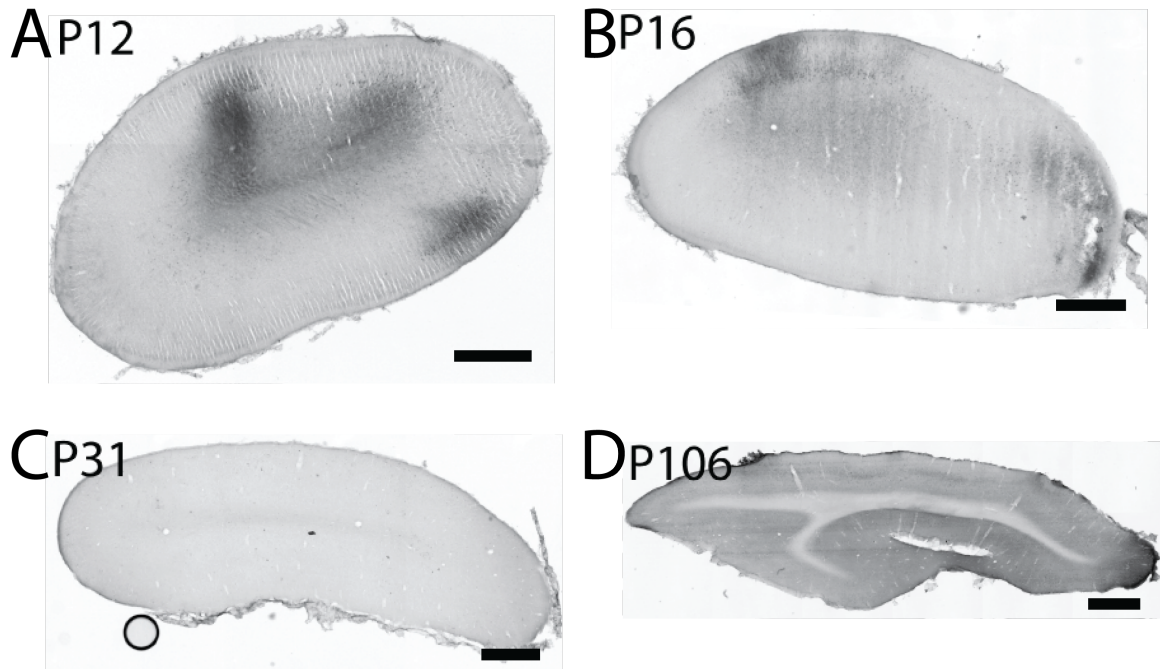


Figure 2.12: Time-course of CRMP2 expression in the visual cortex. Immunohistochemical staining against CRMP2 reveals an early phase of CRMP2 expression (P12 and P16, A and B) that is localized to discrete patches in the neuropil. CRMP2 patches have variable size and spacing making it unlikely that they are marking ocular dominance columns. Animals in the early critical period do not show robust CRMP2 expression (P31, C). Toward the end of the critical period and into adulthood, animals begin to show expression of CRMP2 in a small band of cells across the medial to lateral extent of the visual cortex. Scale bars = 200 $\mu$ m.

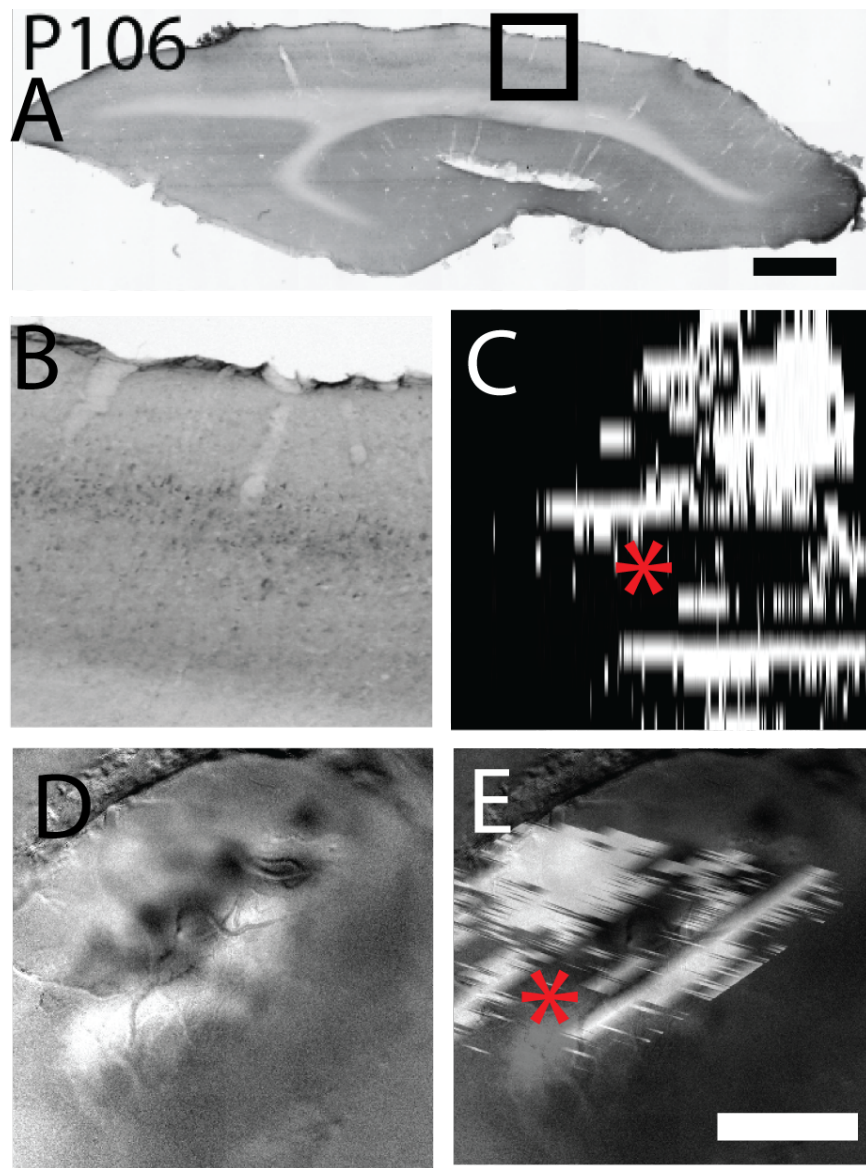


Figure 2.13: CRMP2 is expressed near the V1/V2 border in the mature visual cortex. A, coronal section through a P106 ferret cortex stained for CRMP2. Positively expressing cells appear as a dark stain. A thin band of cells express CRMP2 across the medial to lateral extent of the cortex. B, higher magnification view of the box in A. C, dorsal view of a reconstruction of sequential coronal sections through the cortex. Areas that are positive for CRMP2 expression appear as black patches. D, Ocular dominance map from the same animal. E, overlay of the slice reconstruction series on the functional map in D. The overlay was warped based on marker injections made into the cortex and reconstructed post mortem (not shown). The red asterisk in C and E denotes the position of the slice shown in A and B in the coronal series. Scale bars = 200 $\mu$ m.

Table 2.5: List of protein candidates found to be differentially expressed across ipsilateral and contralateral ocular dominance columns

Protein Name	Expression Direction	Total Hits	EI (I-C) / (I+C)	Matched Species	MW (Da)	pH	Score	Coverage
beta actin	None	4	0	Homo sapiens	42080	5.37	80, 123, 94, 99	30, 47, 34, 45
alpha tubulin	Contra	3	-0.333	Canis familiaris	46781	4.96	139, 169, 107	41, 71, 32
mitochondrial complex beta				Lepus europaeus	44347	5.25	217, 234, 116	46, 60, 28
ATP synthase,F1	Contra	3	-1	Canis familiaris	47821	4.64	93, 97,120	29, 45,47
NADH dehydrogenase	Ipsi	3	1	Homo sapiens	80498	6.11	98,82, 17	24, 39,
collapsin response mediator protein 2	Ipsi	2	1	Canis familiaris	62622	5.95	167, 245	50, 60
Annexin A5	Contra	2	-1	Rattus norvegicus	75706	5.39	75, 165	10, 44
creatine kinase beta	Contra	2	-1	Equus caballus	42926	5.47	78, 82	31, 34
calmodulin isoform 3	None	2	0	Canis familiaris	19144	4.17	88,72	39,35
adenosylhomocysteinate	Contra	1	-1	Canis familiaris	48341	5.82	74	37
fibrinogen, gamma chain	A Ipsi	1	1	Mustela putorius	36053	5.72	91	27
alpha enolase	Ipsi	1	1	Equus caballus	47509	6.37	150	47
Continued on next page								

guanine nucleotide binding protein, beta 1		Contra	1	-1	Canis familiaris	38494	5.61	117	41
ubiquitin carboxy-terminal hydrolase L1		Contra	1	-1	Equus caballus	15865	5.47	137	66
70Kd heat shock protein 8 isoform 2	Ipsi		1	1	Mus musculus	50547	6.17	138	32
Glycogen phosphorylase, Isoform 3		Contra	1	-1	Canis familiaris	96551	6.77	151	26
mitochondrial aconitase 2	Ipsi		1	1	Canis familiaris	85639	8.61	157	23
heat shock 70kDa protein 9B isoform 1	Ipsi		1	1	Pan troglodytes	66788	5.5	180	30
gamma enolase	Contra		1	-1	Canis familiaris	45018	5.04	211	60
Clatherin heavy chain 1 isoform 4		Contra	1	-1	Macaca mulatta	182336	5.41	278	21
ATPase, VI subunit B	Ipsi		1	1	Bos taurus	52613	5.3	296	64
topoisomerase (DNA) III alpha isoform 1		Contra	1	-1	Pan troglodytes	105477	8.22	71	12
oxoglutarate dehydrogenase-like, isoform CRA		Ipsi		1	Homo sapiens	109964	5.96	73	16
septin 2		Contra	1	-1	Homo sapiens	42348	6.05	73	42
DJ-1 (Parkinson disease protein 7 homolog)	(Parkinson disease protein 7 homolog)	Contra	1	-1	Pan troglodytes	21366	6.44	75	40
Continued on next page									

hemoglobin beta subunit	Contra	1	-1	Meles meles	16098	7.96	75	45
2- phosphoglycerate dehydratase	Ipsi	1	1	Canis familiaris	32591	5.78	77	37
70kd Heat Shock Cognate								
Protein Atpase	Ipsi	1	1	Bos taurus	41971	6.36	77	24
Domain, Chain A								
sirtuin 2	Contra	1	-1	Bos taurus	42131	5.49	77	22
clathrin coat assembly pro- tein AP180	Contra	1	-1	Canis familiaris	63299	8.95	78	28
dynamin	Ipsi	1	1	Homo sapiens	97745	6.93	78	20
calcineurin, chain A	Ipsi	1	1	Homo sapiens	43621	5.34	80	38
heat shock protein 60 (GroEL)	Ipsi	1	1	Rattus norvegicus	58061	5.35	80	19
splicing factor proline/glutamin rich (polypyrim- idine tract binding protein associated)	Ipsi	1	1	Homo sapiens	66351	9.42	81	24
14-3-3 protein gamma (Pro- tein kinase C inhibitor protein 1) (KCIP-1)	Ipsi	1	1	Rattus norvegicus	28154	4.8	82	26
collapsin response me- diator protein	Contra	1	-1	Canis familiaris	74485	6.67	84	28
1								
Continued on next page								

peroxiredoxin 2 isoform a	Ipsi	1	1	Homo sapiens	22049	5.66	84	43
Ribose- phosphate pyrophosphok- inase I	Contra	1	-1	Bos taurus	31885	6.39	84	45
voltage gated calcium chan- nel alpha 2	Ipsi	1	1	Sus scrofa	124271	5.11 84	15	
Isocitrate de- hydrogenase [NAD] subunit alpha	Contra	1	-1	Canis famili- aris	40049	6.47	87	30
rab GDI	Contra	1	-1	Homo sapiens	51088	5.94	88	43
Spectrin alpha chain	Contra	1	-1	Canis famili- aris	296540	5.33	98	10

Protein candidates are ordered by highest score from top to bottom. EI: expression index defined as (Ipsilateral expression - Contralateral Expression)/(Ipsilateral expression + Contralateral Expression). Matched Species: identity of the species to which the MS data was matched. MW: predicted molecular weight in daltons. pH: predicted pH. Score: MASCOT score. Coverage: percent of sequence covered by the MASCOT match.

Table 2.6: List of cortical protein candidates sub-cellular locations and functions

Protein Name	Protein Location	Protein Function
14-3-3 protein gamma (Protein kinase C inhibitor protein 1) (KCIP-1)	cytoplasm	Structural
2-phosphoglycerate dehydratase	cytoplasm	Metabolic
70kd Heat Shock Cognate Protein Atpase Domain, Chain A	cytoplasm	Chaperones
70Kd heat shock protein 8 isoform 2	cytoplasm	Chaperones
adenosylhomocysteinase	cytoplasm	Enzymes
alpha enolase	cytoplasm	Enzymes
alpha tubulin	cytoskeleton	Structural
Annexin A5	cytoplasm	Structural
ATPase, VI subunit B	mitochondria	Metabolic
beta actin	cytoskeleton	Structural
beta tubulin	cytoskeleton	Structural
calcineurin, chain A	cytoplasm	Enzymes
calmodulin 1 isoform 3	cytoplasm	Enzymes
Clatherin heavy chain 1 isoform 4	cytoplasm	Structural
clathrin coat assembly protein AP180	nucleus	Structural
collapsin response mediator protein 1	cytoplasm	Axon Guidance
collapsin response mediator protein 2	cytoplasm	Axon Guidance
creatine kinase beta	cytoplasm	Metabolic
DJ-1 (Parkinson disease protein 7 homolog)	cytoplasm	Chaperones
dynamin	cytoplasm	Structural
fibrinogen, gamma A chain	mitochondria	Other
gamma enolase	cytoplasm	Enzymes
Glycogen phosphorylase, Isoform 3	cytoplasm	Enzymes
guanine nucleotide binding protein, beta 1	cytoskeleton	Other
heat shock 70kDa protein 9B isoform 1	mitochondria	Chaperones
heat shock protein 60 (GroEL)	mitochondria	Chaperones
hemoglobin beta subunit	cytoplasm	Other
Isocitrate dehydrogenase [NAD] subunit alpha	cytoplasm	Metabolic
mitochondrial aconitase 2	mitochondria	Metabolic
mitochondrial ATP synthase,F1 complex beta sub	mitochondria	Metabolic
NADH dehydrogenase	mitochondria	Metabolic
oxoglutarate dehydrogenase-like, isoform CRA	mitochondria	Metabolic

Continued on next page

peroxiredoxin 2 isoform a	cytoplasm	Enzymes
rab GDI	endoplasmic reticulum	Enzymes
Ribose-phosphate pyrophosphokinase I	cytoplasm	Enzymes
septin 2	cytoplasm	Enzymes
sirtuin 2	cytoplasm	Structural
Spectrin alpha chain	nucleus	Structural
splicing factor proline/glutamine-rich (polypyrimidine tract binding protein as- sociated), isoform CRAe [Homo sapiens]	nucleus	Other
topoisomerase (DNA) III alpha isoform 1	nucleus	Enzymes
ubiquitin carboxy-terminal hydrolase L1	cytoplasm	Proteolysis
voltage gated calcium channel alpha 2	plasma membrane	Other

Protein candidates are listed alphabetically. All sub-cellular location and function category assignments are based off of protein candidate entries in the UniProt online database (Jain et al., 2009).

## 2.4 Conclusions

### 2.4.1 Summary of findings

At three different levels in the developing visual system (the retina, the LGN, and the visual cortex), I have demonstrated that it is possible to isolate tissue samples for the characterization of genes and/or proteins differentially expressed across circuits that take part in ocular dominance. In the retina, a simple dissection yielding temporal and nasal portions of the retina facilitates contrasts between portions of the retina that project to the ipsilateral LGN vs. those that project to the contralateral LGN. In the LGN, micro-dissection of fluorescently labeled eye specific laminae yields comparisons of samples that process ipsilateral stimuli to contralateral stimuli. In the visual

cortex, functionally guided ocular dominance column biopsies do the same. I have chose to explore these contrasts at the protein level using 2D-DIGE, MALDI-TOF mass spectroscopy, and immunochemistry. Differentially expressed proteins could be isolated from all three levels of the visual system. However, only a small portion of the isolated proteins were isolated again in replicate trials. One protein at each level of the visual system was chosen for further characterization using immunohistochemistry. In the retina, munc13-3 appeared to be expressed in higher abundance in the temporal retina in accord with its differential expression in 2D-DIGE experiments. CRMP4 was found to be expressed at the interlaminar zones in the LGN (see chapters 3 and 4), highlighting both the success of my approach in identifying protein candidates and a possible limitation of the sampling technique used in the LGN. In the cortex, CRMP2 was found to be expressed in ipsilateral ocular dominance columns near the V1/V2 border both in young and adult animals, but not during the beginning of the visual critical period. CRMP2 may thus play a role in the development and maintenance of ocular dominance and/or the V1/V2 border.

#### **2.4.2 Pitfalls and limitations**

This study can be broken down into two major phases. First, the collection of sample tissue and then processing of the generated samples using 2D-DIGE. I will treat them separately here.

First, the process of collecting tissue samples under this methodology is fairly straight forward, but could be improved. In the retina, the manual dissection of the temporal and nasal retina could be improved with the use of a fluorescent label such as and

alexa conjugated -subunit of cholera toxin as is used in LGN dissections. If introduced into one of the LGNs *in vivo* retrogradely label the axons entering that LGN from both eyes and greatly improve the accuracy with which the temporal and nasal samples from the retina could be isolated. In both the retina and the LGN, tissue dissection specificity could be greatly improved by using laser micro-dissection in place of manual dissection.

Second, the process of tissue sample comparison using 2D-DIGE followed by MALD-TOF mass spectroscopy suffers from a number of drawbacks as it is presented here. First, the fidelity with which it is possible to identify ferret proteins is rather low. The ferret genome is not sequenced as thus one must rely on matching mass spectroscopy data from the ferret to other mammalian species in order to positively identify differentially expressed proteins. This fact impacts the reliability of these experiments dramatically. Doing similar experiments in the mouse visual system would yield more reliable data for the retina and LGN where the visual structures in place are analogous to the ferret. Additional complexity is introduced to these experiments when immunohistochemistry and western blot are used to confirm candidate expression. Private and commercial antibodies are largely untested in the ferret and yield highly variable results when used in the ferret. The binding of an antibody to its analogous epitope in the ferret is not guaranteed and is often poor. These factors again make it difficult to perform a screen of this type in the ferret.

### **2.4.3 Discussion**

#### **Novel tissue sampling paradigm**

The main success of this work is the establishment of a pipeline for the isolation of tissue samples that can be used to explore molecular or genetic influences on ocular dominance development. This pipeline could easily be used as a front end for a number of different methodologies across many species for the exploration of ocular dominance. Our attempt to use 2D-DIGE as a back end screen for this sampling methodology was aimed at generating data on the protein level as opposed to the gene level. In order to increase the fidelity with which these studies could be carried out, it will be necessary to work in a species that has a sequenced genome. I have already highlighted some of the drawbacks of using 2D-DIGE in the ferret as a screening methodology after tissue sampling. More success could certainly be achieved by changing experimental model system to the mouse. My tissue sampling strategy could also yield further insight into regulation of gene expression across ocular dominance pathways. Previously, Corriveau et al used differential mRNA display in the cat to explore the contribution of endogenous neural activity on gene expression in the LGN (Corriveau et al., 1998). Their methodology could easily be used as a screen for ocular dominance related genes using the tissue sampling strategies presented here. Additional methods such as those leveraging DNA microarrays and RT-PCR similar to Tropea et als exploration on the impact of visual deprivation on gene expression (Tropea et al., 2006) could yield insight into ocular dominance related gene expression.

### **Collapsin response mediator proteins**

It is of note that multiple members of the collapsin response mediator protein family were identified in both the LGN and cortical screens performed in this chapter. CRMP1, CRMP2, and CRMP4 were identified in the comparison of the A vs. A1 lamina in the LGN. There does not appear to be a consistent pattern of expression across these candidates found in the LGN. CRMP1 was identified as an A candidate, CRMP2 was identified as both an A and an A1 candidate, and although CRMP4 was identified as an A candidate it is only expressed at the interlaminar zones of the LGN (see chapter 3 and 4). CRMP1 and CRMP2 were identified in the comparison of ipsilateral and contralateral ocular dominance columns in the cortex. Again, these candidates do not show a consistent expression direction. CRMP1 was identified once as a contralateral candidate and CRMP2 was identified twice as an ipsilateral candidate.

Given the variability in the apparent expression of the CRMP family members in both the LGN and the cortex, it is unlikely that the family plays a consistent role in development of the visual system. It is more likely that the different family members serve different purposes during development (see section 5.3 for a detailed discussion of possible mechanisms of CRMP4 during development). The CRMP family is one known to mediate a variety functions (Schmidt and Strittmatter, 2007) in neural development and I suspect that this variety is preserved in the development of the visual system.

### **Metabolic proteins**

Another trend in the data presented here that may be noteworthy is that fact that there are a number of metabolic proteins represented. Across the experiments conducted in the retina, LGN, and cortex, eleven proteins with metabolic functions were identified as candidates. Of these eleven proteins, six proteins were identified in the contralateral processing stream and five proteins were found in the ipsilateral processing stream. Without a consistent trend across the processing streams in the retina, LGN and cortex, it is hard to draw a conclusion about the role of metabolic proteins in the development of the visual system.

# Chapter 3

## Developmentally regulated expression of collapsin response mediator protein 4 in the interlaminar zones of the lateral geniculate nucleus

### Abstract

Eye-Specific inputs are separated from each other in the first processing stages of the mammalian visual system. During development, retinal ganglion cell axons from the two eyes move from an initially overlapping state in the lateral geniculate nucleus (LGN) to one in which eye-specific projections are segregated into discrete LGN laminae, defined both anatomically and physiologically. This process is dependent on both activity and molecular paradigms. Here, we report the spatiotemporal distribution of a novel and developmentally regulated molecular marker for LGN lamination; collapsin response mediator protein 4 (CRMP4) in normal ferrets. To determine whether CRMP4 expression is

a conserved feature of mammalian LGN development, we also explore CRMP4 in the mouse and macaque. CRMP4 expression in all three species delineates cytoarchitectonic boundaries in the developing LGN. Our data implicate CRMP4 as a patterning force that operates at LGN laminar boundaries to fine tune and maintain the locations of eye-specific projections in the nucleus after basic relationships between the retina and LGN layers have been established.

### 3.1 Introduction

In binocular mammals, the LGN receives information from both eyes but separates eye-specific inputs into anatomically and physiologically defined laminae. In the adult ferret, retinal afferents originating in the contralateral and ipsilateral retina have major terminations in the A and A1 layers of the LGN, respectively. Additionally, retinal ganglion cell terminations define the three retinorecipient C layers (Linden et al., 1981a; Cucchiaro and Guillery, 1984). Each of these laminae is bounded by cell sparse interlaminar zones. All of these structures develop postnatally in the ferret. At first, cytoarchitectonic laminae and interlaminar zones are not distinguishable and retinal projections from both eyes are intermingled (Linden et al., 1981b; Shatz, 1983; Sretavan and Shatz, 1986b). Over the first ten days of postnatal development, segregation of retinal afferents into eye-specific projections is largely completed, followed by separation of laminae with cell sparse zones within the next week, and adult morphology by the fourth postnatal week (Linden et al.,

1981a; Huberman et al., 2002). The mature A and A1 laminae are further divided into ON and OFF sub-laminar zones. At these ON/OFF boundaries, there are minor cell sparse zones (Stryker and Zahs, 1983).

The refinement of eye-specific inputs and the development of cytoarchitectural laminae in the LGN occur in a developmental epoch characterized by both patterned neural activity and patterned gene expression. Although patterns of neuronal activity are known to be essential for instructing the maturation of the LGN (Sretavan and Shatz, 1986b), less is known about the contribution of molecular paradigms to LGN development. To date, the best example of a molecular paradigm at work in LGN patterning is that of the Eph receptor family of molecules and their ligands, the ephrins. The Ephrin family is known for its role in retinotopy development in the LGN (Pfeiffenberger et al., 2006) but these molecules also influence eye-specific segregation after the initial period of retinal afferent overlap in the LGN (Drescher et al., 1995; Flanagan and Vanderhaeghen, 1998; Huberman et al., 2005; Pfeiffenberger et al., 2005).

Here, we report the spatiotemporal distribution of collapsin response mediator protein 4 (CRMP4, also known as dihydropyrimidinase-like 3/DPYSL3), a novel and developmentally regulated molecular marker for LGN lamination, in normal ferrets as well as in the normal mouse and macaque. CRMP family members have been implicated in growth cone dynamics and guidance and are differentially expressed across the central nervous system (Wang and Strittmatter, 1996). CRMP2, CRMP4, and CRMP5 show developmentally regulated expression profiles in cat primary visual cortex, indicating a possible role for the CRMP family in

visual system patterning (Cnops et al., 2004; Cnops et al., 2006; Van den Bergh et al., 2006a). Consistent with a putative role in neural patterning, juvenile CRMP4 expression is high and adult expression is low (Cnops et al., 2004; Cnops et al., 2006; Van den Bergh et al., 2006a). We hypothesize that spatially confined expression of CRMP4 in the normally developing LGN may act to fine tune retinal axon locations after their initial positioning by early activity dependent and molecular paradigms.

## 3.2 Materials and methods

### 3.2.1 Ferret and mouse tissue preparation

All ferret and mouse experiments were conducted in accordance with protocols approved by the Carnegie Mellon University institutional animal care and use committee. Eighteen (9 normal, 5 monocular enucleate, 4 binocular enucleate) black sable ferrets (*Mustela putorius furo*) between the ages of postnatal day 2 (P2) and adulthood were sacrificed and perfused for histology. Ferrets were sacrificed with an overdose of sodium pentobarbital (250mg/kg) then perfused transcardially with 0.9% NaCl, 4% paraformaldehyde, and 4% parafomaldehyde with 30% sucrose, all in .1M phosphate buffer. Tissue was post-fixed for a minimum of 24 hours before sectioning. Horizontal LGN sections were made from one LGN per animal at 50 $\mu$ m using a freezing microtome. Mice were perfused in the same manner. Mouse brains were sectioned at 50 $\mu$ m in the coronal plane.

### **3.2.2 Macaque tissue preparation**

All procedures were performed according to National Institutes of Health guidelines and in strict compliance with institutional protocols of the California Regional Primate Center at the University of California, Davis. A timed-pregnant macaque was prepared for surgery under ketamine (10 mg/kg), and anesthesia was induced with 1.3% isoflurane. The fetus was delivered by cesarean section and killed by swift decapitation. The brain was removed from the skull and fixed in freshly prepared 4% paraformaldehyde in 0.1M phosphate buffered saline for 5 days then stored at 40C in phosphate buffered saline.

### **3.2.3 Immunohistochemistry**

CRMP4 LGN expression was characterized by immunohistochemical stains with a primary antibody against CRMP4 (1:500 dilution, cat. AB5454, Millipore, Billerica, MA) followed by a fluorescent secondary antibody (Alexa 594, 1:500 dilution, cat. A-11012, Invitrogen, Carlsbad, CA). The polyclonal primary antibody was raised against a synthetic sequence (YDG-PVFDLTTTPK) corresponding to amino acids 499-511 of human CRMP4a and amino acids 612-624 human CRMP4b. In the human, mouse, monkey, rat, and cat, the antibody is reported to react with two isoforms of CRMP4 running at 64kDa and 74kDa. The same protocol was used to visualize CRMP4 expression in mouse and macaque LGNs. This protocol was used to visualize CRMP4 in the retina of P14 and P40 ferrets in egg-yoke embedded horizontal sections made at 50m. Specificity of the CRMP4 primary antibody in ferret LGN tissue was tested using western blot. A single band at 62kDa was

observed in the western blot demonstrating that the antibody reacts specifically with a protein of a similar mass to that of rat CRMP4a and human CRMP4a (Figure 3.2).

### **3.2.4 Western Blotting**

CRMP4 was visualized in western blot using a chemiluminescent substrate (cat. 34077, Fisher, Pittsburgh, PA) after incubation with the same anti-CRMP4 primary antibody used in all immunohistochemical reactions for this study (1:2,500 dilution) and an HRP conjugated secondary antibody (1:2,000 dilution, cat. 111-035-003, Jackson, West Grove, PA). Glyceraldehyde 3-phosphate dehydrogenase (GAPDH) expression was used as a loading control and was visualized after incubation with an anti-GAPDH antibody(1:10,000 dilution, cat. MAB374, Millipore, Billerica, MA) and an HRP conjugated secondary antibody (1:2,000 dilution, cat. 15-035-003, Jackson, West Grove, PA).

### **3.2.5 Myelin staining**

Myelin expression was characterized using a modified Gallyas stain as described previously (Gallyas, 1979; Pistorio et al., 2006). Briefly, tissue sections are fixed thoroughly before impregnation with ammoniacal silver nitrate and development in ammonium nitrate, silver nitrate, and tungstosilic acid.

### **3.2.6 Image analysis**

All images were acquired and analyzed at a resolution of .995m/pixel. To quantify the immunhistochemical staining pat-

terns observed in the ferret LGN, a custom MATLAB software package was employed. Using this software, a contour was drawn at the medial boundary of the binocular LGN between the PGN and the LGN. At every pixel along the drawn contour (pixel resolution = .995m/pixel), lines spanning the medial to lateral axis of the LGN were extended perpendicular to the drawn contour. The middle 25 lines (blue overlay in figure 3.2a) were considered for further analysis, thus ensuring that only the center of the binocular region was used for CRMP4 characterization. For the pixel resolution these analyses were carried out at, the central region of 25 lines corresponded to a region of interest 24.8m wide across the anterior to posterior axis. This width was chosen as a reasonable optimization between the noise reduction and laminar aliasing that occur by averaging in the anterior to posterior axis. Laminar regions and interlaminar zones were manually identified in the average linescan and the summed expression for each was calculated. In all slices where LGN layers could be clearly identified, the ratio of the interlaminar and laminar CRMP4 expression to background staining in the PGN was calculated. For the data presented in this paper, four to seven sequential slices per LGN were quantified according to equation 3.1.

$$\text{RelativeFluorescence} = \frac{\text{LocalFluorescence}}{\text{PGNFluorescence}} * 100 \quad (3.1)$$

Using this method, relative fluorescence was measured at the following locations: PGN-A interlaminar zone, A lamina, A-A1 interlaminar zone, A1 lamina, A1-C interlaminar zone, C lami-nae, as well as the within layer ON/OFF boundaries. Measurements from the interlaminar zones and sublaminar boundaries

(PGN-A border, A-A1 border, A1-C border, A and A1 within layer ON/OFF boundaries) were averaged and compared to the average measurements from the main LGN layers (A, A1, C layers). Significant differences in staining between interlaminar zones and the main LGN layers were assessed by comparison of average relative fluorescence measurements (equation 1) using a paired t-test. Additional characterization of the CRMP4 expression pattern was carried out by separating the within layer ON/OFF boundaries of the A and A1 lamina from the interlaminar zones. In this analysis scheme, CRMP4 expression in the interlaminar zones (PGN-A border, A-A1 border, and A1-C border) and the within layer ON/OFF boundaries (A and A1 ON/OFF boundaries) were compared to main layer expression separately.

### 3.3 Results

In the ferret, there is no significant LGN CRMP4 staining during the first ten days of life (figure 3.1). By P12, there is significant CRMP4 expression in the interlaminar zones between the perigeniculate nucleus (PGN) and the LGN as well as at the boundaries between the A, A1, and C laminae. Additionally, there is sparse labeling in LGN cell bodies. This pattern is maintained throughout the next four weeks before tapering off and was not found after P45 (figure 3.1). Western blot against CRMP4 supports this observation, revealing a stronger band of expression for CRMP4 at P35 than at P55 (figure 3.2). Quantification using a semi-automated algorithm confirmed this developmental expression profile of CRMP4 in the LGN. CRMP4 expression in interlaminar zones is significantly higher than in

the laminar zones from P12 to P45 (paired t-test,  $p < .05$ )(gray box, figure 3.2d). In addition to the expression of CRMP4 in the interlaminar zones, there was weaker but significant (paired t-test,  $p < .05$ ) staining for CRMP4 at the location of the within layer ON/OFF boundaries in both layer A and A1, which have been defined both anatomically and physiologically in the ferret previously (Linden et al., 1981a; Stryker and Zahs, 1983). Staining at the within layer (A and A1) ON/OFF boundaries is significant in a more constrained developmental window (P25-45, figure 3.4) than in the interlaminar zones. Thus, CRMP4 expression in the normally developing LGN appears to be specific to the interlaminar zones and the within layer ON/OFF boundaries.

In the developing ferret retina, CRMP4 expression is concurrent with the LGN expression profile described above. Fibrous processes in the inner and outer plexiform layers are clearly visible along with a labeled subset of retinal ganglion cells (figure 3.5). CRMP4 positive retinal ganglion cell axons can be visualized running across the fiber layer of the retina and into the optic nerve head. This staining pattern was very clear in a P18 ferret and was still recognizable though not as robust at P40.

CRMP4 has been recently identified as a mediator of myelin dependent neurite outgrowth inhibition (Alabed et al ,2007; also see section 5.3.1). In order to determine if this may be a pathway in which CRMP4 is participating in the ferret LGN, I stained the developing ferret LGN for myelin using a modified Gallyas stain. There was a dense stain at the medial boundary of the nucleus as well as at the interlaminar zones in P40 ferret LGN (figure 3.6).

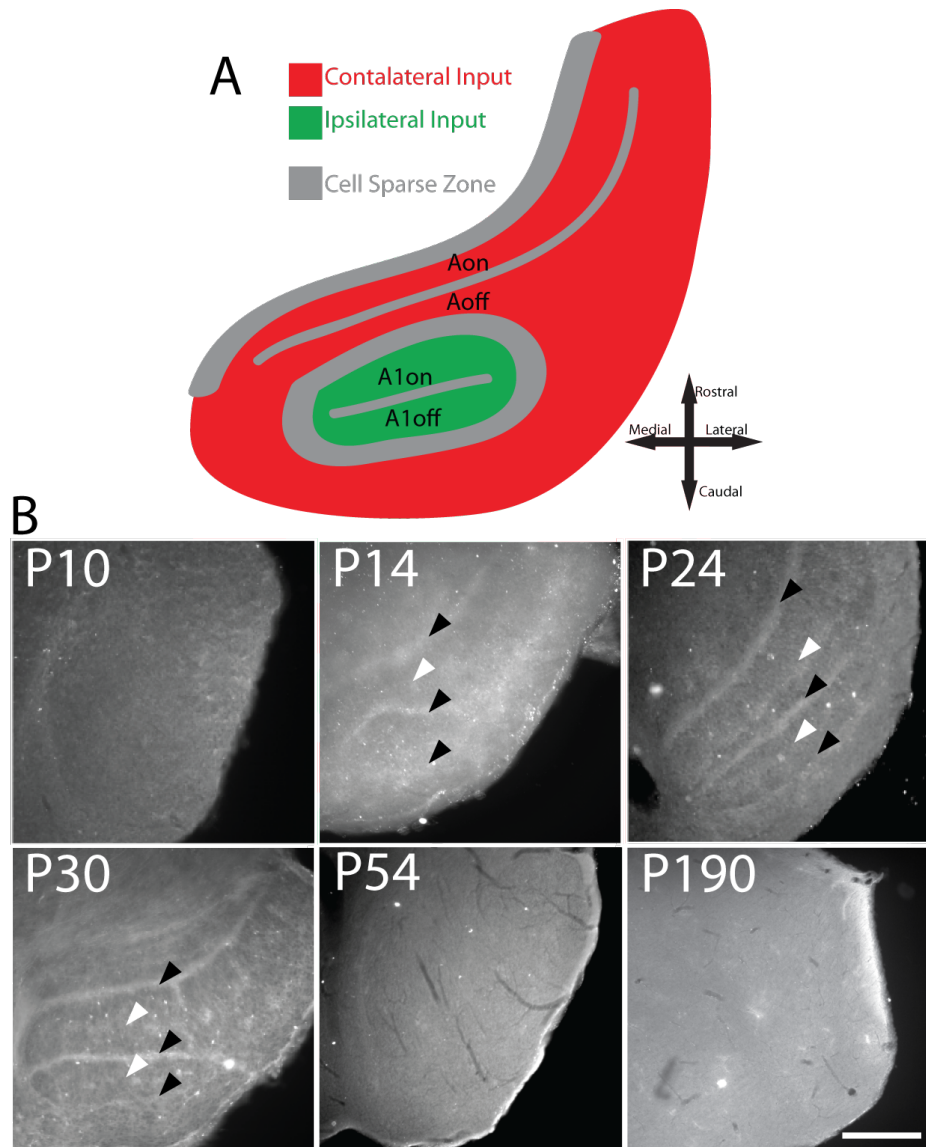


Figure 3.1: Developmentally regulated CRMP4 expression in LGN interlaminar zones of the ferret. A, schematic diagram of the ferret LGN. B, representative CRMP4 staining in horizontal LGN sections. Differential staining between the interlaminar zones and LGN laminae is only present between P12 and P45 (P14, P24, and P30 shown here). Younger (P10) and older animals (P54 and P190) do not show laminar expression of CRMP4. Black arrowheads indicate interlaminar zone staining and white arrowheads indicate staining at the within layer ON/OFF boundaries. Scale bar = 250?m, applies to all.

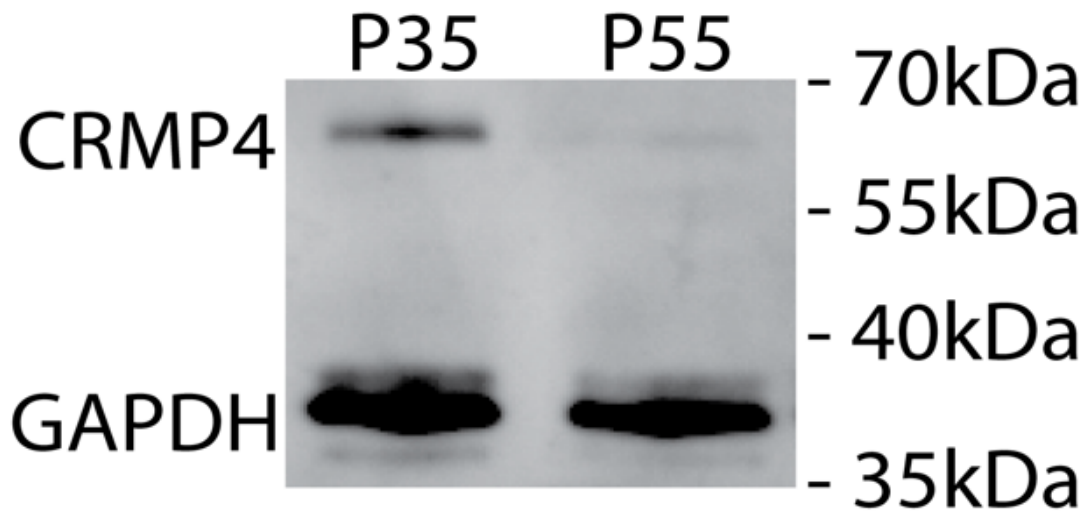


Figure 3.2: Expression of CRMP4 protein in the ferret LGN. Western blot of ferret LGN tissue shows a single immunoreactive band at 62kDa. This is the same as with the mass of CRMP4a in the human and the mouse. CRMP4 expression is strong at P35 and very weak at P55, mirroring its immunohistochemical staining of the LGN.

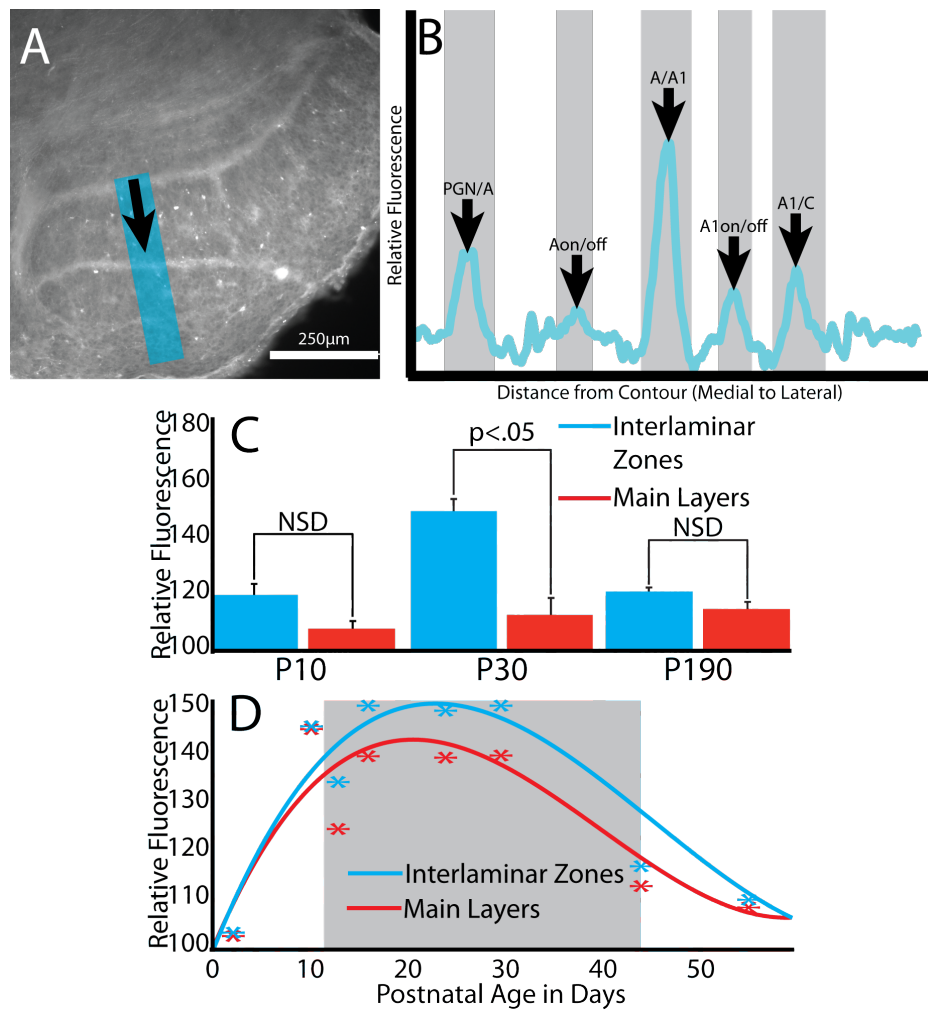


Figure 3.3: Quantification of developmentally regulated CRMP4 expression in the interlaminar zones of the ferret LGN. A, example analysis ROI for quantification of CRMP4 expression in the interlaminar zones of the LGN. The blue overlay is the portion of the LGN used for linescan analysis and the arrow denotes the direction of the linescan. B, a sample average linescan of 25 lines from the image shown in A. The blue line depicts the average linescan derived from the linescans falling in the blue overlay in A. Interlaminar zones and sublaminar boundaries are easily identifiable in the average linescan and are labeled here as well as indicated gray backgrounds. Identification of the interlaminar zones in this way allows for the comparison of interlaminar zone CRMP4 expression relative to the main layers of the LGN. C, example time-points from quantification of differential expression by linescan analysis. There is significant differential CRMP4 expression at P30, and no significant difference (NSD) at P10 or P190. C, Scatterplot of all quantified time-points for normal ferrets (asterisks correspond to individual animal data points) with best fit cubic spline curves overlaid. There is a significant increase in CRMP4 expression in the interlaminar layers over the main layers from P12 to P45 (gray box, students t-test,  $p < .05$ ).

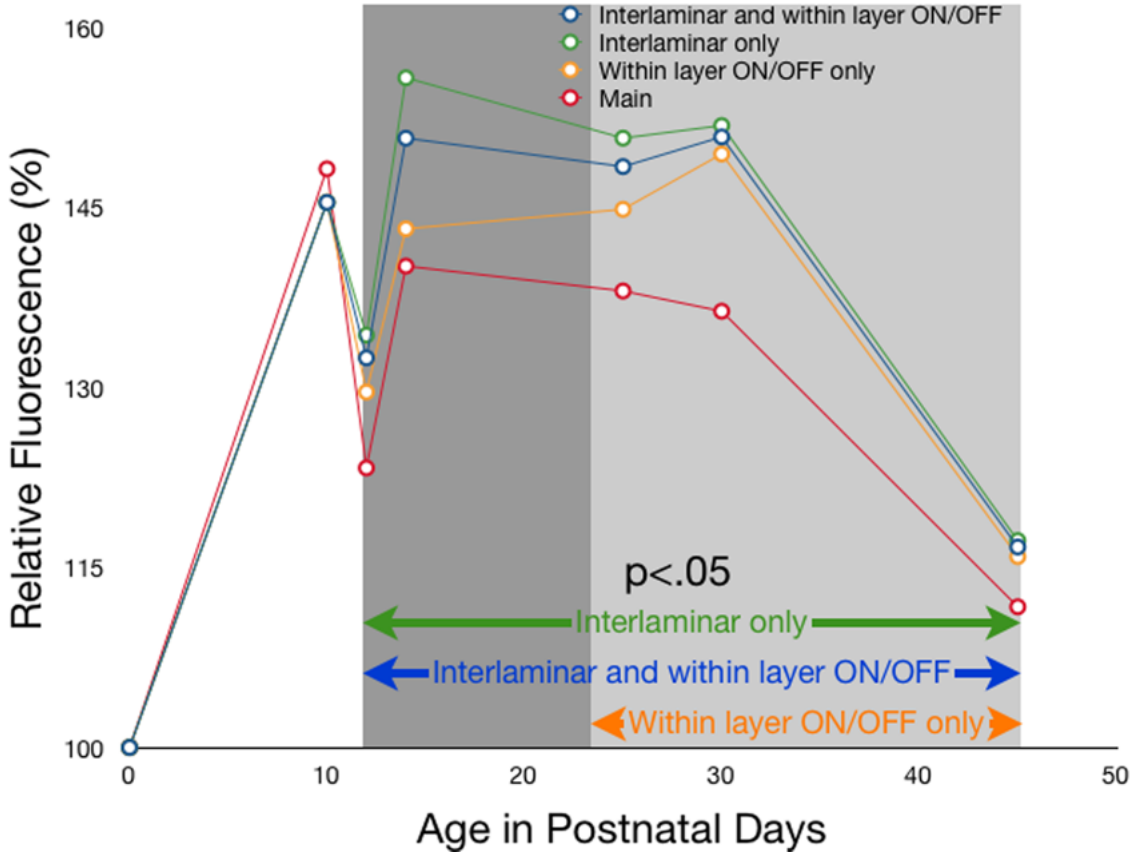


Figure 3.4: Developmentally regulated expression of CRMP4 in both the LGN interlaminar zones and within layer ON/OFF boundaries. The graph displays data for CRMP4 expression in the interlaminar zones and within layer ON/OFF boundaries together (blue line), interlaminar zones only (green line), within layer ON/OFF boundaries only (orange line), and the main LGN layers (red line). When the interlaminar zones and the within layer ON/OFF boundaries are considered together, there is significant CRMP4 expression above the main layers of the LGN between P12 and P45 (as reported in figure 3.2). If the interlaminar zones and ON/OFF boundaries are considered separately, both show significant CMRP4 expression within different but overlapping developmental windows. Interlaminar zone CRMP4 expression remains significant between P12 and P45 and the measured fluorescence is higher than when the within layer ON/OFF boundaries are included. The within layer ON/OFF boundaries express CRMP4 at a lower level that becomes significant by P25. CRMP4 expression in both the interlaminar zones and the within layer ON/OFF boundaries fades after P45 (non-significant time points above P45 are not pictured here).

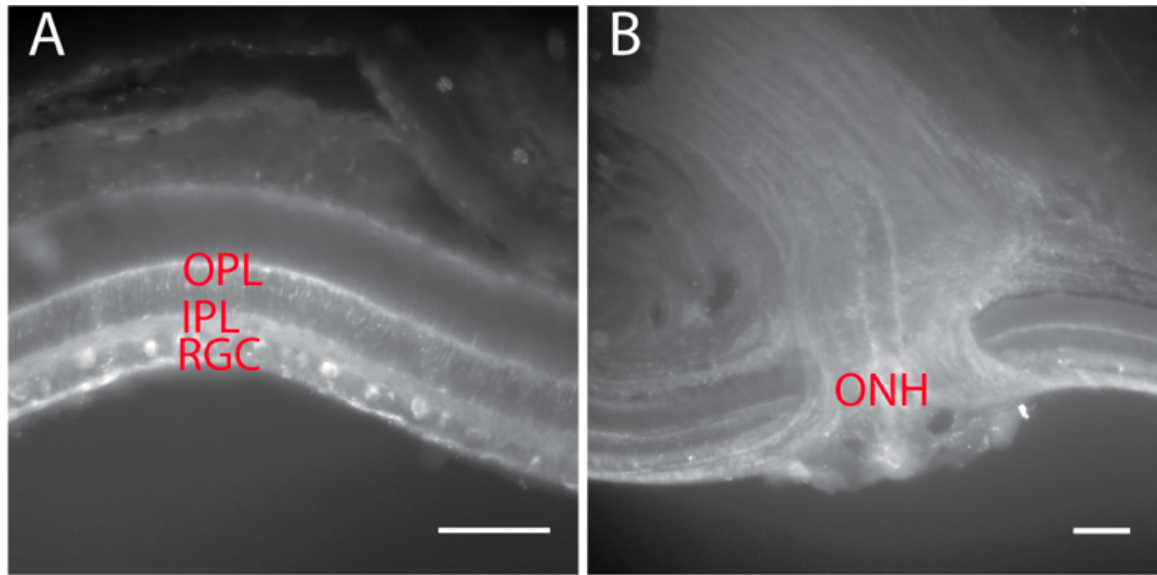


Figure 3.5: CRMP4 expression in the P14 ferret retina. A, CRMP4 is expressed in the outer plexiform (OPL), inner plexiform (IPL), and retinal ganglion cell (RGC) layers. A sub-set of retinal ganglion cell bodies are positive for CRMP4. CRMP4 positive ganglion cell axons are visible in the fiber layer of the retina (A, below RGC layer), the optic nerve head (ONH) and the optic nerve (B). Scale bars =  $50\mu\text{m}$ .

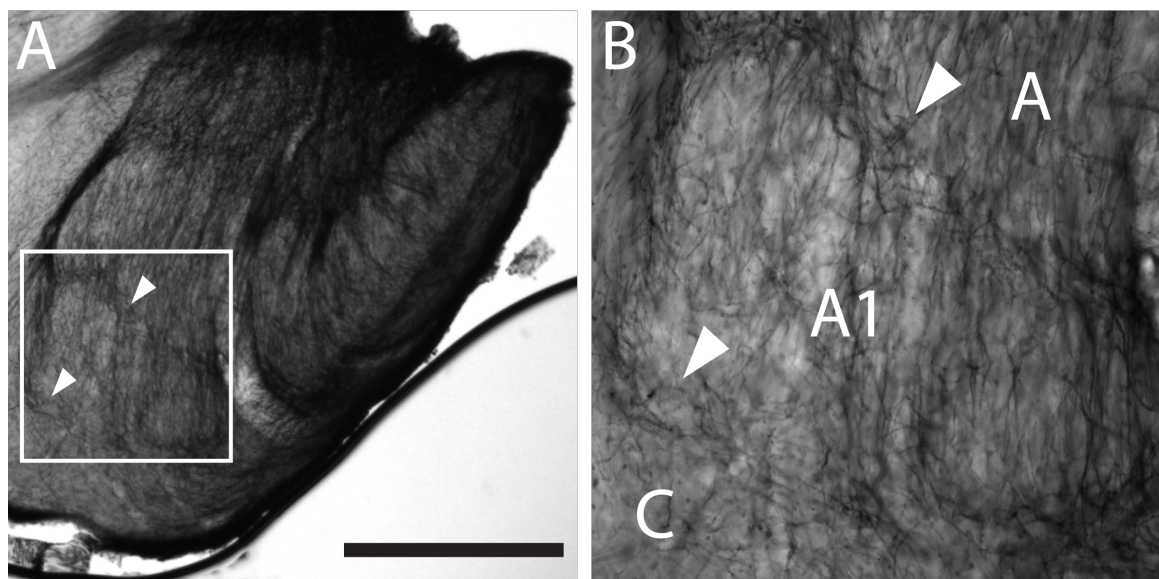


Figure 3.6: Myelin expression in the normal ferret LGN. A, modified gallyas stain for myelin in a P40 ferret LGN. The medial and rostral boundary of the nucleus shows dense myelin staining. In the nucleus, there is more myelinated processes in the interlaminar zones at the A/A1 and A1/C laminar boundaries (denoted by white arrows). B, higher magnification view of the white box in A with the A, A1, and C LGN laminae labeled. Scale bar = 500 $\mu$ m, applies to all.

## 3.4 Conclusions

### 3.4.1 Summary of findings

This study describes the developmentally regulated spatiotemporal expression profile of CRMP4 in the ferret LGN. Immunostaining against CRMP4 shows expression in the interlaminar zones of the LGN, at the medial boundary of the LGN (between the LGN and the PGN), at the boundaries between the A, A1, and C laminae, and at the within layer ON/OFF boundaries. CRMP4 expression at cytoarchitectonic boundary regions in the LGN is also observed in both the developing mouse and macaque LGN. In an E143 macaque, there is expression of CRMP4 in the interlaminar zones reminiscent of our observations in ferret. In the developing mouse, we found robust staining along the medial boundary of the nucleus in the external medullary lamina, but there is no interlaminar expression as is seen in the ferret and the macaque.

Expression of CRMP4 in LGN interlaminar zones is developmentally regulated. Our immunohistochemical stains against CRMP4 reveal a developmental window between P12 and P45 in which the interlaminar zones of the LGN are marked by CRMP4. This is supported by western blot analysis of P35 and P55 LGNs. A third confirmation of the presence of CRMP4 in the ferret LGN from this developmental epoch comes from additional work performed in our lab. CRMP4 has emerged as a laminar marker candidate in an unbiased proteomic screen for differential laminar expression during the final stages of LGN laminar development from P14-P25 (see chapter 2). While this screen was targeted at the molecular characterization of the A

and A1 LGN laminae, our finding of CRMP4 in this screen most likely the result of a small tissue sampling error. Accidental and biased Inclusion of the interlaminar zones into one laminar sample but not the other could result in the identification of an interlaminar marker in this screen.

I also show that CRMP4 is expressed in a subset of retinal ganglion cells during the same developmental epoch in which CRMP4 expression is seen in the LGN. It is likely that retinal ganglion cells are one of the major sources of interlaminar CRMP4 expression in the developing LGN.

### 3.4.2 Pitfalls and limitations

The main shortcoming of this work is the difficulty with which specific expression of CRMP4 in retinogeniculate axons can be determined. While it is clear that a subset of retinal ganglion cells express CRMP4 in the developing retina, it is not clear if they are the only source of CRMP4 in the developing LGN. I have attempted to use high resolution confocal imaging to co-localize cholera toxin  $\beta$ -subunit used as a retinogeniculate tracer (see 4.2 for specific methods) and CRMP4 expression with little definitive success. My attempts at co-localization have been hindered by the fidelity of our chosen CRMP4 antibody at small spatial scales. It is possible that the CRMP4 antibody used in these studies is less specific than we originally thought and that non-specificity only becomes apparent at high magnification. Given that this antibody has not been robustly characterized in the ferret certainly leaves this possibility open. Under high magnification, it is difficult to distinguish CRMP4 expression signal from background and as such it is difficult to

localize CRMP4 expression to retinogeniculate axons. An additional limitation of this study is the relative unavailability of macaque LGN tissue when compared with the ferret. I have robustly characterized the developmentally regulated expression of CRMP4 in the ferret and confirmed that the expression in the macaque LGN mirrors that of the ferret at a single developmentally matched time-point, but I was unable to explore CRMP4 expression in the macaque LGN throughout development.

### 3.4.3 Discussion

Expression of CRMP4 is seen in the interlaminar zones of both the ferret and the macaque during LGN development. CRMP4 is expressed at the medial boundary of the mouse LGN, but there is no laminar expression in the nucleus itself. The lack of laminar CRMP4 expression in the mouse LGN is consistent with CRMP4 as a marker protein for cytoarchitectonically defined boundaries in the nucleus. The mouse LGN has robustly segregated inputs from the two retinas (Godement et al., 1984; Torborg and Feller, 2004), but it lacks the cell sparse zones that accompany eye-specific layers in higher mammals. If CRMP4 delineates cytoarchitectonic boundary regions in the LGN, the presence of laminar CRMP4 expression in ferret and macaque but not in mouse is the expected result. CRMP family mediates axonal dynamics and in this role CRMP4 may help to delineate laminar boundaries through the reorganization of retinogeniculate processes at the cytoarchitectonic boundaries in the LGN where CRMP4 expression is high. Assuming this mode of action, it would be expected that the major source of LGN CRMP4 expression is retinogeniculate axons. CRMP4

expression is evident across the retina in a subset of retinal ganglion cells, lending support to this hypothesis.

The timing of CRMP4 interlaminar zone expression in the ferret LGN is developmentally relevant because this is when the LGN develops mature morphology (Linden et al., 1981a). The earliest expression of CRMP4 in the interlaminar zones is coincident with their initial formation. Before the onset of CRMP4 expression in the ferret LGN, eye-specific segregation of retinal afferents is essentially complete, but cell sparse interlaminar zones have not formed (Linden et al., 1981a).

The segregation of eye-specific inputs in the LGN has been shown to be dependent on both neural activity and molecular cues (Sretavan and Shatz, 1986b; Huberman et al., 2002; Huberman et al., 2005). Altering the expression of key proteins in the retina or the LGN leads to defects in retinothalamic projections, likely resulting from an aberrant molecular contribution to the balance between neural activity and gene expression (Huberman et al., 2005; Pfeiffenberger et al., 2005). A growing list of molecular candidates capable of altering the retinogeniculate projection at different phases of development have emerged over the past decade. These include the Zic family of zinc-finger transcription factors, which affect both the targeting of ipsilateral projections to the LGN and their elaboration once in the nucleus (Herrera et al., 2003; Horng et al., 2009), Ten-m3 which affects ipsilateral afferent targeting (Leamey et al., 2007), and the Ephrins and Eph receptors which mediate proper retinogeniculate targeting as well as topographic patterning (Flanagan and Vanderhaeghen, 1998; Frisen et al., 1998; Williams et al., 2003; Huberman et al., 2005; Pfeiffenberger et al., 2005). I propose that CRMP4 may be acting after these paradigms

have exerted their influence on the development of the LGN. I hypothesize that CRMP4 may fine tune and/or reinforce the final aspects of LGN segregation and lamination.

The CRMP family of phosphoproteins are mediators of semaphorin induced growth cone collapse and dynamics (Goshima et al., 1995) as well as mediators of neurite formation and extension (Inagaki et al., 2001; Fukata et al., 2002). As semaphorin is a diffuseable cue, it is unlikely that CRMP4 in the developing LGN is operating as a mediator of semaphorin signaling, because LGN CRMP4 expression is so spatially precise. Secondary functions of the CRMP family have also been described. CRMP2 has recently been shown to interact with the N-type presynaptic calcium channel CaV2.2, increasing their calcium current density (Brittain et al., 2009). If CRMP4 acted similarly, local modulation of presynaptic calcium levels could influence the behavior of retinal afferents at interlaminar regions by altering neurotransmitter release. However, this mechanism may not be consistent with neurite retraction from interlaminar zones. CRMP4 has also recently been shown to interact with RhoA as a mediator of myelin dependent neurite outgrowth inhibition (Alabed et al., 2007b). In humans and monkeys, the interlaminar zones of the LGN appear to be more heavily myelinated than the main layers of the LGN (Snider and Lee, 1961; Woolsey et al., 2003). My data also shows that the ferret LGN is more heavily myelinated at the cell sparse interlaminar zones. The formation of the interlaminar zones and concomitant increase in CRMP4 expression may reveal refinement of eye-specific projections through myelin dependent neurite outgrowth inhibition.

The spatiotemporal profile of retinogeniculate axon CRMP4 expression is consistent with a model in which CRMP4 helps to

fine tune or reinforce laminar boundaries. As the nucleus matures and begins to exhibit interlaminar zones, CRMP4 expression rises at these boundaries. Once the nucleus has reached its adult form, CRMP4 expression fades. Expression of CRMP4 in retinogeniculate axons could allow them to respond to increased myelination at the interlaminar zones, thus eliminating aberrant projections at LGN boundaries. Immunostains in the developing mouse and macaque LGNs show that CRMP4 expression is also present in these species during late LGN development, suggesting a conserved developmental mechanism. In the primate, the interlaminar zones of the LGN serve particular functions and are targeted by a specific class of retinal ganglion cells(Hendry and Yoshioka, 1994; Hendry and Reid, 2000). Specific expression of CRMP4 in a subset of retinal ganglion cells may reflect the repulsion of some retinal ganglion cell classes (e.g. magnocellular and parvocellular), but not others (e.g. koniocellular). As carnivores and rodents lack a koniocellular pathway, CRMP4 may promote more general refinement of retinal axons into appropriate LGN regions in these species.

# Chapter 4

## Expression of collapsin response mediator protein 4 in the presence of altered retinogeniculate input

### Abstract

Collapsin response mediator protein 4 (CRMP4) is expressed in the interlaminar zones of the developing lateral geniculate nucleus (LGN). CRMP4 expression in the LGN is highest during a developmental epoch in which eye specific segregation of retinal ganglion cells has taken place, but the final cytoarchitecture of the nucleus has not yet been established. The onset of CRMP4 expression is coincident with the formation of cell sparse interlaminar zones in the LGN and CRMP4 expression declines after the cytoarchitecture of the nucleus has reached a mature state. Here, I manipulate the normal development of LGN cytoarchitecture through binocular and monocular enucleation and disruption of cholinergic retinal waves with epibatidine. CRMP4 expression in the presence of aberrant LGN cytoarchitecture is then assayed using immunohisto-

**chemistry.** Enucleation alters the laminar boundaries and expression of CRMP4 in the LGN in a manner consistent with the altered distribution of retinal axons. Blockade of cholinergic retinal waves with epibatidine in the first ten days of life induces aberrant eye specific segregation of retinal ganglion cell afferents as well as abolishes both the formation of normal cell sparse interlaminar zones and CRMP4 expression. Taken Together, the expression pattern of CRMP4 in enucleate and epibatidine treated LGNs demonstrates that CRMP4 expression is driven by the morphology of cell sparse interlaminar zones and not by eye specific segregation.

## 4.1 Introduction

In the normal ferret, retinal afferents from both eyes are intermingled in the LGN at birth and become well segregated by P10 (Linden et al., 1981b). It is clear that the proper segregation of retinal afferents is dependent on the activity of the retinas themselves and is abolished by activity block in the retina (Penn et al., 1998b; Huberman et al., 2002). At birth, endogenous activity in the retina takes the form of traveling waves of cholinergic activity initiated in starburst amacrine cells (Feller et al., 1996; Penn et al., 1998b; Feller, 1999). This pattern of activity persists in the retina for the first two weeks of postnatal life. When retinal waves are blocked for the first ten days of life using epibatidine, a selective cholinergic blocker, the normal segregation of eye specific afferents in the LGN does not occur

and an overlapping distribution of afferents results (Penn et al., 1998b). If recovery is allowed after the initial blockade of retinal waves, segregation is achieved, but the retinal afferents fail to project into the correct LGN laminae. Further, the LGN fails to develop the normal cytoarchitecture associated with mature LGNs (Huberman et al., 2002).

The normal distribution of retinal afferents and organization of the cytoarchitecture in the LGN can also be manipulated by enucleation at birth. Binocular enucleation at birth degrades all retinal afferents in the LGN and eliminates lamination (Brunso-Bechtold and Casagrande, 1981). Monocular enucleation at birth causes the retinal afferents of the spared eye to gradually expand into the normal territory of the enucleated eye after the initial formation of the nucleus. By the third postnatal week, the afferents of the spared eye occupy the full volume of the nucleus (Guillery et al., 1985).

In the first part of this chapter, I confirm the above results from studies of epibatidine treatment as well as a report of epibatidine treatment shifting the ipsilateral projection along the medial to lateral axis of the LGN (Padmanabhan, 2008). Following my characterization of the impact of epibatidine on the projection pattern of retinal afferents in the LGN, I demonstrate that epibatidine treatment abolishes the normal pattern of CRMP4 expression in the LGN reported in chapter 3. In the second part of this chapter, I report the impact of binocular and monocular enucleation on the normal pattern of CRMP4 expression in the LGN.

## **4.2 Materials and methods**

### **4.2.1 Tissue preparation**

All ferret and mouse experiments were conducted in accordance with protocols approved by the Carnegie Mellon University institutional animal care and use committee. Seventeen ( 5 monocular enucleate, 4 binocular enucleate, 5 epibatidine treated, 3 saline controls) black sable ferrets (*Mustela putorius furo*) between the ages of postnatal day 0 (P0) and adulthood were sacrificed and perfused for histology following either enucleation or epibatidine treatment (see 4.2.2 and 4.2.3) and recovery. Ferrets were sacrificed with an overdose of sodium pentobarbital (250mg/kg) then perfused transcardially with 0.9% NaCl, 4% paraformaldehyde, and 4% parafomaldehyde with 30% sucrose, all in .1M phosphate buffer. Tissue was post-fixed for a minimum of 24 hours before sectioning. Horizontal LGN sections were made from one LGN per animal at 50 $\mu$ m using a freezing microtome.

### **4.2.2 Monocular and binocular enucleation**

Ferret enucleations were performed using hypothermia anesthesia and sterile technique on P0 as described previously (Crowley and Katz, 1999). Enucleated animals developed normally until they were processed as above. Two days before monocular enucleates were sacrificed, the spared eye was injected with cholera toxin  $\beta$ -subunit conjugated to alexa-488 under isoflurane anesthesia in order to visualize the organization of the retinogeniculate projection.

#### **4.2.3 Intravitreal application of epibatidine**

*In vivo* intravitreal application of epibatidine was carried out as previously described (Huberman et al., 2002). Briefly, ferrets were anesthetized with inhaled isoflurane and 1-2 $\mu$ l of epibatidine (1mM in sterile saline) or sterile saline was injected into the vitreous humor of each eye every 48 hours from P1 to P9. The animals were allowed to recover until P28 and injection of cholera toxin  $\beta$ -subunit conjugated to alexa-555 in one eye and cholera toxin  $\beta$ -subunit conjugated to alexa-647 in the other as above. Epibatidine or saline control animals were sacrificed at P30 and prepared for histology as described above.

#### **4.2.4 Immunohistochemistry**

Immunohistochemical stains against CRMP4 were carried out as described in 3.2.3.

#### **4.2.5 Myelin staining**

Myelin staining was carried out as described in 3.2.5.

#### **4.2.6 Image analysis for epibatidine disruption of retinothalamic projections**

All images were acquired and converted to binary images using maximum correlation thresholding (Padmanabhan et al., 2010). Percent overlap values for the contralateral and ipsilateral retinothalamic projection were calculated by counting the number of yellow pixels in binarized images vs. the total number of pixels in the projection domain. For the calculation of mediolateral and rostrocaudal position, the weighted centroid

of the ipsilateral projection was calculated and expressed as a normalized position along the two axes of the nucleus. For perimeter to area calculations, a single pixel edge was calculated around all projection domains. This edge was calculated by uniformly shrinking the boundaries of binarized projection domains and subtracting this shrunk version from the original binarized domain leaving a single pixel edge at the projection boundaries. The number of pixels in the edge regions was compared to the total number of pixels in the projection domains themselves for perimeter to area measures. All epibatidine morphological measures are same as used previously for the same analysis in our lab (Padmanabhan, 2008).

#### **4.2.7 Image analysis for laminar expression of CRMP4 and Myelin**

Analysis of CRMP4 and myelin laminar patterns was carried out as described in 3.2.6.

### **4.3 Results**

#### **4.3.1 Transient epibatidine block of retinal activity disrupts normal retinal projections, normal cytoarchitecture, and normal CRMP4 expression in the LGN**

Retinal activity was blocked using epibatidine for the first 10 days of postnatal life followed by recovery until P30. The resultant projection pattern and laminar organization of the LGN mirrored what has been previously reported (Huberman et al., 2002; Padmanabhan, 2008). In normal P30 ferrets there is a rather stereotyped retinothalamic connection and lamina-

tion pattern consisting of a single major projection of ipsilateral retinal ganglion cells to the A1 lamina and minor projection in the C1 lamina of the LGN (Linden et al., 1981b). Saline controls in the present study exhibit this typical morphology (figure 4.1a). Epibatidine treated animals did not show the normal projection and lamination pattern and were instead characterized by multiple major ipsilateral projections (figure 4.1b,c). In order to determine the degree to which the ipsilateral projection was scattered in epibatidine animals, I quantified the number of ipsilateral projections, ipsilateral projection surface area/volume ratio, and the contralateral surface area/volume ratio. There were significantly more ipsilateral projections to the LGNs of epibatidine animals (figure 4.1c, saline =  $1.0 \pm 0.0$  patches, epibatidine =  $3.2 \pm 0.2$  patches,  $P < .001$ , students t-test). There was also a significantly higher surface area/volume ratio of the ipsilateral projection in epibatidine animals (figure 4.1d, saline =  $0.037 \pm 0.005$ , epibatidine =  $0.070 \pm 0.006$ ,  $p = 0.004$ , students t-test), but not of the contralateral projection (figure 4.1e, saline =  $0.030 \pm 0.005$ , epibatidine =  $0.028 \pm 0.004$ ,  $p = .787$ , students t-test). Although the normal pattern of retinothalamic projections to the LGN was altered in these animals, there was no difference in the total volume of the contralateral (figure 4.2a, saline =  $81.84 \pm 2.83\%$ , epibatidine =  $86.48 \pm 2.00\%$ ,  $p = 0.12$ , students t-test) and ipsilateral (figure 4.2b, saline =  $18.67 \pm 3.50\%$ , epibatidine =  $14.53 \pm 2.26\%$ ,  $p = 0.22$ , students t-test) projections between saline controls and epibatidine treated animals. Further, the segregation between ipsilateral and contralateral projections was unchanged in epibatidine animals (figure 4.2c, saline percent overlap =  $0.64 \pm 0.45\%$ , epibatidine percent overlap =  $1.02 \pm 0.50\%$ ,  $p =$

.56, students t-test). In addition to the above measures, I quantified the mean rostrocaudal and mediolateral position of the ipsilateral projection in epibatidine treated animals (figure 4.3). There was no difference in the rostrocaudal position of the ipsilateral projection into the LGN (figure 4.3b, saline =  $0.71 \pm 0.04$ , epibatidine =  $0.75 \pm 0.04$ ,  $p = 0.43$ , students t-test), but there was a significant medial shift epibatidine treated animals (figure 4.3c, saline =  $0.50 \pm 0.04$ ,  $0.31 \pm 0.03$ ,  $P < 0.01$ , students t-test). All morphological parameters measured above are in agreement with previous studies of epibatidine treated animals in our lab (Padmanabhan, 2008).

In addition to the observed disruption in retinothalamic projection morphology, epibatidine treatment disrupts the normal cytoarchitecture of the LGN. In the normal P30 LGN, the laminae of the nucleus are separated by cell sparse interlaminar zones along with ON/OFF cell sparse sublaminar boundaries in the A and A1 laminae (Linden et al., 1981b; Stryker and Zahs, 1983). These cell sparse zones are abolished in my epibatidine treated animals (figure 4.4). The lack of cell sparse interlaminar zones in the epibatidine treated P30 ferret is consistent with previous work by Huberman et al (Huberman et al., 2002).

To assess the extent to which CRMP4 expression is linked to the normal eye specific segregation in the developing LGN, we stained epibatidine treated LGNs for CRMP4 at P30. Epibatidine treatment decouples eye specific segregation from lamination in the LGN and allows us to study the correlation of CRMP4 expression to the two processes independently (Huberman et al., 2002). In P30 epibatidine treated animals, the pat-

tern of eye specific projections into the LGN was disrupted compared to normal animals and there was no laminar expression of CRMP4 above background (figure 4.5). Myelin expression in the LGN of epibatidine treated animals was also disrupted. In normal animals, there is dense myelin staining both at the PGN/LGN boundary and at interlaminar zones (see figure 3.6). In epibatidine treated animals, there is very little myelin expression above background at the interlaminar zones and only the LGN/PGN boundary shows significant myelin expression (figure 4.6).

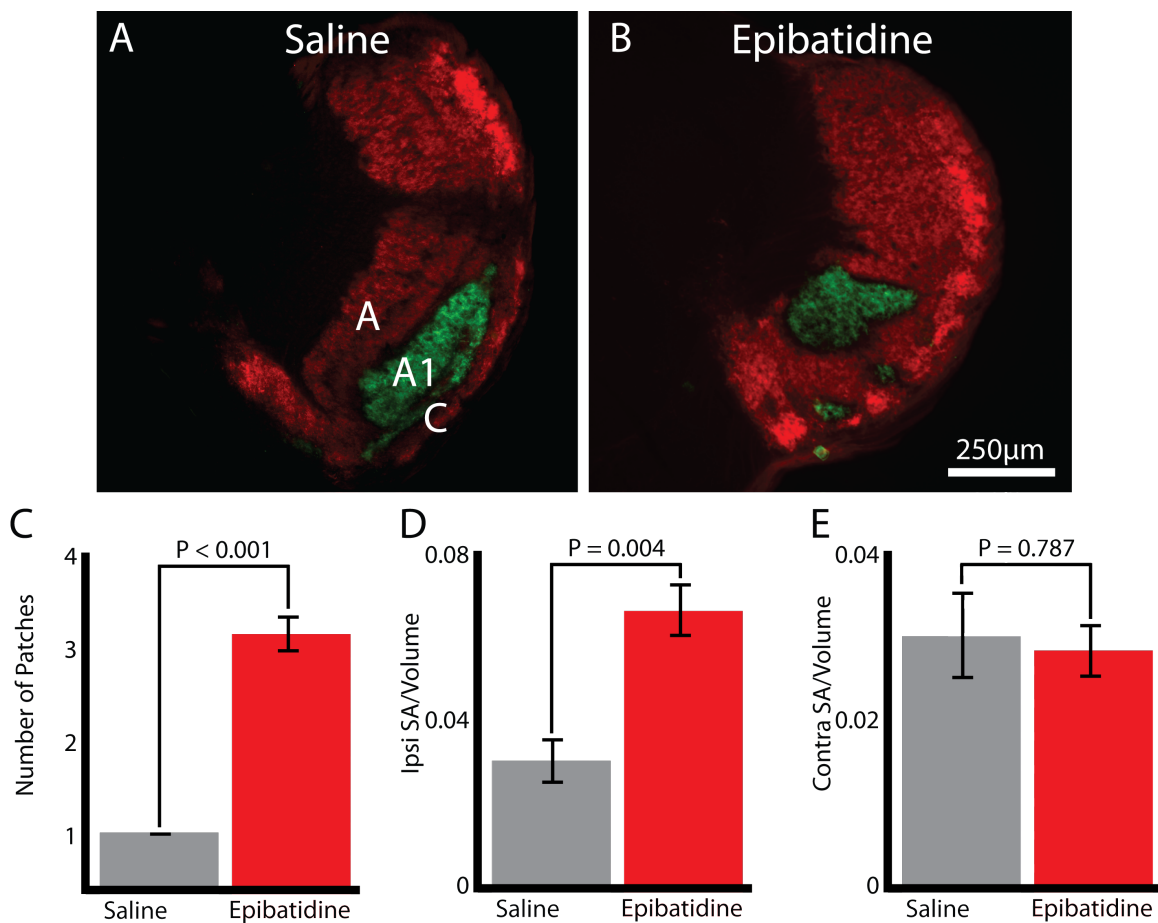


Figure 4.1: Epibatidine treatment alters the pattern of retinothalamic projections into the LGN. A, normal P30 ferret LGN in horizontal section. contralateral projections (red) display major terminations into the A lamina while major terminations from the ipsilateral retina (green) terminate in the A1 lamina. Minor projections from both retinas terminate in the C laminae. B, epibatidine treated ferrets show disrupted retinothalamic projection patterns at P30. Multiple ipsilateral projections are visible and the contralateral projection is reorganized to fill the space normally occupied by parts of the ipsilateral projection. C, epibatidine treated ferrets display more ipsilateral patches in the LGN than saline controls. D, epibatidine animals also show smaller ipsilateral projection domains as measured by the surface area/volume of these projections. E, There is no difference between the surface area/volume measure of the contralateral projection.

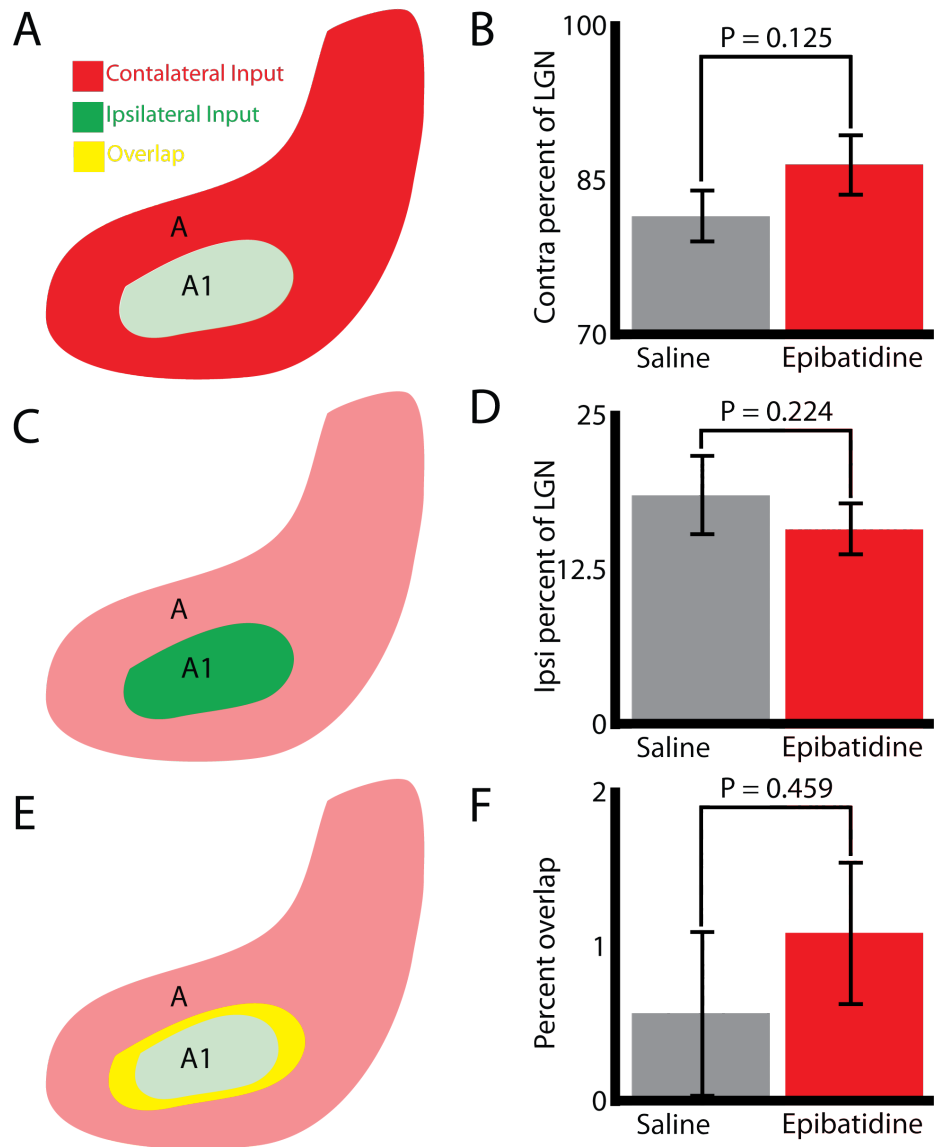


Figure 4.2: Epibatidine treatment does not alter the size or segregation of ipsilateral and contralateral retinothalamic projections to the LGN. A, C, and E, diagrams of the contralateral projection, ipsilateral projection, and overlap between the two, respectively. B, there is no difference in the percentage of the total LGN volume occupied by the contralateral projection between saline and epibatidine treated animals. D, there is also no difference in the percentage of the LGN occupied by the ipsilateral projection. F, the degree of overlap between the ipsilateral and contralateral projections is not altered in epibatidine treated animals.

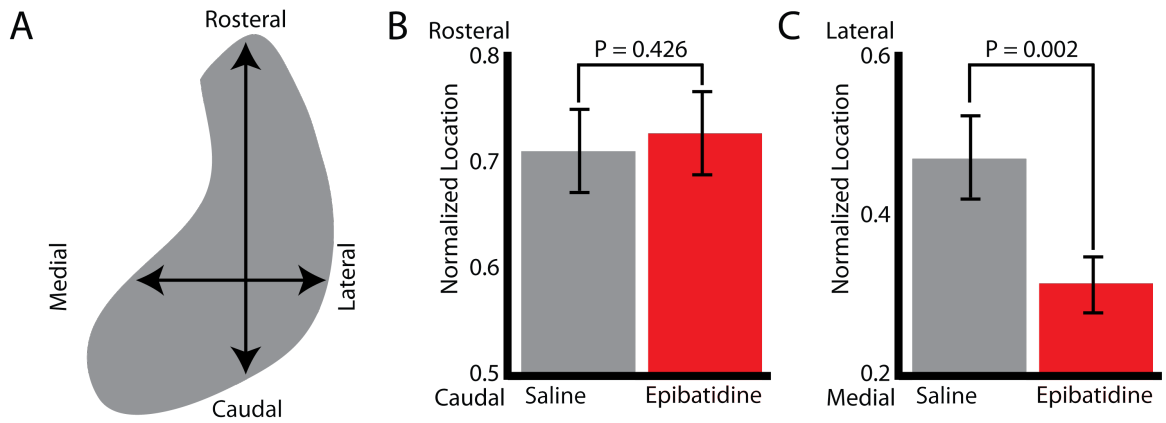
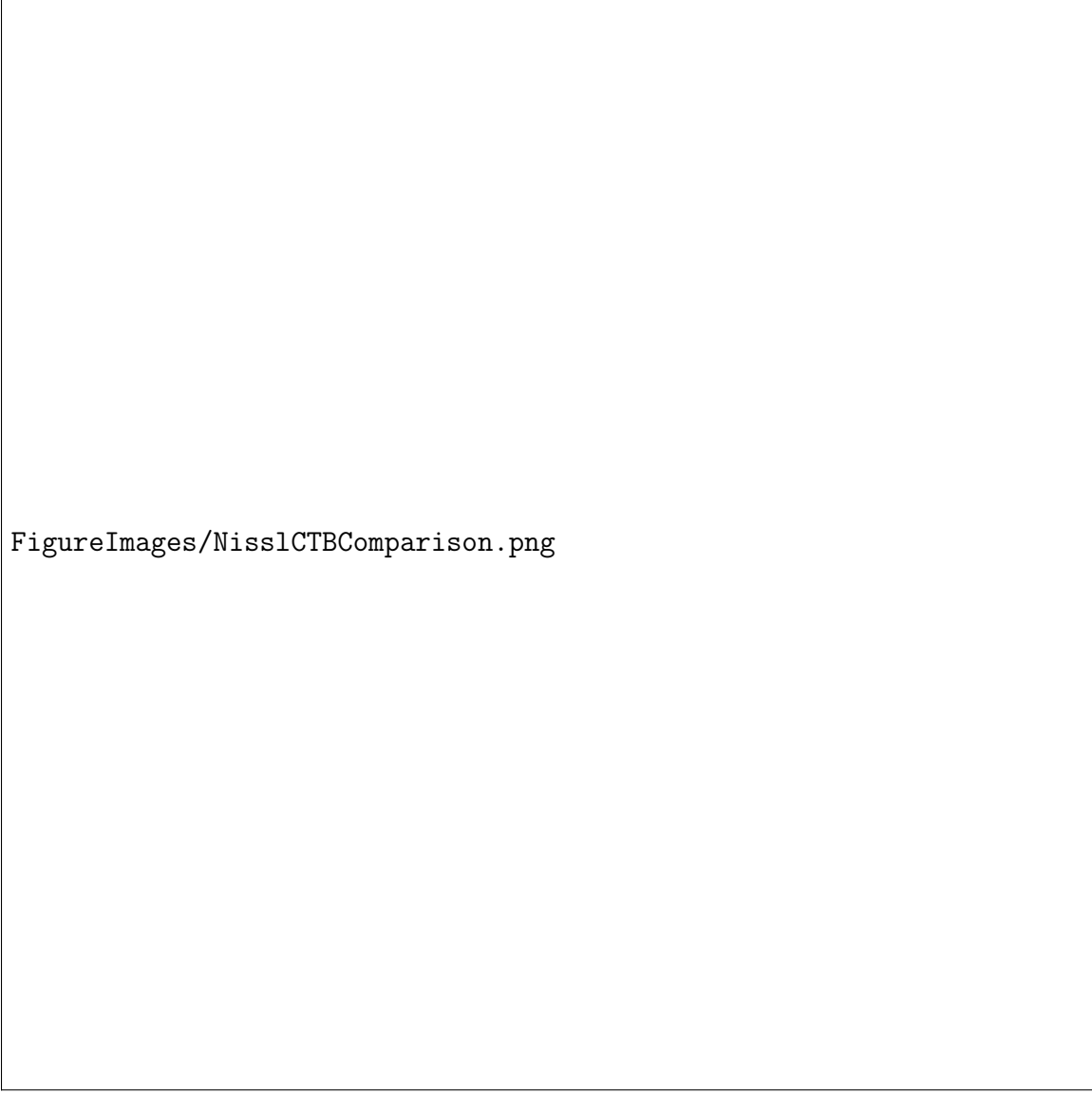


Figure 4.3: Epibatidine treatment causes a medial shift in the ipsilateral retinothalamic projection to the LGN. A, diagram of the position of the rostrocaudal and mediolateral axes in a horizontal section of the ferret LGN. B, there is no significant shift in the position of ipsilateral projections to the LGN along the rostrocaudal axis under epibatidine treatment. C, there is a significant medial shift in the position of the ipsilateral projection along the mediolateral axis under epibatidine treatment.



FigureImages/NisslCTBComparison.png

Figure 4.4: Epibatidine treatment abolishes normal LGN cytoarchitecture. A, horizontal slice of a normal P30 LGN with ipsilateral retinal projections labeled in green and contralateral projections labeled in red. Clear gaps in the density of projections are visible at the laminar and ON/OFF sublaminar boundaries (white arrows). B, Nissl stain of an adjacent slice to A. Cell sparse regions are visible at laminar and ON/OFF sublaminar boundaries (black arrows). C, larger view of the white box in A. D, larger view of the red box in B. E, horizontal slice of an epibatidine treated P30 LGN with ipsilateral retinal projections labeled in green and contralateral projections labeled in red. The organization of the retinothalamic projections is disrupted relative to saline controls. F, Nissl stain of an adjacent slice to E. There are no clear cell sparse zones akin to those seen in saline controls. G and H, larger views of the white and red boxes in E and F, respectively. scale bar = 250  $\mu$ m, applies to all

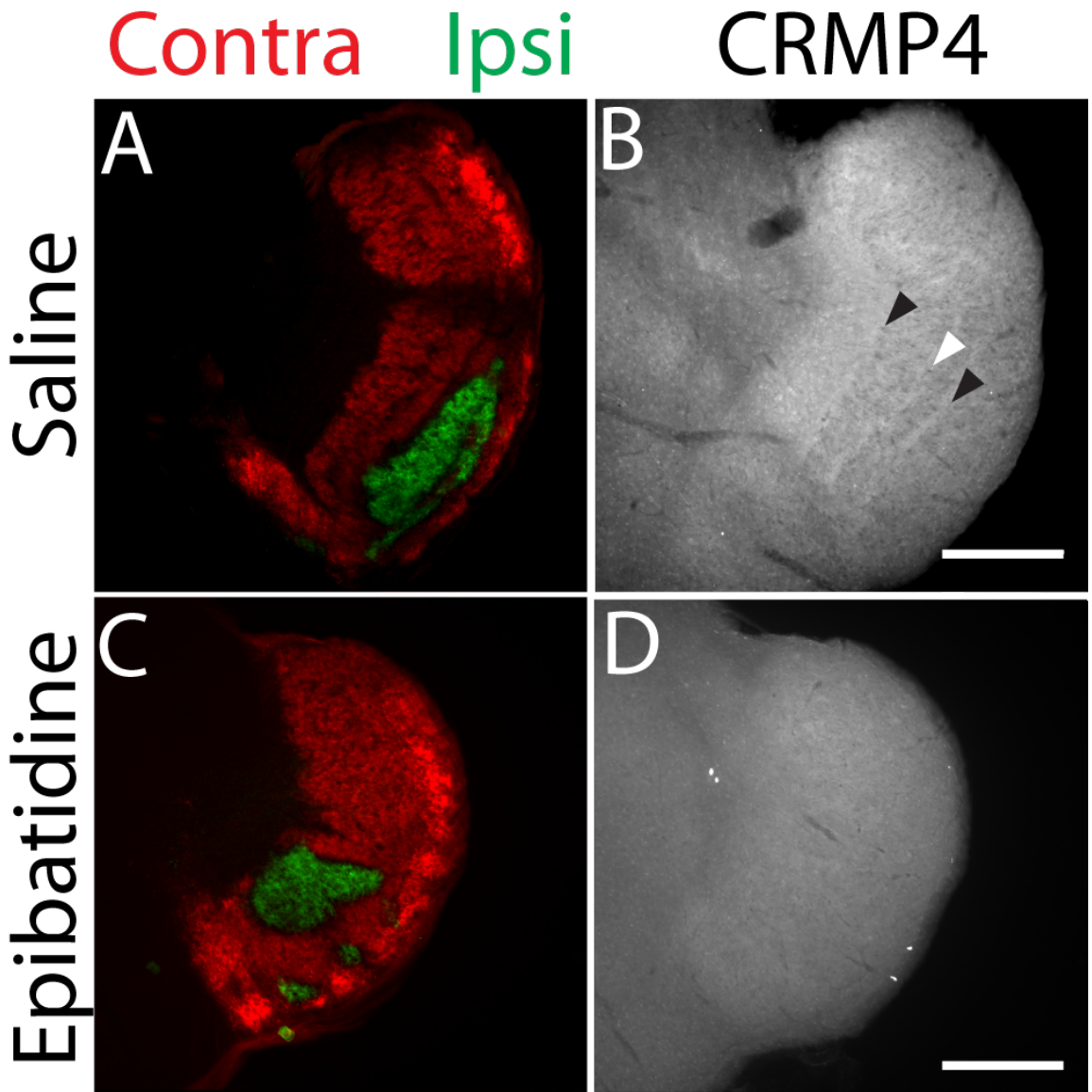


Figure 4.5: Epibatidine treatment abolishes CRMP4 expression in the ferret LGN. Bilateral intraocular treatment with epibatidine (1mM) from P1-P9 followed by recovery until P30 results in a disorganized retinothalamic projection (A, saline treated vs. C, epibatidine treated). Epibatidine treatment abolishes normal CRMP4 expression in the nucleus (B, saline treated vs. D, epibatidine treated). Black arrowheads indicate interlaminar zone staining and white arrowheads indicate staining at the within layer ON/OFF boundaries. Epibatidine treated animals exhibit robust segregation of eye specific inputs to the LGN in the absence of CRMP4 expression suggesting that CRMP4 expression in the LGN is not linked to eye specific segregation. scale bars = 250 $\mu$ m.

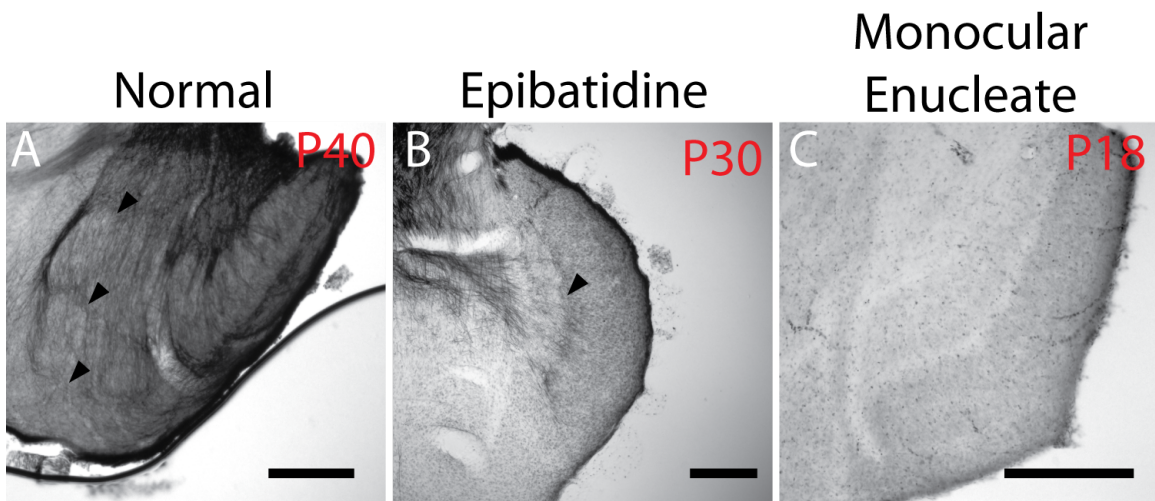


Figure 4.6: Myelination of normal and epibatidine treated LGNs. A, In the normal LGN, the interlaminar zones are more heavily myelinated than the main layers (arrows). B, In the epibatidine treated ferret, only the PGN/LGN boundary is heavily myelinated (arrow). This myelination pattern mirrors the pattern of CRMP4 in the epibatidine treated LGN. The correlation of CRMP4 expression and myelination across both normal and epibatidine treated animals is suggestive of an interaction between the two. CRMP4 is a mediator of myelin dependent outgrowth inhibition and may be shaping boundaries in the LGN through this mechanism. C, In the young monocular enucleate (P18), there is no evidence of heavy myelination in the LGN. scale bars = 250 $\mu$ m.

#### **4.3.2 Monocular or binocular enucleation at birth abolishes normal development of cytoarchitecture in the LGN and normal interlaminar CRMP4 expression**

In chapter 3, I reported that CRMP4 is expressed in a developmentally regulated manner in the interlaminar zones of the ferret LGN. In order to further characterize the expression of CRMP4 in the developing LGN and shed light on the source of this protein's expression, we performed monocular and binocular P0 enucleations followed by 16 to 55 days of recovery and immunostaining against CRMP4. Shorter post-enucleation survival times were not explored because we aimed to characterize the impact of enucleation when CRMP4 expression is the most robust. Binocular enucleation at P0 completely eliminates CRMP4 expression in the LGN at all ages tested (P20, P26, P45, P55; figure 4.7). CRMP4 expression in the LGNs of three ferrets (P16, figure 4.7; P18 and P20, data not shown) that were monocularly enucleated at P0 resembles a less organized version of the interlaminar expression profile seen in a normal ferret at this age. CRMP4 is expressed around the boundaries of the A1 lamina of the LGN ipsilateral to the enucleated eye, but the expression appears to be more diffuse than in normal ferrets from this age range. Additionally, a few CRMP4 positive cell bodies can be found in the LGN. CRMP4 expression is not present in the LGN of older monocular enucleates at P26 and P48 (figure 4.7). From the third to fourth postnatal week in a monocular enucleate life, there is a loss of the normal cytoarchitectonic laminar boundaries in the LGN. The nucleus moves from a cytoarchitectonic state indistinguishable from age matched normals to one in which there are no discernible laminar bound-

aries (Guillery et al., 1985). CRMP4 expression tracks the loss of laminar boundaries during this transition period.

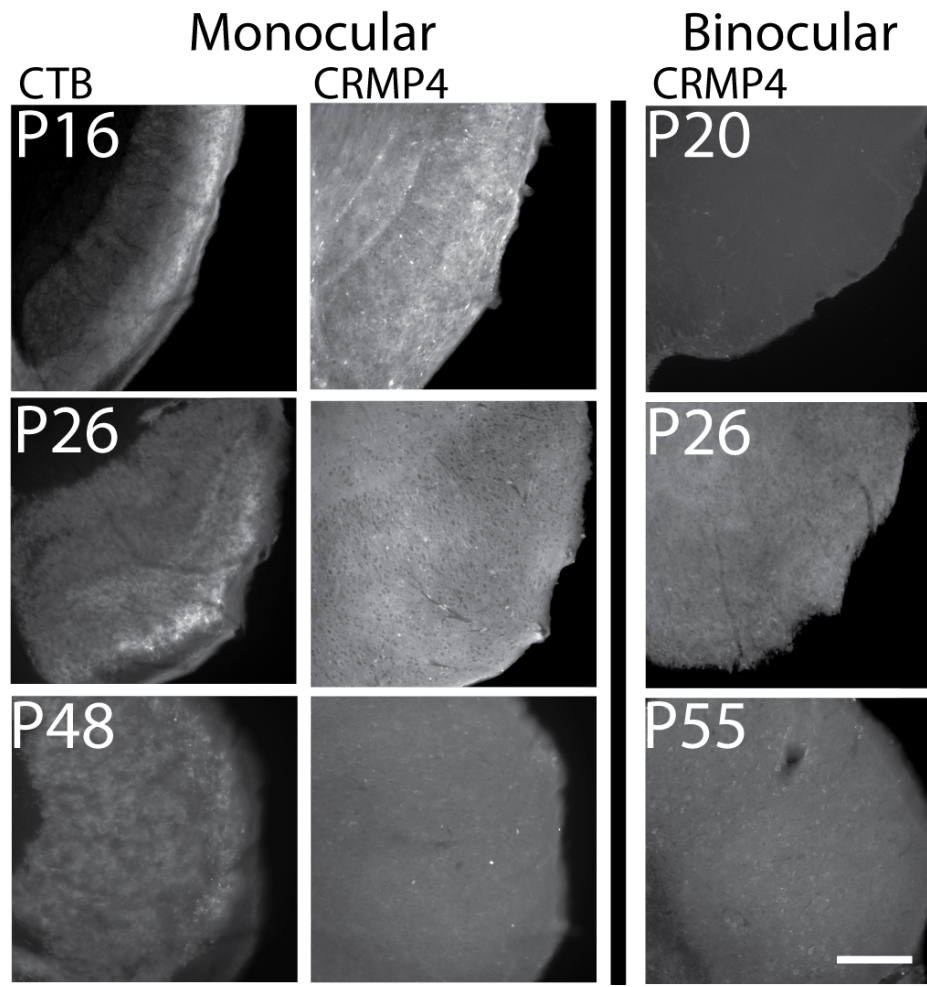


Figure 4.7: LGN CRMP4 expression in enucleate ferrets. GN expression of CRMP4 in ferrets enucleated at P0 and sacrificed at the ages shown. Left column, spared contralateral retinal afferents in monocularly enucleated ferrets labeled with cholera toxin subunit conjugated to alexa 488. By P26, the contralateral projection has begun to fill the whole volume of the LGN with robust contralateral projections throughout the nucleus by P48. Middle column, CRMP4 immunostaining data from the same sections as the left column, the expansion of the contralateral projection is coincident with loss of CRMP4 expression. Right column, binocular enucleation completely abolishes laminar expression of CRMP4 at all survival periods tested as shown by immunostaining. All sections are horizontal and 50 $\mu$ m thick. Scale bar =250 $\mu$ m, applies to all.

## 4.4 Conclusions

### 4.4.1 Summary of Findings

I confirm here that transient block of cholinergic retinal waves from P0 to P10 using epibatidine disrupts the normal projection pattern of retinal afferents into the LGN and eliminates normal cytoarchitectural laminar boundaries. These results are consistent with previous reports (Huberman et al., 2002; Padmanabhan, 2008). Further, I obtain the same results using methods employed previously in our lab (Padmanabhan, 2008). I show that epibatidine results in the loss of normal CRMP4 expression and abolishes normal myelination patterns in the LGN.

I also show that a loss of CRMP4 expression in the LGN is observed in animals subjected to either binocular or monocular enucleation at birth. In the binocular enucleate, CRMP4 expression appears to never develop in the LGN. In the monocular enucleate, CRMP4 expression is initially present at P16 when CRMP4 expression normally develops. However, CRMP4 expression is more diffuse and disorganized than in the normal animal and rapidly declines. The decline of CRMP4 expression tracks the loss of cell sparse interlaminar zones in monocular enucleates.

### 4.4.2 Pitfalls and limitations

First, because of the length of time between epibatidine injections (48 hrs), it is almost certainly the case that the blockade of retinal waves is incomplete throughout the first ten days of life, but it is rather intermittent with some recovery between injections. Intermittent recovery of this kind most likely induces

variability into the final disruption of retinothalamic targeting in epibatidine treated animals. In spite of this, it is remarkable that epibatidine animals can be treated as a group and be distinguished from controls on some salient measures of retinothalamic morphology (i.e. number of ipsilateral patches). A second limitation of this study is that no other retinal activity modulation paradigm was carried out. It is not possible to know for sure if the observed reduction in CRMP4 expression in the LGN is specific to epibatidine treatment or if it is a result of modulated retinal activity in general. However, the aim of this chapter is simply to measure the impact of altered LGN morphology on CRMP4 expression and my data is useful in that regard.

#### 4.4.3 Discussion

In both epibatidine treated animals and enucleate animals, CRMP4 expression in the LGN appears to be linked to the cytoarchitectural landscape of the nucleus. Specifically, CRMP4 expression tracks the presence, absence, or change in the cell sparse interlaminar zones that define the boundaries of LGN laminae in normal animals. I reported in chapter 3 that CRMP4 expression is apparent at the interlaminar zones in the normal ferret and that CRMP4 expression is developmentally regulated. Here, I have shown that abolishing the interlaminar zones through enucleation or blockade of cholinergic retinal waves with epibatidine also abolishes CRMP4 expression. Further, CRMP4 expression tracks the degradation of interlaminar zones in monocular enucleates. In these animals, normal LGN cytoarchitecture develops initially and persists into the third week

of postnatal life but interlaminar zones are soon lost and the mature monocular enucleate lacks them altogether (Guillery et al., 1985). CRMP4 expression in monocular enucleates mirrors this pattern, showing diffuse expression around the interlaminar zones during the third postnatal week and disappearing by the end of the forth postnatal week. Taken together, these results indicate that the presence of cell sparse interlaminar zones and CRMP4 expression are at least coincidentally linked.

Myelination in the LGN also appears to be linked to the presence or absence of the cell sparse interlaminar zones. In chapter 3, I reported that the interlaminar zones of the ferret LGN are more heavily myelinated than the rest of the nucleus. Dense myelination of this kind fails to develop in epibatidine treated animals and in enucleates. Instead, only the medial boundary of the nucleus exhibits dense myelination. The fact that myelination and CRMP4 expression both track the presence or absence of the cell sparse interlaminar zones suggests a possible mechanism by which CRMP4 may be sculpting the locations of retinal afferents in the LGN. CRMP4 has been shown to be a mediator of myelin dependent neurite outgrowth inhibition (Alabed et al., 2007). It is possible that CRMP4 expression in retinal ganglion cell afferents serves to mediate the translation of extracellular myelination cues into axon outgrowth inhibition at laminar boundaries (see general discussion for a more in depth treatment). Under this scheme, the failure of myelination to develop in epibatidine and monocular enucleate LGNs is permissive for axonal rearrangement in the area of normal laminar boundaries. In both cases, retinal ganglion cell afferents cross regions that would be defined by heavily myelinated and cell sparse interlaminar zones and would normally serve as

barriers to axonal outgrowth. Myelination may also be partially required for the maintenance of CRMP4 expression. There is no detectable laminar myelination in young monocular enucleates. The fact that CRMP4 expression initially develops in the LGNs of these animals but does not persist lends support to the hypothesis that LGN CRMP4 expression may be maintained in part by the presence of local myelination cues.

# Chapter 5

## General Discussion

### 5.1 Toward a molecular characterization of ocular dominance

In chapter 2, I presented a novel tissue sampling strategy for the elucidation of molecular correlates of visual development. This strategy centers around the study of ocular dominance in the developing ferret. Through a combination of dissection, fluorescent tracer, and *in vivo* imaging experiments, I show that it is possible to isolate structures in the retina, LGN, and cortex that form the anatomical basis of ocular dominance. These samples were then used as the substrate for proteomic analysis using two dimensional difference gel electrophoresis (2D-DIGE) and matrix assisted LASER desorption/ionization time of flight (MALDI-TOF) mass spectroscopy. We identified molecular candidates from the retina, LGN, and visual cortex that may contribute to the formation and/or maintenance of ocular dominance columns in the ferret.

The tissue sampling strategy employed in chapter 2 could be easily used as the sample generation scheme for other screens targeted at providing a genetic characterization of ocular dominance. In the past, differential mRNA display (Corriveau et al.,

1998), DNA microarrays (Tropea et al., 2006), and 2D-DIGE (Van den Bergh et al., 2006a) have been successfully employed in the study of visual development. All of these screens share a basic common methodology in that they are comparisons of two sample pools to one another. I show that it is possible to generate pairs of samples in the retina, LGN, and cortex such that ocular dominance may be explored. These samples could be processed with the above techniques to yield further insights into the establishment and/of maintenance of ocular dominance at the level of mRNA expression or at the level of protein expression.

The choice of an appropriate screen for use with the tissue sampling strategy presented in this dissertation will depend on the experimental goals at hand. The use of a gel based screening system such as the 2D-DIGE system presented here leads to one fundamental advantage over many other screens. Gel based methods operate at the protein level where many other methods operate at the mRNA level. As a result, gel based techniques are capable of directly measuring differences in protein expression across samples where other techniques force the experimenter to infer protein expression levels from mRNA levels. Due to the direct measurement of protein expression, a more fine grained analysis of the samples is permitted. Specifically, differential regulation of mRNA expression or splice variants across samples will be shown in a proteomic screen but not in other techniques based on mRNA. Additionally, studies such as those using DNA microarrays followed by RT-PCR frequently suffer from a high signal to noise ratios and can be difficult to interpret because of this (Murray et al., 2008). Gel based tech-

niques such as the one presented here do not rely on amplification methods and typically show a much better signal to noise ratio with detection limits as low as 0.5 fmol of protein (Unlu et al., 1997; Gong et al., 2004; Viswanathan et al., 2006). However, gel based methods provide less coverage across the genome of samples than other techniques based on an unbiased screens of mRNA. Making use of the 2D-DIGE system presented here, membrane bound proteins are underrepresented in my resultant data due to a bias of 2D-DIGE toward cytosolic proteins during the IEF separation phase of the experiment. Other two dimensional gel techniques involving doubled SDS-PAGE separation rather than the IEF/SDS-PAGE approach taken here have been developed in order to include membrane bound proteins (Rais et al., 2004), but these methods suffer from poor mass resolution when compared to standard IEF/SDS-PAGE techniques. As a result doubled SDS-PAGE methods are not particularly useful for comparative screens in which only small proteomic changes are expected.

For the molecular characterization of ocular dominance using the tissue strategy provided here, 2D-DIGE appears to be a good choice of screening system. The proteomic changes across retina, LGN, and visual cortex sample pairs can be rather small and as such it is important to choose a system that is capable of detecting subtle expression differences. These changes may not be apparent in other techniques where signal to noise is higher. Changes may also manifest themselves at the level of protein expression and slice variation. Again, the ability of 2D-DIGE to detect these changes makes it a good choice of screening system. 2D-DIGE does suffer from bias away from membrane bound proteins and the data recovered from these experiments

must be interpreted in this light.

Beyond the choice of methodology selected, the choice of animal model will impact both the scope and quality of experiments implementing the tissue sampling strategy presented here. The majority of the work that was carried out in this dissertation was done in the ferret, but these methods are directly translatable to many other mammalian models. In the case of the retina and the LGN, it is possible to generate samples for comparison of ocular dominance at the molecular level in any rodent, carnivore, or primate. The anatomy of the retina and LGN that allows us to isolate these samples in the ferret is common to all rodents, carnivores, and primates. In carnivores and primates, the LGN is laid out in a similar fashion to that of the ferret. Eye specific lamina are separated by cell sparse interlaminar zones and can easily be isolated using visual methods such as fluorescence guided micro-dissection(Kawasaki et al., 2004). In the primate, visual dissection of fresh tissue has also be used to isolate different portions of the LGN (Murray et al., 2008). The LGN is separated into eye specific domains like the LGNs of higher mammals, but it lacks cell sparse interlaminar zones (Godement et al., 1984). The eye specific patches of the mouse LGN could be isolated using fluorescence guided micro-dissection, but great care would have to be taken not to contaminate eye specific samples by including small portions of the adjacent tissue.

The methods presented here for the generation of cortical ocular dominance samples translate to other carnivores and many primates. Direct analogues of the cortical sampling and screening procedure presented in this dissertation exist for all animals with physiologically defined ocular dominance columns. Some

animals such as tree shrews do not appear to show physiologically defined ocular dominance columns (Hubel, 1975; Humphrey et al., 1977). Others, such as the new world monkeys have sparked debate as to the presence or absence of ocular dominance columns in their visual cortices. Marmosets, in particular, have been the source of this debate. Ocular dominance columns in adult marmosets have been detected by some groups (Chappert-Piquemal et al., 2001), but not by all (Spatz, 1979, 1989). Cortical sample generation depends on the use of optical imaging of intrinsic signal in order to generate functional maps of ocular dominance columns for sample biopsy. As such, the methods presented here will be sufficient for sample generation in all animals with physiologically identifiable ocular dominance columns.

In the rodent, ocular dominance columns do not exist. Instead, the rodent has a single binocular zone inside of a larger monocular response zone. At the single cell level, rodents exhibit ocular dominance, but ocular dominance is not detectable at the spatial scales employed here for both optical imaging of intrinsic signal and sample biopsy. Because of the structure of rodent visual cortex, there is no direct analog to the work presented here in the ferret cortex and as such the scope of these experiments in the mouse would be altered. Instead, one could use similar methodology to assay the molecular differences between the binocular and monocular zones in rodent visual cortex. This experiment, while informative, would not be a direct characterization of ocular dominance. Instead, it may be better framed as a study of the plasticity mechanisms that are specific to the monocular zone of the rodent.

Comparisons of samples generated using the methods pre-

sented here will be particularly useful in an animal model in which the genome has been sequenced. For example, working in the mouse, I have found that data processing and interpretation after MALDI-TOF mass spectrometry is much more straight forward and reliable than working in the ferret. The ferret genome is yet to be sequenced and as such studies in the ferret are hindered by cross-species comparisons to known genomes. In the mouse, within-species comparison undoubtably increases the quality of the experimental pipeline.

## 5.2 Molecular development of the LGN

In chapter 3 and chapter 4, I showed that collapsin response mediator 4 (CRMP4) is a novel and developmentally regulated molecular marker of LGN development. CRMP4 expression is developmentally regulated in the interlaminar zones of the lateral geniculate nucleus and linked to the normal development of LGN cytoarchitecture. I characterized CRMP4 expression in the developing LGN after detecting CRMP4 as a putative molecular candidate in a comparative ocular dominance screen (chapter 2). Other comparative screens of the LGN during development or of the different laminae within the LGN have also yielded a wealth of data on the molecular pathways at work during LGN development (Kawasaki et al., 2004; Horng et al., 2009). These studies along with more direct tests have shown that the molecular specification of the LGN is characterized by a diverse set of proteins including but not limited to transcription factors (Horng et al., 2009), cell surface receptors (Flanagan and Vanderhaeghen, 1998; Frisen et al., 1998; Huberman et al., 2005; Pfeiffenberger et al., 2005), components

of intracellular signaling and plasticity (Hendry and Yoshioka, 1994; Hendry and Reid, 2000), glial markers (Hutchins and Casagrande, 1988, 1990), and myelin (Snider and Lee, 1961; Woolsey et al., 2003). Clearly the topic of LGN development from a molecular perspective is quite complex and it is becoming more complex with the addition of novel molecular pathways as the molecular study of the visual system continues to evolve. The challenge in much of this work is that of interpretation. Given that the structure of the LGN is complex and that its development is shaped by both genetic and activity based factors, it is difficult to interpret the role that any one molecular marker or pathway takes during development. To elucidate the role of any given molecular marker during development, it must be considered in the face of other known markers that carry some salient relationship to the marker under consideration. Beyond insights gained from the expression profiles of many co-varying molecular markers, it would be very beneficial to manipulate the expression profile of the molecular marker under consideration where possible. Manipulations of this sort could be carried out through genetic alterations in species with mapped genomes or by using over-expression and under-expression systems such as viral mediated siRNA delivery.

In the case of the work presented here, CRMP4 is shown to be dependent on both the developmental state of the LGN and of its cytoarchitecture. However, it is not abundantly clear what the mechanistic role of CRMP4 in LGN development may be. I have shown that CRMP4 expression and myelination covary in the LGN of both normal ferrets and those with abnormal cytoarchitecture. This fact leads to a natural hypothesis of the

mechanistic role of CRMP4 during LGN development. This hypothesis is treated in detail in section 5.3.1 and alternative hypotheses are treated in sections 5.3.2 and 5.3.3.

Further insight into the mechanism of CRMP4 action could be gained through virally mediated over-expression of CRMP4 or delivery of a CRMP4 antagonist in retinal ganglion cells. It is possible to transfect retinal ganglion cells in the newborn ferret retina using electroporation (Huberman et al., 2005). This system could be used to deliver a viral construct designed to over-express CRMP4 in developing retinal ganglion cells entering the LGN. Similarly, CRMP4 expression in retinal ganglion cells could be decreased through the delivery of a CRMP4 siRNA (Alabed et al., 2007a). Further, a test of the specific hypothesis that CRMP4 mediates myelin dependent outgrowth inhibition (see section 5.3.1), could be carried out by the delivery of CRMP4-RhoA inhibitor protein (C4RIP). In short, myelin dependent outgrowth inhibition has been shown to require the binding of CRMP4 to RhoA and C4RIP disrupts this binding event(Alabed et al., 2007a). These experiments fall outside of the scope of this dissertation.

### **5.3 Hypothesized roles of CRMP4 during LGN development**

In chapter 3 and chapter 4, I make brief references to three possible mechanistic roles of CRMP4 during LGN development. In the sections that follow, I expand upon these references in order to treat them more fully and to illustrate my preferred hypothesis for the role of CRMP4 during LGN development. The hypotheses are as follows:

- i. CRMP4 serves as a response factor downstream of myelin signaling and mediates myelin dependent outgrowth inhibition in the cell sparse interlaminar zones.*
- ii. CRMP4 serves as a response factor downstream of semaphorin signaling and mediates growth cone collapse in the cell sparse interlaminar zones*
- iii. CRMP4 serves to modulate calcium signaling in RGC axon terminals in the cell sparse interlaminar zones.*

I first discuss the hypothesis that CRMP4 serves as response factor downstream of myelin signaling and mediates myelin dependent outgrowth inhibition in the cell sparse interlaminar zones since it is my preferred hypothesis for the role of CRMP4 during LGN development. The second two hypotheses are next discussed along with an explanation of why I do not favor them.

### **5.3.1 Hypothesis i: CRMP4 serves as a response factor downstream of myelin signaling and mediates myelin dependent outgrowth inhibition in the cell sparse interlaminar zones.**

In both chapter 2 and chapter 3, I show that the pattern of CRMP4 and myelination in the LGN of the developing ferret covary. Both expression of CRMP4 and myelination are high at the medial boundary of the LGN as well as at the cell sparse interlaminar zones that separate the individual LGN laminae from one another. This covariance in expression leads to a mechanistic hypothesis of the role that CRMP4 may take

during LGN development. CRMP family members are known regulators of growth cone dynamics (Goshima et al., 1995) as well as mediators of neurite formation and extension (Inagaki et al., 2001; Fukata et al., 2002). CRMP4 has also been specifically identified as a mediator of myelin dependent outgrowth inhibition (Alabed et al., 2007b).

Normally, growing axons do not extend processes across heavily myelinated regions. These regions thus serve as boundaries or borders to neuronal growth and regeneration. In this way, myelination is an important factor in shaping the structure of the brain both during initial development and in response to injury. A number of factors associated with myelin expression serve as the molecular basis of this inhibition of axonal growth. These factors are collectively referred to as myelin associated inhibitors (MAIs) (Yiu and He, 2003). MAIs exert their influence on axons by binding to cell surface receptors and triggering intracellular signaling cascades that inhibit axonal outgrowth (Mandemakers and Barres, 2005). The MAIs include glycoproteins such as myelin-associated glycoprotein (McKerracher et al., 1994) and oligodendrocyte-myelin glycoprotein (Kottis et al., 2002) as well as other proteins expressed at the cell surface including Nogo-A (Chen et al., 2000). MAIs inhibit the growth of axonal processes through the disruption of normal cytoskeletal dynamics mediated by Rho-GTPases. If RhoA and one of its downstream effectors Rho kinase (ROCK) are blocked, exuberant axonal outgrowth results (Dergham et al., 2002). Conversely, if RhoA signaling is activated by MAIs, axonal outgrowth is stunted (Yiu and He, 2003).

CRMP4 physically and functionally interacts with RhoA. The strength of this interaction is increased by the application

of the MAI Nogo-A (see figure 5.1 for a summary of CRMP4 activation by MAIs). Nogo-A signals through a complex of the Nogo receptor (NgR) and p75. A signal through the complex of NgR and p75 activates RhoA and allows RhoA to bind to CRMP4 (Yiu and He, 2003; Alabed et al., 2007a). Further, the disruption of this interaction facilitates axon outgrowth in the presence of MAIs indicating that the RhoA-CRMP4 interaction is necessary and sufficient for axon outgrowth inhibition *in vitro* (Alabed et al., 2007b). The association of CRMP4 with RhoA is known to be driven by the phosphorylation state of CRMP4. Phosphorylated CRMP4 is inactive and does not interact with RhoA. Glycogen synthase kinase 3 $\beta$ (GSK3 $\beta$ ) is known to phosphorylate CRMP4 and is itself phosphorylated and inactivated by MAIs (Alabed et al., 2010). With the inactivation of GSK3 $\beta$ , CRMP4 is released from its normal inhibition and is free to bind with RhoA. This interaction then leads to axon outgrowth inhibition. Through this signaling cascade, the presence of CRMP4 may be a critical player in axonal rearrangements *in vivo*.

In the LGN, CRMP4 may respond to the presence of extracellular myelination and serve as a control of laminar specificity in retinogeniculate axonal targeting. At the onset of CRMP4 expression in the LGN (P12-14), the initial segregation of retinogeniculate inputs into eye specific layers is complete and the beginnings of cell sparse interlaminar zones are apparent (Figure 5.2, row A). The cell sparse zones are not heavily myelinated at this time, but as the nucleus matures, myelination becomes more apparent (Figure 5.2, row C). Coincident with the increase in myelination, CRMP4 expression in the nucleus increases (Figure 5.2, row D). Both heavy myelination and CRMP4 expression

are observed in the cell sparse interlaminar zones by P30. During the onset of myelination and peak of CRMP4 expression, the interlaminar zones expand and retinogeniculate projections crossing these regions must contract and pull out of inappropriate connections with the wrong eye specific lamina. CRMP4 may thus serve as an agent of fine scale changes in the retinogeniculate circuit during the final stages of LGN development. By P40-P50, the LGN has achieved its final adult morphology and CRMP4 expression fades (Figure 5.2). If the normal cytoarchitecture of the nucleus is manipulated, normal expression of CRMP4 and myelin as well as the normal formation of cell sparse interlaminar zones is disrupted. This result can be viewed as a breakdown of the normal signaling mechanisms in place at the cell sparse interlaminar zones. With the break down of normal cytoarchitecture comes the loss of proper myelination and a failure of normal CRMP4 signaling. Without CRMP4 signaling at the interlaminar zones, normal boundaries in the LGN are lost. This is highlighted in the case of monocularly enucleated ferrets. In these animals, the normal beginnings of proper targeting of the spared eye, cytoarchitecture, and CRMP4 expression are evident early in development. However, at P18-20, the spared eye expands its footprint in the LGN and takes over the territory normally occupied by the enucleated eye. At the same time, the beginnings of normal cytoarchitecture are lost and CRMP4 expression becomes more diffuse and ultimately disappears. The loss of CRMP4 expression in these animals may be one of the factors that allows the release of spared eye afferents from normal outgrowth inhibition and facilitates the expansion of the spared eye into the enucleated eyes territory.

One of the missing links in this hypothesis is the presence

or absence of myelination in the early interlaminar zones. It is clear that there is myelination at the interlaminar zones by P30 and beyond, but it is not clear that there is significant myelination at the interlaminar zones at the onset of LGN CRMP4 expression at P12-14. I have not been able to identify significant myelination in the LGN of animals at this age, but the sample size of these pilot studies was very limited (2 animals). The modified Gallyas stain used for detection of myelin in this work has proven to be rather variable in ferret tissue. Due to this methodological variation, it is unclear if our failure to find myelination in the young ferret LGN (Figure 5.2, C2) is the result of poor detection in our myelin stain or of the results reveal a true lack of myelination at this age.

## Myelinated interlaminar zone axon

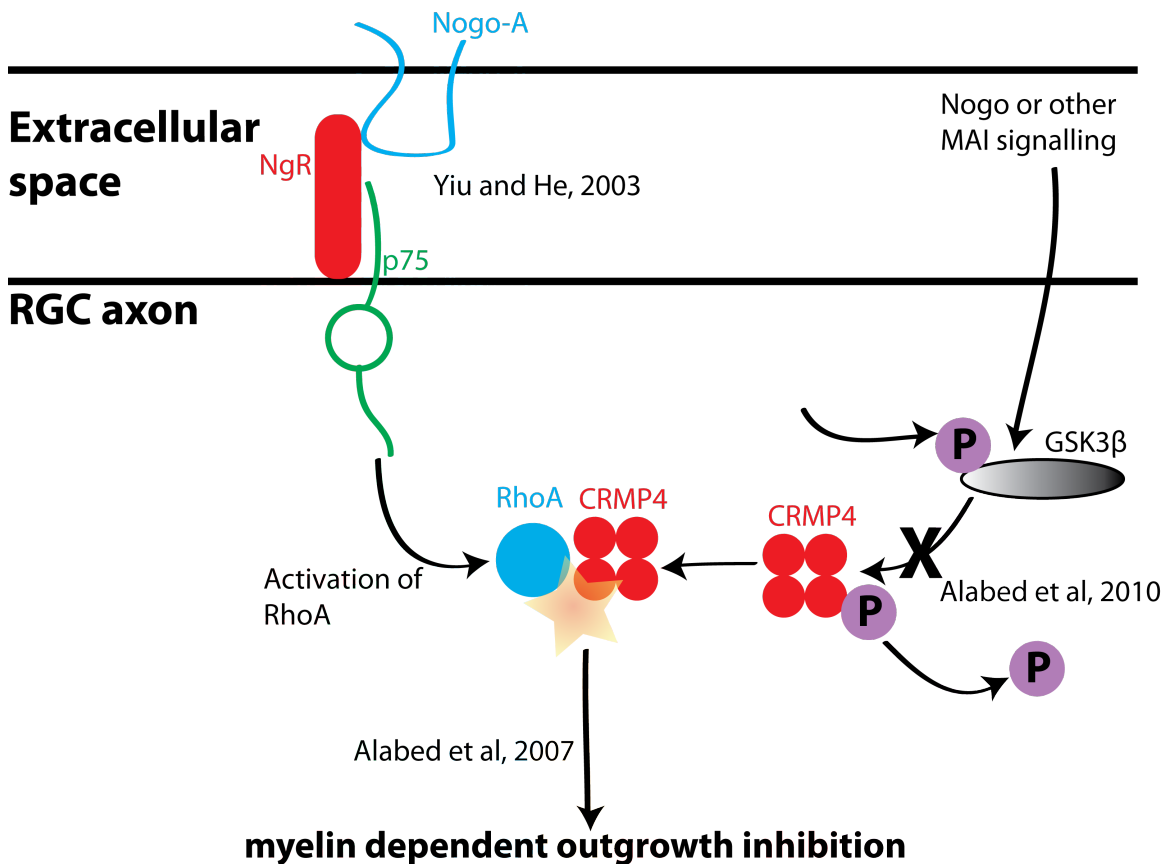


Figure 5.1: MAI signaling through CRMP4 and RhoA results in myelin dependent outgrowth inhibition. Nogo-A signaling through the complex of the Nogo receptor (NgR) and p75 results in the activation of RhoA (Yiu and He, 2003). This activation allows RhoA to bind to CRMP4 (Alabed et al, 2007). Signaling through Nogo or other myelin associated inhibitors (MAIs) results in the phosphorylation of glycogen synthase kinase 3 $\beta$  (GSK3 $\beta$ ). Phosphorylation inactivates GSK3 $\beta$  and leads to a loss of phosphorylation of CRMP4 (Alabed et al, 2010). Unphosphorylated CRMP4 becomes active and is free to bind with RhoA. Binding of RhoA and CRMP4 leads to myelin dependent outgrowth inhibition (Alabed et al, 2007). In the context of the ferret interlaminar zone, MAIs are present on myelinated axons passing through the interlaminar zones and RGC axons expressing CRMP4 could exhibit myelin dependent outgrowth inhibition at interlaminar boundaries through these signaling cascades.

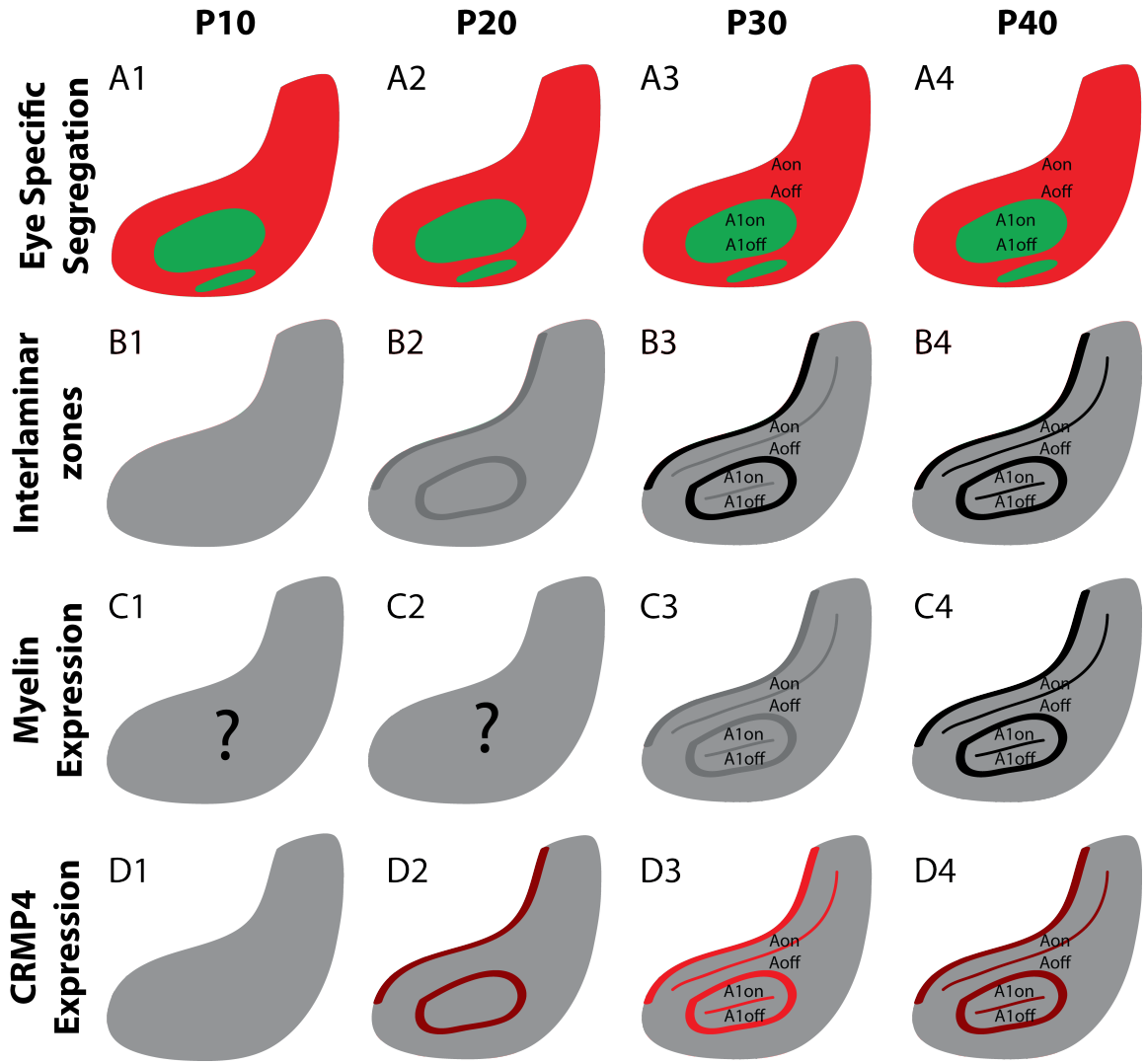


Figure 5.2: Development of eye specific segregation, interlaminar zones, myelination, and CRMP4 expression in the normal ferret LGN. Row A, eye specific segregation is complete by P10 and is maintained throughout adult hood. ON and OFF sub-domains appear in segregated eye specific lamina by P30. Row B, Interlaminar zones are not present at P10 but begin to develop by P20. Nascent interlaminar zones mature and minor cell sparse regions at the ON/OFF sub-laminar boundaries appear by P30. Row C, It is unclear if any myelination is present in the LGN of animals at P10 and P20. By P30, the interlaminar zones and ON/OFF sub-laminar boundaries zones become myelinated. This myelination pattern becomes more dense as the animal ages. Row D, CRMP4 expression is absent at P10 and apparent at the interlaminar zones by P20. By P30, the interlaminar zones and sub-laminar ON/OFF boundaries robustly express CRMP4. Around P40, CRMP4 expression begins to fade across the nucleus.

### **5.3.2 Hypothesis ii: CRMP4 serves as a response factor downstream of semaphorin signaling and mediates growth cone collapse in the cell sparse interlaminar zones.**

The Semaphorin family of proteins includes both secreted and membrane bound proteins that are implicated in both attractive and repellent axon guidance (Raper, 2000). Canonically, semaphorin signaling is transduced at the cellular membrane through the action of the plexin family of transmembrane receptors. Different plexin family members bind to different classes of semaphorins (Nakamura et al., 2000). For the remainder of this section, I will limit my discussion of the semaphorin family to class 3 semaphorins. Class 3 semaphorins are secreted proteins that bind to a receptor complex composed of plexinA and either neuropilin-1 or neuropilin-2. PlexinA and one of the two neuropilins are obligate co-receptors for functional class 3 semaphorin signaling (Kolodkin et al., 1997). Specifically, a class 3 semaphorin, Sema3a, is known to cause growth cone collapse through the intracellular action of CRMP4 (Goshima et al., 1995; Schmidt and Strittmatter, 2007) and as such will be the focus of discussion here.

To mediate axon dynamics only in the interlaminar zones of the LGN, a diffusible molecule such as Sema3a would have to originate from point sources in the interlaminar zones and not diffuse out of the interlaminar zones into the main layers of the LGN. It is unlikely that this is the case in the developing LGN for two reasons. First, the interlaminar zones are very thin. The width of the interlaminar zone in adult LGNs is no wider than 50m. This estimate is conservative and the width of the interlaminar zones is certainly smaller as the LGN is developing and

slowly progressing toward the morphology seen in the adult. It is unlikely that the diffusion of Sema3a would be limited to the interlaminar zones given that a Sema3a molecule originating in a point source in the middle of an interlaminar zone would only need to diffuse  $25\mu\text{m}$  to encroach upon the main layers of the LGN. As a point of reference, molecules close to the size of Sema3a (125 kDa) diffuse through water with a diffusion coefficient of  $0.45 \times 10^{-3} \text{ m}^2/\text{s}$  (Nauman et al., 2007). If this diffusion coefficient is assumed for Sema3a in the interlaminar zones of the LGN, it would take 15 hours for a point source of Sema3a at the center of an interlaminar zone to drive Sema3a signaling outside of the interlaminar zone. The actual diffusion coefficient observed for Sema3a in the interlaminar zones would depend on the influence of the extra cellular matrix in the interlaminar zones. If Sema3a fails to diffuse as indicated above due to an excess of binding partners or if Sema3a leaves the secreting cell but remains bound to its surface, the diffusion of Sema3a in the interlaminar zones may be much lower than expected.

Even if it is taken as a given that a point source of Sema3a in the interlaminar zones of the LGN will not result in Sema3a signaling outside of the interlaminar zones, the hypothesis that CRMP4 expression in the interlaminar zones serves to mediate Sema3a signaling suffers from a lack of spatially confined Sema3a sources in the LGN. Within the LGN, there are different classes of cells that are molecularly distinct from one another. In the primate, these cells are divided into two major classes, magnocellular and parvocellular. Different layers in the primate LGN are composed of either magnocellular or parvocellular cells. A third, molecularly distinct, set of cells found

in the interlaminar zones has also been identified (Livingstone and Hubel, 1984; Hendry and Yoshioka, 1994; Hendry and Reid, 2000). These cells form the koniocellular pathway in the LGN. In the cat, the observed cell types of the LGN are X and Y cells. These cells are physiologically and morphologically distinct from one another. Unlike the primate, cell types in the cat LGN are not neatly organized into different laminae (LeVay and Ferster, 1977). Additionally, the cells in the interlaminar zones of the cat do not appear to have a distinct molecular phenotype. The ferret LGN resembles the LGN of the cat more than the primate in both its constituent cell types and in its anatomy. As an example, I attempted to identify ferret LGN cells analogous to those reported in the primate koniocellular pathway in a pilot study. Staining for calcium/calmodulin-dependent protein kinase 2 (CamK2) in the primate LGN reveals cells in the koniocellular pathway. Staining for CamK2 in the ferret LGN revealed CamK2 positive cells throughout the volume of the LGN. With the observed homogeneity in cell type across the LGN, it is unlikely that only cells found in the interlaminar zones of the ferret LGN would secrete Sema3a. It is much more likely that Sema3a secretion would be evenly distributed throughout the nucleus.

Due to both the spatial precision over which CRMP4 expression occurs in the developing LGN and the lack of a molecularly distinct cell type in the interlaminar zones of the ferret LGN, it is unlikely that CRMP4 serves as a response factor downstream of semaphorin signaling and mediates growth cone collapse in the cell sparse interlaminar zones.

### **5.3.3 Hypothesis iii: CRMP4 serves to modulate calcium signaling in RGC axon terminals in the cell sparse interlaminar zones**

Recent studies have shown that CRMP2 has an alternative role in synaptic plasticity beyond its typical role in growth cone dynamics. CRMP2 has been shown to interact with the N-type presynaptic Ca<sup>2+</sup> channel (CaV2.2) and this interaction serves to modulate the of Ca<sup>2+</sup> current moving through presynaptic CaV2.2 channels (Brittain et al., 2009). Modulation of calcium channels influences the action of presynaptic calcium flux in turn modulates neurotransmitter release at the synapse (Catterall and Few, 2008). Specifically, an increase in CRMP2 levels leads to an increase in calcium flux and a consequent increase in neurotransmitter release. It is unknown if the observed interaction with CaV2.2 and CRMP2 is specific to CRMP2 or if it may be a general property of the CRMP family. If CRMP4 is also capable of modulating synaptic plasticity, CRMP4 may serve to modulate calcium signaling in RGC axon terminals in the cell sparse interlaminar zones and thus modulate synaptic plasticity in the cell sparse interlaminar zones through an increase in neurotransmitter release. An increase in neurotransmitter release could lead to increase synaptic efficacy in portions of the LGN with high local calcium concentrations through the action of CRMP4. For this hypothesis to hold there should be a difference in calcium signaling between the cell sparse interlaminar zones and the main laminae of the LGN. This difference would then provide a substrate upon which CRMP4 could serve to shape the projections of RGC into the LGN. Under this scheme CRMP4 expression at the interlaminar zones would re-

sult in increased sensitivity to different local calcium levels and thus larger differences in the synaptic strength of developing synapses in the interlaminar zones and main LGN layers. If local calcium levels were lower in the interlaminar zones than the main LGN layers, this scheme could lead to a strengthening of synapses onto the main LGN laminae a weakening of synapses onto the interlaminar zones. Differential synaptic plasticity of this kind could assist in fine tuning laminar boundaries in the LGN.

In order to test this hypothesis, it will be necessary to characterized the magnitude of calcium flux across the LGN. Characterization of the LGN in this way could be carried out using calcium imaging in LGN slice preparations. If the interlaminar zones of the LGN are identified either directly by characterization of cytoarchitecture or indirectly by fluorescent tracer injections into the retina, an imaging location could be chosen such that it includes an interlaminar zone as well as the bordering main LGN laminae. Calcium flux in response to stimulation across the slice could then be visualized in order to determine if the interlaminar zones behave differently from the main LGN laminae.

I do not favor this hypothesis due to the fact that CRMP4 has not definitively been shown to interact with calcium channels at the synapse or hold sway over any other synaptic properties directly. The CRMP family is defined by a common structural similarity and is actually composed of members that have a significant variation around a the base CRMP structure. As a result, the family has been shown to participate in a wide variety of functions (Schmidt and Strittmatter, 2007). Not all members of the CRMP family share all of the functions of the

family and it is not a good assumption that an atypical CRMP function such as interaction with CaV2.2 channels is common to all CRMPs. Without direct evidence for an interaction of CRMP4 with calcium signaling or other synaptic phenomenon, I do not find it likely that CRMP4 serves to modulate synaptic plasticity directly in the interlaminar zones.

## 5.4 Conclusions

### 5.4.1 Specific conclusions

In this dissertation, I have outlined a strategy for the characterization of molecular correlates of visual development. Specifically, I present a novel strategy for the exploration of the molecular basis of ocular dominance. The study of visual development in this way led to the characterization of a novel marker for LGN development, CRMP4. I show that CRMP4 expression is both developmentally regulated and subject to manipulation through classic alterations of LGN anatomy through enucleation and activity modulation in the retina. CRMP4 expression covaries with the expression of myelin in the LGN and CRMP4 may serve to fine tune the laminar wiring of the LGN through myelin dependent outgrowth inhibition. Alternative explanations of the mechanism of CRMP4 action in the developing LGN include mediation of semaphorin signaling or the mediation of synaptic plasticity through an interaction with calcium signaling. Definitive proof of the mechanism of CRMP4 action in the developing LGN will require additional experimentation beyond the scope of this dissertation.

It is also worth noting that the methods presented here for

the molecular characterization of the visual system are applicable to other modular neural systems. In many neural systems, it is possible to generate pairs of samples that represent closely related functional modules. These pairs of modules could easily be assayed using the methods presented here. As an example, many of the primary sensory modalities could be examined using similar approaches to what is seen here. It would be straight forward extension of the methods presented here to characterize the molecular compliments of different barrels in S1 of the rodent, different tonotopic representations in auditory cortex, or different odor representations in the olfactory bulb, to list a few. In all of these cases, an adaptation of the tissue sampling paradigms presented in this dissertation followed by a differential screen using 2D-DIGE or other screening system could lead to a novel perspective on the influence of molecular cues in these systems.

#### **5.4.2 General conclusions**

Historically, much of neural development was viewed as a result of endogenous and externally driven activity paradigms. In this view the remarkable reliability of neural anatomy across both individuals and generations was thought to be a result of stereotyped environmental influences on the nervous system. From the view of a single neuron, the pattern of activity that it receives and the pattern of activity that its potential synaptic partners display were thought to be the driving forces behind wiring decisions. This perspective has been at the root of many successes and breakthroughs in our understanding of neural function. However, the story of neural development is

much more complex than it would seem when viewed simply as a result of neural activity. Molecular influences on neural systems have come to be known as driving forces in development as well. From the perspective of a single neuron, the full complement of its molecules and that of its potential synaptic partners augments wiring decisions in the face of activity paradigms. These two developmental schemes appear to be at odds with one another, but I believe that they are in fact synergetic.

Over the last two decades, there has been an massive proliferation of methods aimed at genetic and molecular characterization of biological systems and the field of developmental neuroscience has borrowed heavily from these tools. In the most general sense, the work presented in this dissertation represents an additional borrowing. It is my belief that application of tools such as those presented in this dissertation to the study of neural development will paint a much more holistic picture of neural development than what is found in many current textbooks. Rather than viewing neural development through the lens of activity dependent mechanisms or molecular mechanisms, we will come to realize that the actual mechanics of neural development are a marriage of both. Activity and molecular influences on neural systems will lose their discrete labels as we study the two systems in tandem. We will see that one influences the other and feeds back onto itself. There is a sort of beautiful completeness to this perspective on the operation of neural systems.

# References

- Alabed YZ, Pool M, Tone SO, Fournier AE (2007) Identification of CRMP4 as a Convergent Regulator of Axon Outgrowth Inhibition. *Journal of Neuroscience* 27:1702-1711.
- Alabed YZ, Pool M, Ong Tone S, Sutherland C, Fournier AE (2010) GSK3 beta regulates myelin-dependent axon outgrowth inhibition through CRMP4. *J Neurosci* 30:5635-5643.
- Antonini A, Stryker M (1993) Development of individual geniculocortical arbors in cat striate cortex and effects of binocular impulse blockade. *The Journal of Neuroscience* 13:3549-3573.
- Antonini A, Stryker M (1996) Plasticity of geniculocortical afferents following brief or prolonged monocular occlusion in the cat. *J Comp Neurol* 369:64-82.
- Antonini A, Gillespie D, Crair M, Stryker M (1998) Morphology of single geniculocortical afferents and functional recovery of the visual cortex after reverse monocular deprivation in the kitten. *J Neurosci* 18:9896-9909.
- Augustin I, Betz A, Herrmann C, Jo T, Brose N (1999) Differential expression of two novel Munc13 proteins in rat brain. *Biochem J* 337 ( Pt 3):363-371.
- Bal T, von Krosigk M, McCormick D (1995) Synaptic and membrane mechanisms underlying synchronized oscillations in the ferret lateral geniculate nucleus in vitro. *J Physiol (Lond)* 483:641-663.
- Bishop KM, Goudreau G, O'Leary DD (2000) Regulation of area identity in the mammalian neocortex by Emx2 and Pax6. *Science* 288:344-349.
- Bishop KM, Rubenstein JL, O'Leary DD (2002) Distinct actions of Emx1, Emx2, and Pax6 in regulating the specification of areas in the developing neocortex. *J Neurosci* 22:7627-7638.
- Bishop KM, Garel S, Nakagawa Y, Rubenstein JL, O'Leary DD (2003) Emx1 and Emx2 cooperate to regulate cortical size, lamination, neuronal differentiation, development of cortical efferents, and thalamocortical pathfinding. *J Comp Neurol* 457:345-360.
- Blumenfeld H, McCormick D (2000) Corticothalamic inputs control the pattern of activity generated in thalamocortical networks. *J Neurosci* 20:5153-5162.
- Bonhoeffer T, Grinvald A (1991) Iso-orientation domains in cat visual cortex are arranged in pinwheel-like patterns. *Nature* 353:429-431.
- Bonhoeffer T, Grinvald A (1996) Optical Imaging Based on Intrinsic Signals: The Methodology. In: *Brain Mapping: The Methods*, pp 55-97.
- Bosking W, Zhang Y, Schofield B, Fitzpatrick D (1997) Orientation selectivity and the arrangement of horizontal connections in tree shrew striate cortex. *J Neurosci* 17:2112-2127.
- Brittain J, Piekarz A, Wang Y, Kondo T, Cummins T, Khanna R (2009) An atypical role for collapsin response mediator protein 2 (CRMP-2) in neurotransmitter release via interaction with presynaptic voltage-gated Ca<sup>2+</sup> channels. *J Biol Chem*.
- Brunso-Bechtold J, Casagrande V (1981) Effect of bilateral enucleation on the development of layers in the dorsal lateral geniculate nucleus. *Neuroscience* 6:2579-2586.

- Bulfone A, Martinez S, Marigo V, Campanella M, Basile A, Quaderi N, Gattuso C, Rubenstein JL, Ballabio A (1999) Expression pattern of the Tbr2 (Eomesodermin) gene during mouse and chick brain development. *Mech Dev* 84:133-138.
- Butts D (2002) Retinal waves: implications for synaptic learning rules during development. *Neuroscientist* 8:243-253.
- Butts D, Feller M, Shatz C, Rokhsar D (1999) Retinal waves are governed by collective network properties. *J Neurosci* 19:3580-3593.
- Cabelli R, Hohn A, Shatz C (1995) Inhibition of ocular dominance column formation by infusion of NT-4/5 or BDNF. *Science* 267:1662-1666.
- Cabelli R, Shelton D, Segal R, Shatz C (1997) Blockade of endogenous ligands of trkB inhibits formation of ocular dominance columns. *Neuron* 19:63-76.
- Cang J, Wang L, Stryker MP, Feldheim DA (2008a) Roles of ephrin-as and structured activity in the development of functional maps in the superior colliculus. *J Neurosci* 28:11015-11023.
- Cang J, Kaneko M, Yamada J, Woods G, Stryker M, Feldheim D (2005) Ephrin-as guide the formation of functional maps in the visual cortex. *Neuron* 48:577-589.
- Cang J, Niell CM, Liu X, Pfeiffenberger C, Feldheim DA, Stryker MP (2008b) Selective disruption of one Cartesian axis of cortical maps and receptive fields by deficiency in ephrin-As and structured activity. *Neuron* 57:511-523.
- Catalano SM, Shatz CJ (1998) Activity-Dependent Cortical Target Selection by Thalamic Axons. *Science* 281:559-562.
- Catterall WA, Few AP (2008) Calcium channel regulation and presynaptic plasticity. *Neuron* 59:882-901.
- Chapman B, Zahs K, Stryker M (1991) Relation of cortical cell orientation selectivity to alignment of receptive fields of the geniculocortical afferents that arborize within a single orientation column in ferret visual cortex. *J Neurosci* 11:1347-1358.
- Chappert-Piquemal C, Fonta C, Malecaze F, Imbert M (2001) Ocular dominance columns in the adult New World Monkey *Callithrix jacchus*. *Vis Neurosci* 18:407-412.
- Chen MS, Huber AB, van der Haar ME, Frank M, Schnell L, Spillmann AA, Christ F, Schwab ME (2000) Nogo-A is a myelin-associated neurite outgrowth inhibitor and an antigen for monoclonal antibody IN-1. *Nature* 403:434-439.
- Chiu C, Weliky M (2001) Spontaneous Activity in Developing Ferret Visual Cortex In Vivo. *The Journal of Neuroscience* 21:8906-8914.
- Chiu C, Weliky M (2002) Relationship of correlated spontaneous activity to functional ocular dominance columns in the developing visual cortex. *Neuron* 35:1123-1134.
- Cnops L, Van de Plas B, Arckens L (2004) Age-dependent expression of collapsin response mediator proteins (CRMPs) in cat visual cortex. *Eur J Neurosci* 19:2345-2351.
- Cnops L, Hu T-T, Burnat K, Arckens L (2007a) Influence of Binocular Competition on the Expression Profiles of CRMP2, CRMP4, Dyn I, and Syt I in Developing Cat Visual Cortex. *Cerebral Cortex* 18:1221-1231.
- Cnops L, Hu T-T, Eysel UT, Arckens L (2007b) Effect of binocular retinal lesions on CRMP2 and CRMP4 but not Dyn I and Syt I expression in adult cat area 17. *Eur J Neurosci* 25:1395-1401.
- Cnops L, Hu T-T, Burnat K, Van Der Gucht E, Arckens L (2006) Age-dependent alterations in CRMP2 and CRMP4 protein expression profiles in cat visual cortex. *Brain Research* 1088:109-119.
- Cnops L, Hu T-T, Vanden Broeck J, Burnat K, Van Den Bergh G, Arckens L (2007c) Age- and experience-dependent expression of Dynamin I and Synaptotagmin I in cat visual system. *J Comp Neurol* 504:254-264.

- Corriveau R, Huh G, Shatz C (1998) Regulation of class I MHC gene expression in the developing and mature CNS by neural activity. *Neuron* 21:505-520.
- Cramer K, Sur M (1997) Blockade Of Afferent Impulse Activity Disrupts On/Off Sublamination In the Ferret Lateral Geniculate Nucleus. *Brain Research Developmental Brain Research* 98:287-290.
- Crowley J, Katz L (1999) Development of ocular dominance columns in the absence of retinal input. *Nat Neurosci* 2:1125-1130.
- Crowley J, Katz L (2000) Early development of ocular dominance columns. *Science* 290:1321-1324.
- Crowley J, Katz L (2002) Ocular dominance development revisited. *Curr Opin Neurobiol* 12:104-109.
- Cucchiaro J, Guillory R (1984) The development of the retinogeniculate pathways in normal and albino ferrets. *Proc R Soc Lond B Biol Sci* 223:141-164.
- Dergham P, Ellezam B, Essagian C, Avedissian H, Lubell WD, McKerracher L (2002) Rho signaling pathway targeted to promote spinal cord repair. *J Neurosci* 22:6570-6577.
- Drescher U, Kremoser C, Handwerker C, Lschinger J, Noda M, Bonhoeffer F (1995) In vitro guidance of retinal ganglion cell axons by RAGS, a 25 kDa tectal protein related to ligands for Eph receptor tyrosine kinases. *Cell* 82:359-370.
- Dufour A, Seibt J, Passante L, Depaepe V, Ciossek T, Frisen J, Kullander K, Flanagan J, Polleux F, Vanderhaeghen P (2003) Area specificity and topography of thalamocortical projections are controlled by ephrin/Eph genes. *Neuron* 39:453-465.
- Ellsworth CA, Lyckman AW, Feldheim DA, Flanagan JG, Sur M (2005) Eprhin-A2 and -A5 influence patterning of normal and novel retinal projections to the thalamus: Conserved mapping mechanisms in visual and auditory thalamic targets. *J Comp Neurol* 488:140-151.
- Famiglietti E, Kolb H (1976) Structural basis for ON-and OFF-center responses in retinal ganglion cells. *Science* 194:193-195.
- Feller M, Wellis D, Stellwagen D, Werblin F, Shatz C (1996) Requirement for cholinergic synaptic transmission in the propagation of spontaneous retinal waves. *Science* 272:1182-1187.
- Feller MB (1999) Spontaneous Correlated Activity in Developing Neural Circuits. *Neuron* 22:653-656.
- Feller MB, Butts DA, Aaron HL, Rokhsar DS, Shatz CJ (1997) Dynamic Processes Shape Spatiotemporal Properties of Retinal Waves. *Neuron* 19:293-306.
- Flanagan J, Vanderhaeghen P (1998) The ephrins and Eph receptors in neural development. *Annu Rev Neurosci* 21:309-345.
- Frisen J, Yates P, McLaughlin T, Friedman G, O'Leary D, Barbacid M (1998) Eprhin-A5 (AL-1/RAGS) is essential for proper retinal axon guidance and topographic mapping in the mammalian visual system. *Neuron* 20:235-243.
- Frostig R, Lieke E, Ts'o D, Grinvald A (1990) Cortical functional architecture and local coupling between neuronal activity and the microcirculation revealed by in vivo high-resolution optical imaging of intrinsic signals. *Proc Natl Acad Sci U S A* 87:6082-6086.
- Fukata Y, Itoh TJ, Kimura T, Mnager C, Nishimura T, Shiromizu T, Watanabe H, Inagaki N, Iwamatsu A, Hotani H, Kaibuchi K (2002) CRMP-2 binds to tubulin heterodimers to promote microtubule assembly. *Nat Cell Biol* 4:583-591.
- Galli L, Maffei L (1988) Spontaneous impulse activity of rat retinal ganglion cells in prenatal life. *Science* 242:90-91.
- Gallyas F (1979) Silver staining of myelin by means of physical development. *Neurol Res* 1:203-209. Ghosh A, Shatz C (1992a) Involvement of subplate neurons in the formation of ocular dominance columns. *Science* 255:1441-1443.

- Ghosh A, Shatz C (1992b) Pathfinding and target selection by developing geniculocortical axons. *J Neurosci* 12:39-55.
- Goddard C, Butts D, Shatz C (2007) Regulation of CNS synapses by neuronal MHC class I. *Proc Natl Acad Sci U S A* 104:6828-6833.
- Godement P, Salaun J, Imbert M (1984) Prenatal and postnatal development of retinogeniculate and retinocollicular projections in the mouse. *J Comp Neurol* 230:552-575.
- Gong L, Puri M, Unlu M, Young M, Robertson K, Viswanathan S, Krishnaswamy A, Dowd S, Minden J (2004) Drosophila ventral furrow morphogenesis: a proteomic analysis. *Development* 131:643-656.
- Goshima Y, Nakamura F, Strittmatter P, Strittmatter SM (1995) Collapsin-induced growth cone collapse mediated by an intracellular protein related to UNC-33. *Nature* 376:509-514.
- Guillery R (1971) An abnormal retinogeniculate projection in the albino ferret (*Mustela furo*). *Brain Res* 33:482-485.
- Guillery R, LaMantia A, Robson J, Huang K (1985) The influence of retinal afferents upon the development of layers in the dorsal lateral geniculate nucleus of mustelids. *J Neurosci* 5:1370-1379.
- Hendry SH, Yoshioka T (1994) A neurochemically distinct third channel in the macaque dorsal lateral geniculate nucleus. *Science* 264:575-577.
- Hendry SH, Reid RC (2000) The koniocellular pathway in primate vision. *Annual Review of Neuroscience* 23:127-153.
- Hensch TK (2005) Critical period plasticity in local cortical circuits. *Nat Rev Neurosci* 6:877-888.
- Herrera E, Marcus R, Li S, Williams SE, Erskine L, Lai E, Mason C (2004) Foxd1 is required for proper formation of the optic chiasm. *Development* 131:5727-5739.
- Herrera E, Brown L, Aruga J, Rachel RA, Dolen G, Mikoshiba K, Brown S, Mason CA (2003) Zic2 patterns binocular vision by specifying the uncrossed retinal projection. *Cell* 114:545-557.
- Herrmann K, Antonini A, Shatz C (1994) Ultrastructural evidence for synaptic interactions between thalamocortical axons and subplate neurons. *Eur J Neurosci* 6:1729-1742.
- Hogan D, Williams RW (1995) Analysis of the retinas and optic nerves of achiasmic Belgian sheepdogs. *J Comp Neurol* 352:367-380.
- Hogan D, Garraghty P, Williams R (1999) Asymmetric connections, duplicate layers, and a vertically inverted map in the primary visual system. *J Neurosci* 19:RC38.
- Horng S, Kreiman G, Ellsworth C, Page D, Blank M, Millen K, Sur M (2009) Differential gene expression in the developing lateral geniculate nucleus and medial geniculate nucleus reveals novel roles for Zic4 and Foxp2 in visual and auditory pathway development. *J Neurosci* 29:13672-13683.
- Horton J, Hocking D (1996a) Intrinsic variability of ocular dominance column periodicity in normal macaque monkeys. *J Neurosci* 16:7228-7239.
- Horton J, Hocking D (1996b) An adult-like pattern of ocular dominance columns in striate cortex of newborn monkeys prior to visual experience. *J Neurosci* 16:1791-1807.
- Horton J, Hocking D (1997) Timing of the critical period for plasticity of ocular dominance columns in macaque striate cortex. *J Neurosci* 17:3684-3709.
- Huang Z, Kirkwood A, Pizzorusso T, Porciatti V, Morales B, Bear M, Maffei L, Tonegawa S (1999) BDNF regulates the maturation of inhibition and the critical period of plasticity in mouse visual cortex. *Cell* 98:739-755.
- Hubel D, Wiesel T (1963a) Shape and arrangement of columns in cat's striate cortex. *J Physiol* 165:559-568.

- Hubel D, Wiesel T (1968) Receptive fields and functional architecture of monkey striate cortex. *J Physiol (Lond)* 195:215-243.
- Hubel D, Wiesel T (1969) Anatomical demonstration of columns in the monkey striate cortex. *Nature* 221:747-750.
- Hubel D, Wiesel T (1977a) Ferrier lecture. Functional architecture of macaque monkey visual cortex. *Proc R Soc Lond B Biol Sci* 198:1-59.
- Hubel D, Wiesel T (1998) Early exploration of the visual cortex. *Neuron* 20:401-412.
- Hubel D, Wiesel T, LeVay S (1977) Plasticity of ocular dominance columns in monkey striate cortex. *Philos Trans R Soc Lond B Biol Sci* 278:377-409.
- Hubel DH (1975) An Autoradiographic Study of the Retinal-Cortical Projections in the Tree Shrew (*Tupaia glis*). *Brain Research* 96:41-60.
- Hubel DH (1982) Exploration of the Primary Visual Cortex, 1955-78. *Nature* 299:515-524.
- Hubel DH, Wiesel TN (1959) Receptive fields of single neurones in the cat's striate cortex. *J Physiol* 148:574-591.
- Hubel DH, Wiesel TN (1962) Receptive Fields, Binocular Interaction and Functional Architecture in the Cat's Visual Cortex. *Journal of Physiology* 160:106-154.
- Hubel DH, Wiesel TN (1963b) Receptive Fields of Cells in Striate Cortex of Very Young, Visually Inexperienced Kittens. *Journal of Neurophysiology* 26:994-1002.
- Hubel DH, Wiesel TN (1966) Effects of varying stimulus size and color on single lateral geniculate cells in Rhesus monkeys. *Proc Natl Acad Sci U S A* 55:1345-1346.
- Hubel DH, Wiesel TN (1970) The Period of Susceptability to the Physiological Effects of Unilateral Eye Closure in Kittens. *Journal of Physiology (Lond)* 206:419-436.
- Hubel DH, Wiesel TN (1972) Laminar and Columnar Distribution of Geniculo-cortical Fibers in the Macaque Monkey. *The Journal of Comparative Neurology* 146:421-450.
- Hubel DH, Wiesel TN (1974) Sequence Regularity and Geometry of Orientation Columns in the Monkey Striate Cortex. *The Journal of Comparative Neurology* 158:267-294.
- Hubel DH, Wiesel TN (1977b) Ferrier Lecture: Functional Architecture of the Macaque Monkey Visual Cortex. *Proceedings of the Royal Society of London, Series B* 198:1-59.
- Hubener M (2003) Mouse visual cortex. *Curr Opin Neurobiol* 13:413-420.
- Huberman A, Stellwagen D, Chapman B (2002) Decoupling eye-specific segregation from lamination in the lateral geniculate nucleus. *J Neurosci* 22:9419-9429.
- Huberman A, Murray K, Warland D, Feldheim D, Chapman B (2005) Ephrin-As mediate targeting of eye-specific projections to the lateral geniculate nucleus. *Nat Neurosci* 8:1013-1021.
- Huberman A, Wang G, Liets L, Collins O, Chapman B, Chalupa L (2003) Eye-specific retino-geniculate segregation independent of normal neuronal activity. *Science* 300:994-998.
- Huberman AD, Feller MB, Chapman B (2008) Mechanisms underlying development of visual maps and receptive fields. *Annu Rev Neurosci* 31:479-509.
- Huh G, Boulanger L, Du H, Riquelme P, Brotz T, Shatz C (2000) Functional requirement for class I MHC in CNS development and plasticity. *Science* 290:2155-2159.
- Humphrey A, Albano J, Norton T (1977) Organization of ocular dominance in tree shrew striate cortex. *Brain Res* 134:225-236.
- Hutchins JB, Casagrande VA (1988) Glial cells develop a laminar pattern before neuronal cells in the lateral geniculate nucleus. *Proc Natl Acad Sci U S A* 85:8316-8320.
- Hutchins JB, Casagrande VA (1990) Development of the lateral geniculate nucleus: interactions between retinal afferent, cytoarchitectonic, and glial cell process lamination in ferrets and tree shrews. *J Comp Neurol* 298:113-128.

- Inagaki N, Chihara K, Arimura N, Mnager C, Kawano Y, Matsuo N, Nishimura T, Amano M, Kaibuchi K (2001) CRMP-2 induces axons in cultured hippocampal neurons. *Nature Neuroscience* 4:781-782.
- Issa N, Trachtenberg J, Chapman B, Zahs K, Stryker M (1999) The critical period for ocular dominance plasticity in the Ferret's visual cortex. *J Neurosci* 19:6965-6978.
- Jackson C, Peduzzi J, Hickey T (1989) Visual cortex development in the ferret. I. Genesis and migration of visual cortical neurons. *The Journal of Neuroscience* 9:1242-1253.
- Jacobs S, Van De Plas B, Van Der Gucht E, Clerens S, Cnops L, Van Den Bergh G, Arckens L (2008) Identification of new regional marker proteins to map mouse brain by 2-D difference gel electrophoresis screening. *Electrophoresis* 29:1518-1524.
- Jain E, Bairoch A, Duvaud S, Phan I, Redaschi N, Suzek BE, Martin MJ, McGarvey P, Gasteiger E (2009) Infrastructure for the life sciences: design and implementation of the UniProt website. *BMC Bioinformatics* 10:136.
- Kanold P, Kara P, Reid R, Shatz C (2003) Role of subplate neurons in functional maturation of visual cortical columns. *Science* 301:521-525.
- Kaschube M, Wolf F, Geisel T, Lowel S (2002) Genetic influence on quantitative features of neocortical architecture. *J Neurosci* 22:7206-7217.
- Kaschube M, Schnabel M, Wolf F, Lowel S (2009) Interareal coordination of columnar architectures during visual cortical development. *Proc Natl Acad Sci U S A* 106:17205-17210.
- Kaschube M, Wolf F, Puhlmann M, Rathjen S, Schmidt K, Geisel T, Lowel S (2003) The pattern of ocular dominance columns in cat primary visual cortex: intra- and interindividual variability of column spacing and its dependence on genetic background. *Eur J Neurosci* 18:3251-3266.
- Katz L, Crowley J (2002) Development of cortical circuits: lessons from ocular dominance columns. *Nat Rev Neurosci* 3:34-42.
- Kawasaki H (2004) Molecular Organization of the Ferret Visual Thalamus. *Journal of Neuroscience* 24:9962-9970.
- Kawasaki H, Crowley JC, Livesey FJ, Katz LC (2004) Molecular organization of the ferret visual thalamus. *J Neurosci* 24:9962-9970.
- Keil W, Schmidt KF, Lowel S, Kaschube M (2010) Reorganization of columnar architecture in the growing visual cortex. *Proc Natl Acad Sci U S A* 107:12293-12298.
- Kerschensteiner D, Wong RO (2008) A precisely timed asynchronous pattern of ON and OFF retinal ganglion cell activity during propagation of retinal waves. *Neuron* 58:851-858.
- Kim U, Bal T, McCormick D (1995) Spindle waves are propagating synchronized oscillations in the ferret LGNd in vitro. *J Neurophysiol* 74:1301-1323.
- Kolodkin AL, Levengood DV, Rowe EG, Tai YT, Giger RJ, Ginty DD (1997) Neuropilin is a semaphorin III receptor. *Cell* 90:753-762.
- Kottis V, Thibault P, Mikol D, Xiao ZC, Zhang R, Dergham P, Braun PE (2002) Oligodendrocyte-myelin glycoprotein (OMgp) is an inhibitor of neurite outgrowth. *J Neurochem* 82:1566-1569.
- Krishna K, Nuernberger M, Weth F, Redies C (2009) Layer-specific expression of multiple cadherins in the developing visual cortex (V1) of the ferret. *Cereb Cortex* 19:388-401.
- Law M, Zahs K, Stryker M (1988) Organization of primary visual cortex (area 17) in the ferret. *J Comp Neurol* 278:157-180.
- Leamey CA, Merlin S, Lattouf P, Sawatari A, Zhou X, Demel N, Glendining KA, Oohashi T, Sur M, Fssler R (2007) Ten-m3 Regulates Eye-Specific Patterning in the Mammalian Visual Pathway and Is Required for Binocular Vision. *Plos Biol* 5:e241.
- Lee K, McCormick D (1997) Modulation of spindle oscillations by acetylcholine, cholecystokinin

- and 1S,3R-ACPD in the ferret lateral geniculate and perigeniculate nuclei in vitro. *Neuroscience* 77:335-350.
- Lein E, Shatz C (2000) Rapid regulation of brain-derived neurotrophic factor mRNA within eye-specific circuits during ocular dominance column formation. *J Neurosci* 20:1470-1483.
- Lein E, Hohn A, Shatz C (2000) Dynamic regulation of BDNF and NT-3 expression during visual system development. *J Comp Neurol* 420:1-18.
- LeVay S, Ferster D (1977) Relay cell classes in the lateral geniculate nucleus of the cat and the effects of visual deprivation. *J Comp Neurol* 172:563-584.
- LeVay S, Stryker MP, Shatz CJ (1978) Ocular Dominance Columns and Their Development in Layer IV of the Cat's Visual Cortex: A Quantitative Study. *Journal of Comparative Neurology* 179:223-244.
- LeVay S, Wiesel TN, Hubel D (1980) The Development of Ocular Dominance Columns in Normal and Visually Deprived Monkeys. *The Journal of Comparative Neurology* 191:1-51.
- LeVay S, McConnell S, Luskin M (1987) Functional organization of primary visual cortex in the mink (*Mustela vison*), and a comparison with the cat. *J Comp Neurol* 257:422-441.
- LeVay S, Connolly M, Houde J, Van Essen D (1985) The complete pattern of ocular dominance stripes in the striate cortex and visual field of the macaque monkey. *J Neurosci* 5:486-501.
- Linden D, Guillory R, Cucchiaro J (1981a) The dorsal lateral geniculate nucleus of the normal ferret and its postnatal development. *J Comp Neurol* 203:189-211.
- Linden DC, Guillory RW, Cucchiaro J (1981b) The dorsal lateral geniculate nucleus of the normal ferret and its postnatal development. *The Journal of Comparative Neurology* 203:189-211.
- Livingstone MS, Hubel DH (1984) Anatomy and Physiology of a Color System in the Primate Visual Cortex. *The Journal of Neuroscience* 4:309-356.
- Lyckman AW, Horng S, Leamey CA, Tropea D, Watakabe A, Van Wart A, McCurry C, Yamamori T, Sur M (2008) Gene expression patterns in visual cortex during the critical period: synaptic stabilization and reversal by visual deprivation. *Proceedings of the National Academy of Sciences of the United States of America* 105:9409-9414.
- Mandemakers WJ, Barres BA (2005) Axon regeneration: it's getting crowded at the gates of TROY. *Curr Biol* 15:R302-305.
- McConnell S, LeVay S (1986) Anatomical organization of the visual system of the mink, *Mustela vison*. *J Comp Neurol* 250:109-132.
- McCormick D, Trent F, Ramoa A (1995) Postnatal development of synchronized network oscillations in the ferret dorsal lateral geniculate and perigeniculate nuclei. *The Journal of Neuroscience* 15:5739-5752.
- McKerracher L, David S, Jackson DL, Kottis V, Dunn RJ, Braun PE (1994) Identification of myelin-associated glycoprotein as a major myelin-derived inhibitor of neurite growth. *Neuron* 13:805-811.
- Meister M, Wong RO, Baylor DA, Shatz CJ (1991) Synchronous bursts of action potentials in ganglion cells of the developing mammalian retina. *Science* 252:939-943.
- Miyashita-Lin EM, Hevner R, Wasserman KM, Martinez S, Rubenstein JLR (1999) Early Neocortical Regionalization in the Absence of Thalamic Innervation. *Science* 285:906-909.
- Morgan JE, Henderson Z, Thompson ID (1987) Retinal decussation patterns in pigmented and albino ferrets. *Neuroscience* 20:519-535.
- Mountcastle V (1957) Modality and topographic properties of single neurons of cat's somatic sensory cortex. *J Neurophysiol* 20:408-434.
- Mountcastle V, Davies P, Berman A (1957) Response properties of neurons of cat's somatic sensory cortex to peripheral stimuli. *J Neurophysiol* 20:374-407.

- Murray KD, Rubin CM, Jones EG, Chalupa LM (2008) Molecular correlates of laminar differences in the macaque dorsal lateral geniculate nucleus. *J Neurosci* 28:12010-12022.
- Murre JM, Sturdy DP (1995) The connectivity of the brain: multi-level quantitative analysis. *Biol Cybern* 73:529-545.
- Nakamura F, Kalb RG, Strittmatter SM (2000) Molecular basis of semaphorin-mediated axon guidance. *Journal of Neurobiology* 44:219-229.
- Nauman JV, Campbell PG, Lanni F, Anderson JL (2007) Diffusion of insulin-like growth factor-I and ribonuclease through fibrin gels. *Biophys J* 92:4444-4450.
- Padmanabhan K (2008) On the role of spontaneous retinal activity in the anatomical development of early visual circuits (Doctoral Dissertaion). Carnegie Mellon University, Pittsburgh, Pennsylvania.
- Padmanabhan K, Eddy WF, Crowley JC (2010) A novel algorithm for optimal image thresholding of biological data. *J Neurosci Methods* 193:380-384.
- Pak W, Hindges R, Lim Y-S, Pfaff SL, O'Leary DDM (2004) Magnitude of binocular vision controlled by islet-2 repression of a genetic program that specifies laterality of retinal axon pathfinding. *Cell* 119:567-578.
- Pang ZP, Sudhof TC (2010) Cell biology of Ca<sup>2+</sup>-triggered exocytosis. *Curr Opin Cell Biol* 22:496-505.
- Penn A, Riquelme P, Feller M, Shatz C (1998a) Competition in Retinogeniculate Patterning Driven by Spontaneous Activity. *ScienceNew Series* 279:2108-2112.
- Penn AA, Riquelme PA, Feller MB, Shatz CJ (1998b) Competition in retinogeniculate patterning driven by spontaneous activity. *Science* 279:2108-2112.
- Perkins D, Pappin D, Creasy D, Cottrell J (1999) Probability-based protein identification by searching sequence databases using mass spectrometry data. *Electrophoresis* 20:3551-3567.
- Pfeiffenberger C, Yamada J, Feldheim D (2006) Ephrin-As and patterned retinal activity act together in the development of topographic maps in the primary visual system. *J Neurosci* 26:12873-12884.
- Pfeiffenberger C, Cutforth T, Woods G, Yamada J, Renteria R, Copenhagen D, Flanagan J, Feldheim D (2005) Ephrin-As and neural activity are required for eye-specific patterning during retinogeniculate mapping. *Nat Neurosci* 8:1022-1027.
- Pistorio AL, Hendry SH, Wang X (2006) A modified technique for high-resolution staining of myelin. *Journal of Neuroscience Methods* 153:135-146.
- Rais I, Karas M, Schgger H (2004) Two-dimensional electrophoresis for the isolation of integral membrane proteins and mass spectrometric identification. *Proteomics* 4:2567-2571.
- Rakic P (1981) Development of Visual Centers in the Primate Brain Depends on Binocular Competition Before Birth. *Science* 214:928-931.
- Raper JA (2000) Semaphorins and their receptors in vertebrates and invertebrates. *Current Opinion in Neurobiology* 10:88-94.
- Redies C, Diksic M, Riml H (1990) Functional organization in the ferret visual cortex: a double-label 2-deoxyglucose study. *The Journal of Neuroscience* 10:2791-2803.
- Rockland K (1985) Anatomical organization of primary visual cortex (area 17) in the ferret. *J Comp Neurol* 241:225-236.
- Rowell JJ, Mallik AK, Dugas-Ford J, Ragsdale CW (2010) Molecular analysis of neocortical layer structure in the ferret. *J Comp Neurol* 518:3272-3289.
- Rubenstein JL, Anderson S, Shi L, Miyashita-Lin E, Bulfone A, Hevner R (1999) Genetic control of cortical regionalization and connectivity. *Cereb Cortex* 9:524-532.

- Rusoff A, Dubin M (1977) Development of receptive-field properties of retinal ganglion cells in kittens. *J Neurophysiol* 40:1188-1198.
- Ruthazer E, Stryker M (1996) The role of activity in the development of long-range horizontal connections in area 17 of the ferret. *J Neurosci* 16:7253-7269.
- Schmidt EF, Strittmatter SM (2007) The CRMP family of proteins and their role in Sema3A signaling. *Adv Exp Med Biol* 600:1-11.
- Seung HS (2009) Reading the book of memory: sparse sampling versus dense mapping of connectomes. *Neuron* 62:17-29. Shatz C, Luskin M (1986) The relationship between the geniculocortical afferents and their cortical target cells during development of the cat's primary visual cortex. *J Neurosci* 6:3655-3668.
- Shatz CJ (1983) The prenatal development of the cat's retinogeniculate pathway. *J Neurosci* 3:482-499.
- Shatz CJ, Kirkwood PA (1984) Prenatal Development of Functional Connections in the Cat's Retinogeniculate Pathway. *The Journal of Neuroscience* 4:1378-1397.
- Shatz CJ, Stryker MP (1988) Prenatal Tetrodotoxin Infusion Blocks the Segregation of Retinogeniculate Afferents. *Science* 242:87-89.
- Snider RS, Lee JC (1961) *A Stereotaxic Atlas of the Monkey Brain*. Chicago and London, The University of Chicago Press.
- Spatz WB (1979) The retino-geniculo-cortical pathway in Callithrix. II. The geniculo-cortical projection. *Exp Brain Res* 36:401-410.
- Spatz WB (1989) Loss of ocular dominance columns with maturity in the monkey, *Callithrix jacchus*. *Brain Res* 488:376-380.
- Sperry R (1963) Chemoaffinity in the Orderly Growth of Nerve Fiber Patterns and Connections. *Proc Natl Acad Sci U S A* 50:703-710.
- Sporns O (2011) The human connectome: a complex network. *Ann N Y Acad Sci*.
- Sporns O, Tononi G, Kotter R (2005) The human connectome: A structural description of the human brain. *PLoS Comput Biol* 1:e42.
- Sretavan DW, Shatz CJ (1986a) Prenatal Development of Retinal Ganglion Cell Axons: Segregation into Eye-Specific Layers Within the Cat's Lateral Geniculate Nucleus. *The Journal of Neuroscience* 6:234-251.
- Sretavan DW, Shatz CJ (1986b) Prenatal development of cat retinogeniculate axon arbors in the absence of binocular interactions. *J Neurosci* 6:990-1003.
- Stacy R, Wong R (2003) Developmental relationship between cholinergic amacrine cell processes and ganglion cell dendrites of the mouse retina. *J Comp Neurol* 456:154-166.
- Stellwagen D, Shatz C (2002) An instructive role for retinal waves in the development of retinogeniculate connectivity. *Neuron* 33:357-367.
- Stellwagen D, Shatz C, Feller M (1999) Dynamics of retinal waves are controlled by cyclic AMP. *Neuron* 24:673-685.
- Stryker M (1978) Postnatal development of ocular dominance columns in layer IV of the cat's visual cortex and the effects of monocular deprivation. *Arch Ital Biol* 116:420-426.
- Stryker M, Zahs K (1983) On and off sublaminae in the lateral geniculate nucleus of the ferret. *J Neurosci* 3:1943-1951.
- Stryker M, Harris W (1986) Binocular impulse blockade prevents the formation of ocular dominance columns in cat visual cortex. *The Journal of Neuroscience* 6:2117-2133.
- Thompson ID, Morgan JE (1993) The development of retinal ganglion cell decussation patterns in postnatal pigmented and albino ferrets. *Eur J Neurosci* 5:341-356.
- Tian NM, Pratt T, Price DJ (2008) Foxg1 regulates retinal axon pathfinding by repressing an

- ipsilateral program in nasal retina and by causing optic chiasm cells to exert a net axonal growth-promoting activity. *Development* 135:4081-4089.
- tom Dieck S, Altrock WD, Kessels MM, Qualmann B, Regus H, Brauner D, Fejtova A, Bracko O, Gundelfinger ED, Brandstatter JH (2005) Molecular dissection of the photoreceptor ribbon synapse: physical interaction of Bassoon and RIBEYE is essential for the assembly of the ribbon complex. *J Cell Biol* 168:825-836. Torborg CL, Feller MB (2004) Unbiased analysis of bulk axonal segregation patterns. *Journal of Neuroscience Methods* 135:17-26.
- Tropea D, Van Wart A, Sur M (2009) Molecular mechanisms of experience-dependent plasticity in visual cortex. *Philos Trans R Soc Lond, B, Biol Sci* 364:341-355.
- Tropea D, Kreiman G, Lyckman A, Mukherjee S, Yu H, Horng S, Sur M (2006) Gene expression changes and molecular pathways mediating activity-dependent plasticity in visual cortex. *Nat Neurosci* 9:660-668.
- Unlu M, Morgan M, Minden J (1997) Difference gel electrophoresis: a single gel method for detecting changes in protein extracts. *Electrophoresis* 18:2071-2077.
- Van den Bergh G, Clerens S, Cnops L, Vandesande F, Arckens L (2003) Fluorescent two-dimensional difference gel electrophoresis and mass spectrometry identify age-related protein expression differences for the primary visual cortex of kitten and adult cat. *J Neurochem* 85:193-205.
- Van den Bergh G, Clerens S, Firestein B, Burnat K, Arckens L (2006a) Development and plasticity-related changes in protein expression patterns in cat visual cortex: a fluorescent two-dimensional difference gel electrophoresis approach. *Proteomics* 6:3821-3832.
- Van Den Bergh G, Clerens S, Firestein BL, Burnat K, Arckens L (2006b) Development and plasticity-related changes in protein expression patterns in cat visual cortex: A fluorescent two-dimensional difference gel electrophoresis approach. *Proteomics* 6:3821-3832.
- Van Essen DC, Newsome WT, Maunsell JH (1984) The visual field representation in striate cortex of the macaque monkey: asymmetries, anisotropies, and individual variability. *Vision Res* 24:429-448.
- Vanderhaeghen P (2007) The ephrins and the eph receptors in neural development. 1-38.
- Vanderhaeghen P, Polleux F (2004) Developmental mechanisms patterning thalamocortical projections: intrinsic, extrinsic and in between. *Trends Neurosci* 27:384-391.
- Venter JC et al. (2001) The sequence of the human genome. *Science* 291:1304-1351.
- Viswanathan S, nl M, Minden JS (2006) Two-dimensional difference gel electrophoresis. *Nat Protoc* 1:1351-1358.
- von Krosigk M, Bal T, McCormick D (1993) Cellular mechanisms of a synchronized oscillation in the thalamus. *Science* 261:361-364.
- Wang LH, Strittmatter SM (1996) A family of rat CRMP genes is differentially expressed in the nervous system. *J Neurosci* 16:6197-6207.
- Weliky M (2000) Correlated Neuronal Activity and Visual Cortical Development. *Neuron* 27:427-430.
- Weliky M, Katz LC (1999) Correlational structure of spontaneous neuronal activity in the developing lateral geniculate nucleus *in vivo*. *Science* 285:599-604.
- White LE, Bosking WH, Williams SM, Fitzpatrick D (1999a) Maps of central visual space in ferret V1 and V2 lack matching inputs from the two eyes. *J Neurosci* 19:7089-7099.
- White LE, Bosking WH, Williams SM, Fitzpatrick D (1999b) Maps of Central Visual Space in Ferret V1 and V2 Lack Matching Inputs from the Two Eyes. *The Journal of Neuroscience* 19:7089-7099.
- Wiesel TN, Hubel DH (1963a) Single Cell Responses in Striate Cortex of Kittens Deprived of Vision in One Eye. *Journal of Neurophysiology* 26:1003-1017.

- Wiesel TN, Hubel DH (1963b) Effects of Visual Deprivation on Morphology and Physiology of Cells in the Cat's Lateral Geniculate Body. *Journal of Neurophysiology* 26:978-993.
- Wiesel TN, Hubel DH (1965) Extent of Recovery from the Effects of Visual Deprivation in Kittens. *Journal of Neurophysiology* 28:1060-1072.
- Wiesel TN, Hubel DH (1966) Spatial and chromatic interactions in the lateral geniculate body of the rhesus monkey. *J Neurophysiol* 29:1115-1156.
- Williams RW, Hogan D, Garraghty PE (1994) Target recognition and visual maps in the thalamus of achiasmatic dogs. *Nature* 367:637-639.
- Williams SE, Mann F, Erskine L, Sakurai T, Wei S, Rossi DJ, Gale NW, Holt CE, Mason CA, Henkemeyer M (2003) Ephrin-B2 and EphB1 mediate retinal axon divergence at the optic chiasm. *Neuron* 39:919-935.
- Wong R (1999) Retinal waves and visual system development. *Annu Rev Neurosci* 22:29-47.
- Wong RO, Meister M, Shatz CJ (1993) Transient period of correlated bursting activity during development of the mammalian retina. *Neuron* 11:923-938.
- Wong ROL, Oakley DM (1996) Changing Patterns of Spontaneous Bursting Activity of On and Off Retinal Ganglion Cells During Development. *Neuron* 16:1087-1095.
- Woolsey TA, Hanaway J, Gado MH (2003) *The Brain Atlas: A Visual Guide to the Human Central Nervous System*. Hoboken, NJ, John Wiley and Sons, Inc.
- Yiu G, He Z (2003) Signaling mechanisms of the myelin inhibitors of axon regeneration. *Curr Opin Neurobiol* 13:545-551.
- Zahs K, Stryker M (1988) Segregation of ON and OFF afferents to ferret visual cortex. *The Journal of Neurophysiology* 59:1410-1429.